ISM Dynamics and Star Formation

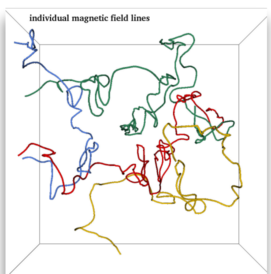

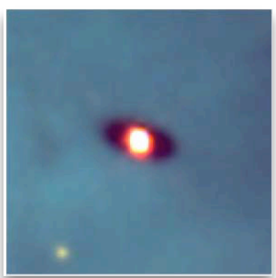
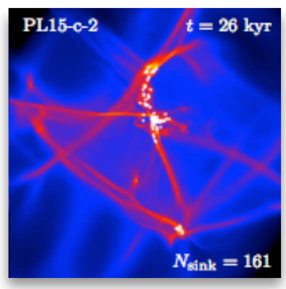


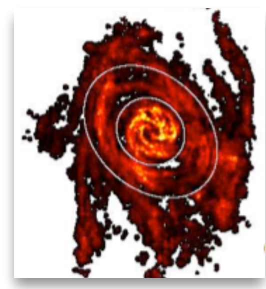
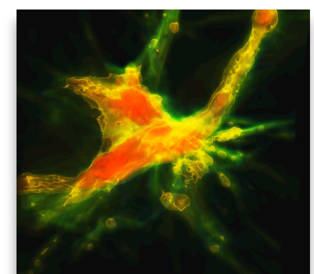

Ralf Klessen

Zentrum für Astronomie der Universität Heidelberg
Institut für Theoretische Astrophysik

thanks to ...

... people in the star formation group at Heidelberg University:

Christian Baczynski, Erik Bertram, Frank Bigiel, Andre Bubel, Diane Cormier, Volker Gaibler, Simon Glover, Dimitrious Gouliermis, Tilman Hartwig, Juan Ibanez, Christoph Klein, Lukas Konstandin, Mei Sasaki, Jennifer Schober, Rahul Shetty, Rowan Smith, László Szűcs

... former group members:

Robi Banerjee, Ingo Berentzen, Paul Clark, Christoph Federrath, Philipp Girichidis, Thomas Greif, Milica Micic, Thomas Peters, Dominik Schleicher, Stefan Schmeja, Sharanya Sur, . . .

... many collaborators abroad!

Deutsche Forschungsgemeinschaft DFG
DFG Priority Program 1573 ISM-SPP Interstellar Medium
BADEN-WÜRTTEMBERG STIFTUNG Wir stiften Zukunft
HGSFP
IMPRS
erc European Research Council

Preface

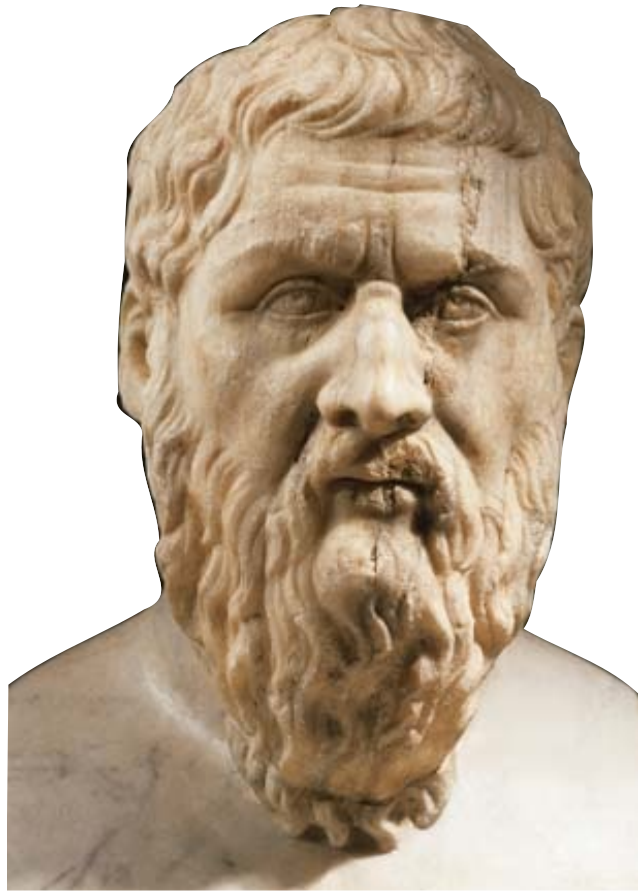

Platon
428/427–348/347 BC

Capitoline Museum, Rome.

3

Plato's allegory of the cave*

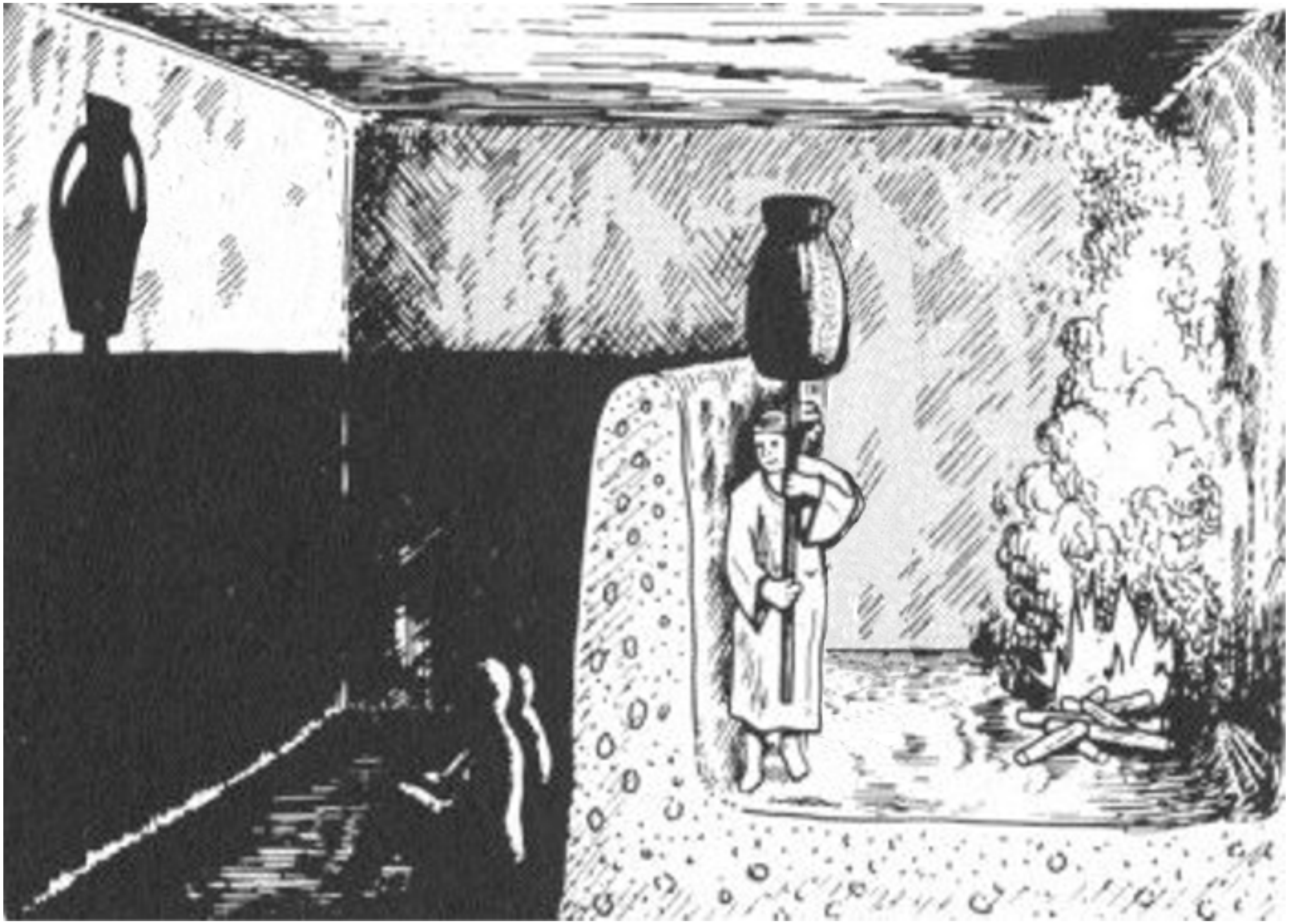

Laszlo Szücs, image from criticalthinking-mc205.wikispaces.com

* The Republic (514a-520a)

Plato's allegory of the cave*

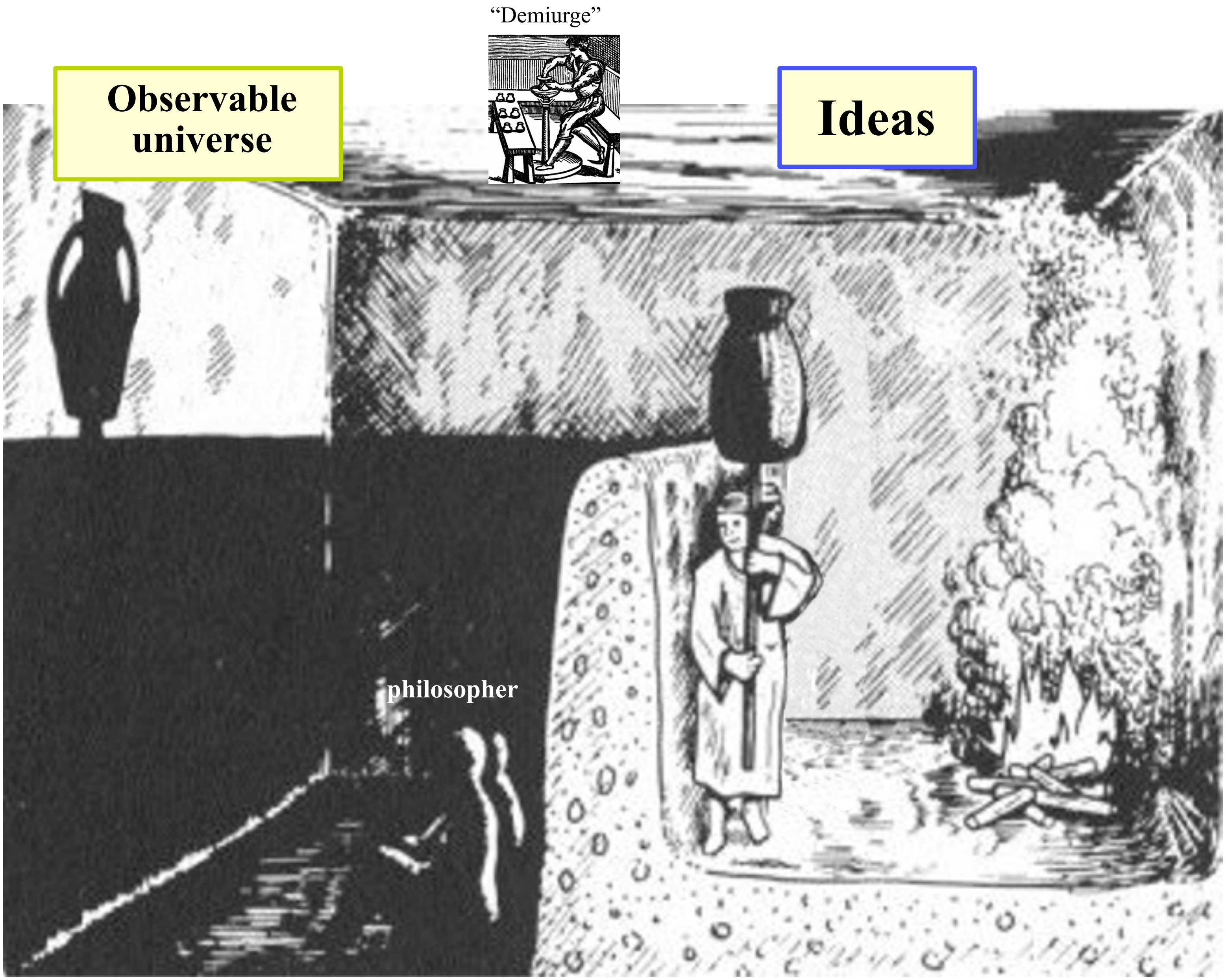

* The Republic (514a-520a)

Laszlo Szücs, image from criticalthinking-mc205.wikispaces.com

}

Plato's allegory of the cave* ↔ Astronomical observations

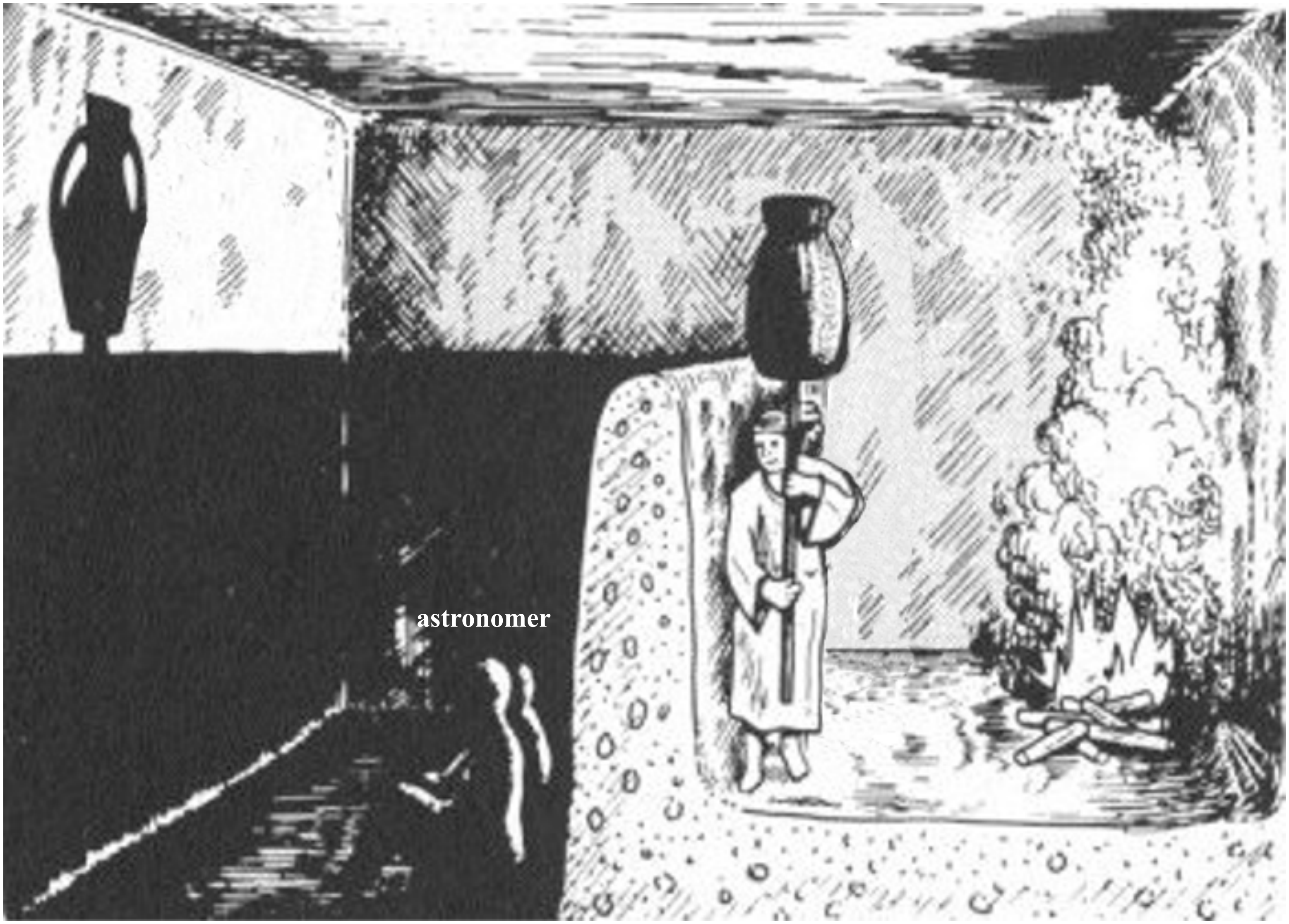

Laszlo Szücs, image from criticalthinking-mc205.wikispaces.com

* The Republic (514a-520a)

8

Plato's allegory of the cave* ↔ Astronomical observations

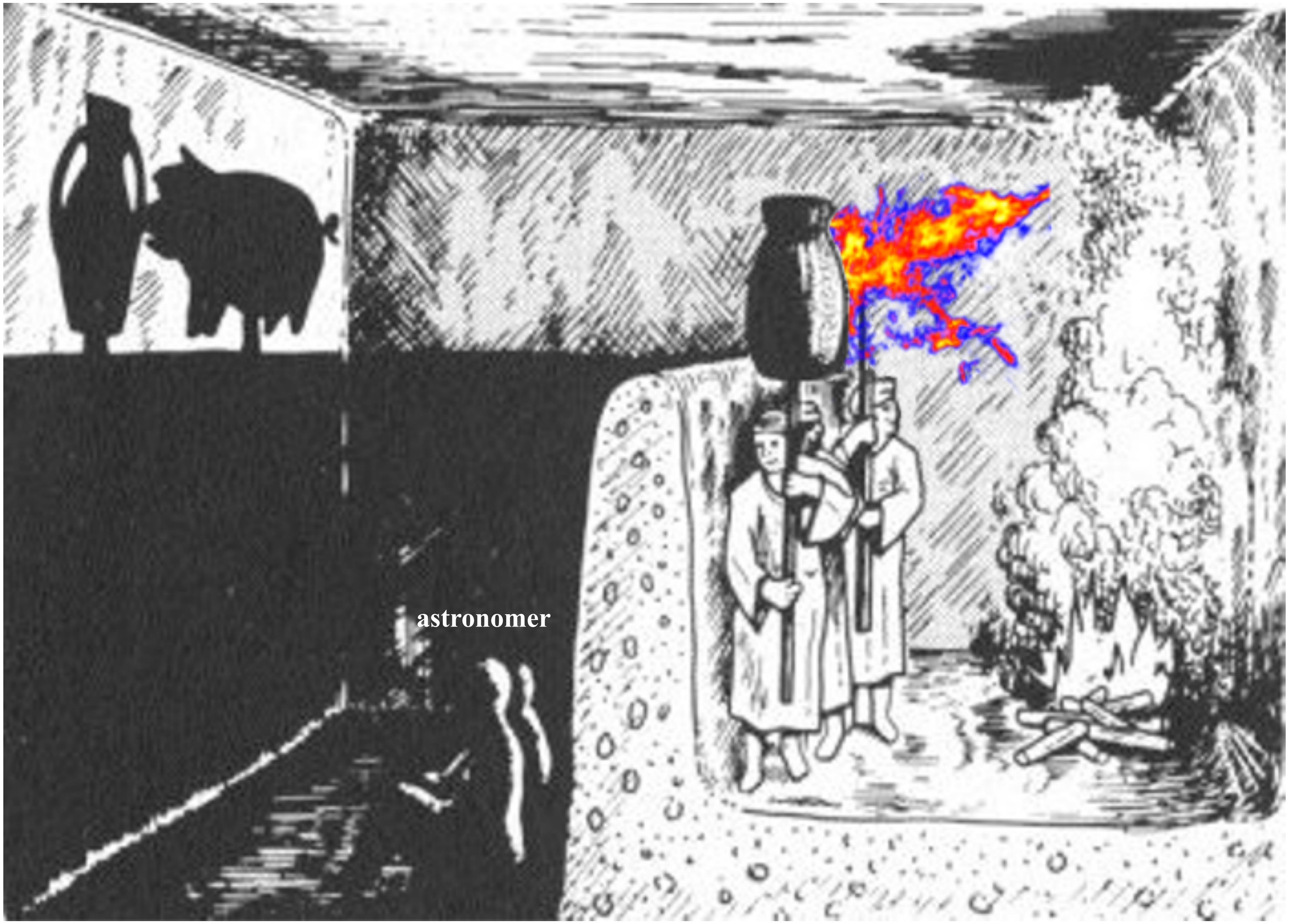

Laszlo Szücs, image from criticalthinking-mc205.wikispaces.com

* The Republic (514a-520a)

Plato's allegory of the cave* ↔ Astronomical observations

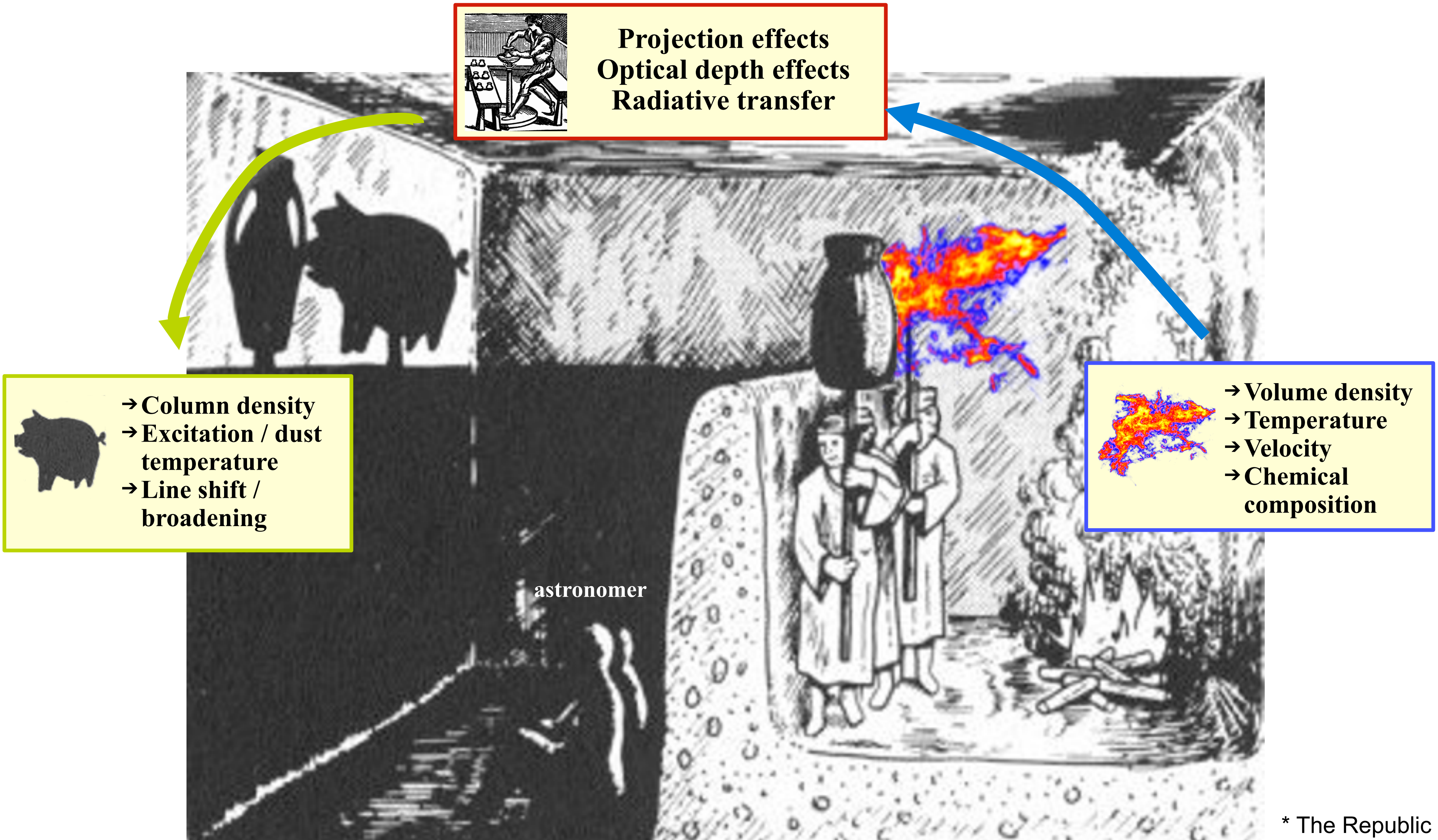

Laszlo Szücs, image from criticalthinking-mc205.wikispaces.com

* The Republic (514a-520a)

Plato's allegory of the cave* ↔ Astronomical observations

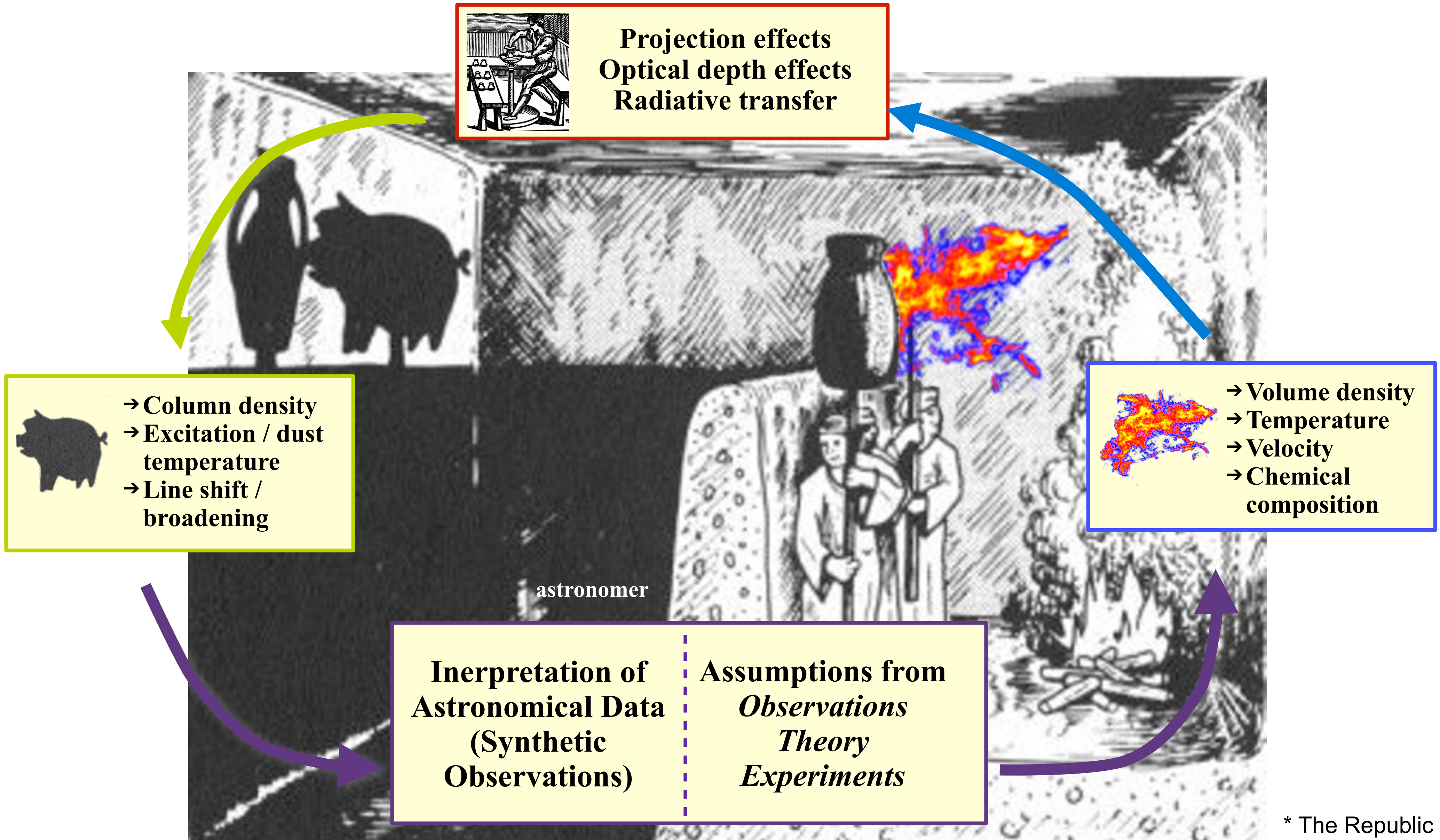

Laszlo Szücs, image from criticalthinking-mc205.wikispaces.com

* The Republic (514a-520a)

Example: from CO emission to total column density

Following Wilson et al. 2009

J=1-0

I$(^{12}$**CO)**
115.271 GHz

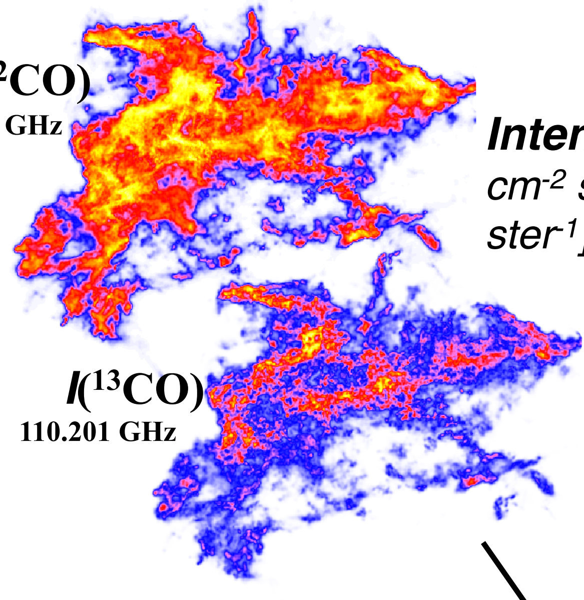

I$(^{13}$**CO)**
110.201 GHz

Intensity *[erg cm^{-2} s^{-1} Hz^{-1} ster^{-1}]*

Brightness temperature *[K]*

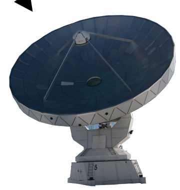

T_B^{12}

T_B^{13}

Assumptions I.

I$(^{12}$**CO) is optically thick**

I$(^{13}$**CO) is optically thin**

Along a line of sight uniform T$_{ex}$ and same for ^{12}CO and ^{13}CO

$$T_{\rm ex} = 5.5/\ln\left(1 + \frac{5.5}{T_B^{12} + 0.82}\right)$$

$$\tau_{13}(v) = -\ln\left[1 - \frac{T_{\rm B}^{13}}{5.3}\left\{\exp\left(\frac{5.3}{T_{\rm ex}} - 1\right)^{-1} - 0.16\right\}^{-1}\right]$$

LTE

$$N(^{13}{\rm CO}) = 3.0\times10^{14}\frac{T_{\rm ex}\int\tau_{13}(v)dv}{1-\exp(-5.3/T_{\rm ex})}$$

Assumptions II.

Uniform N(^{12}CO)/N(^{13}CO) ~ 60 *

N(H$_2$)/N(^{12}CO) ratio ~ 6.6×10^3 **

Column density [cm^{-2}]

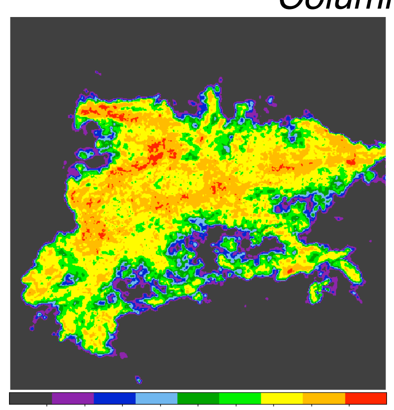

Comparison to observations.

Laszlo Szücs et al., MNRAS, submitted.

* Langer & Penzias (1990)
** Pineda et al. (2009)

phenomenology

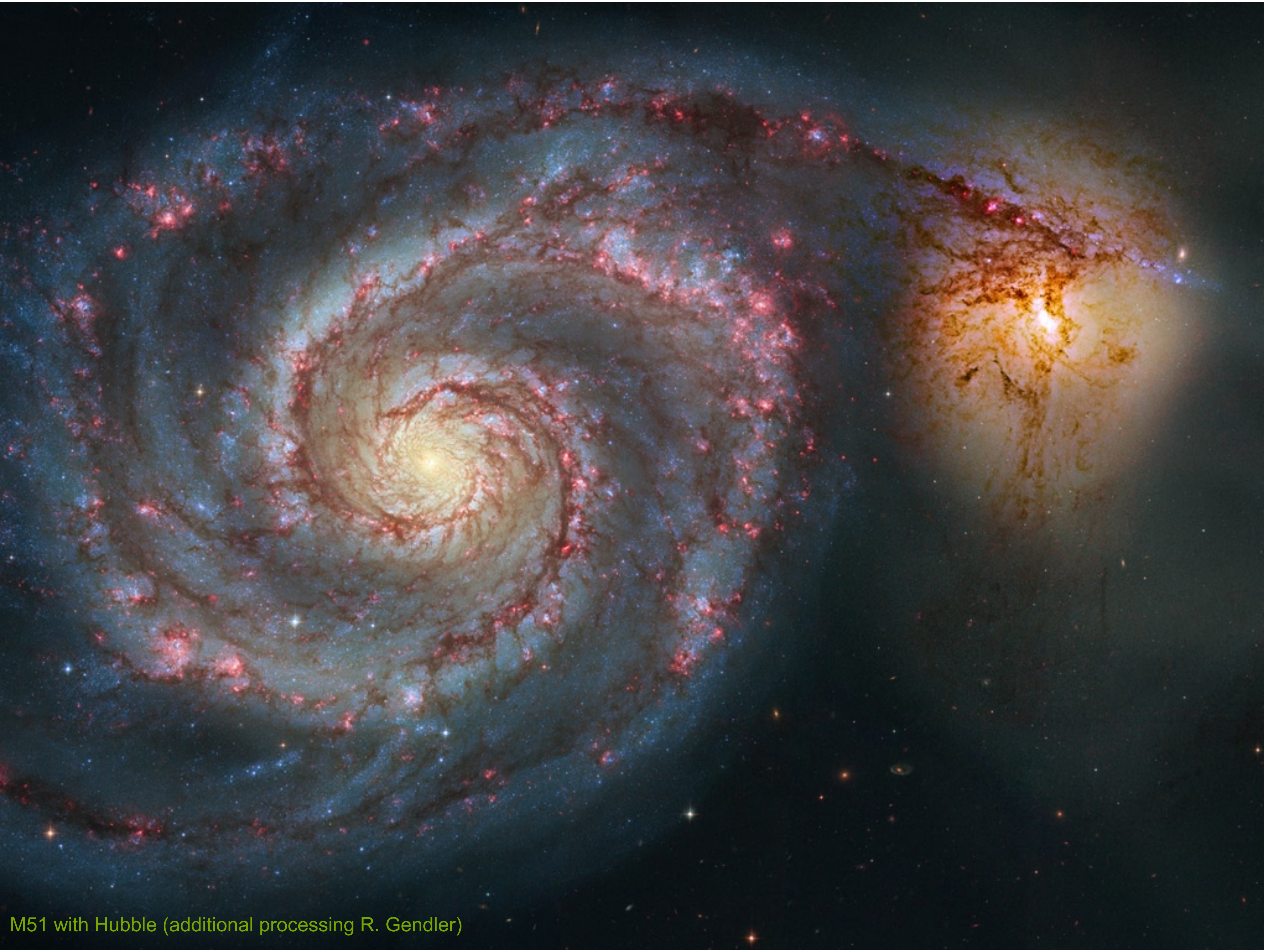

M51 with Hubble (additional processing R. Gendler)

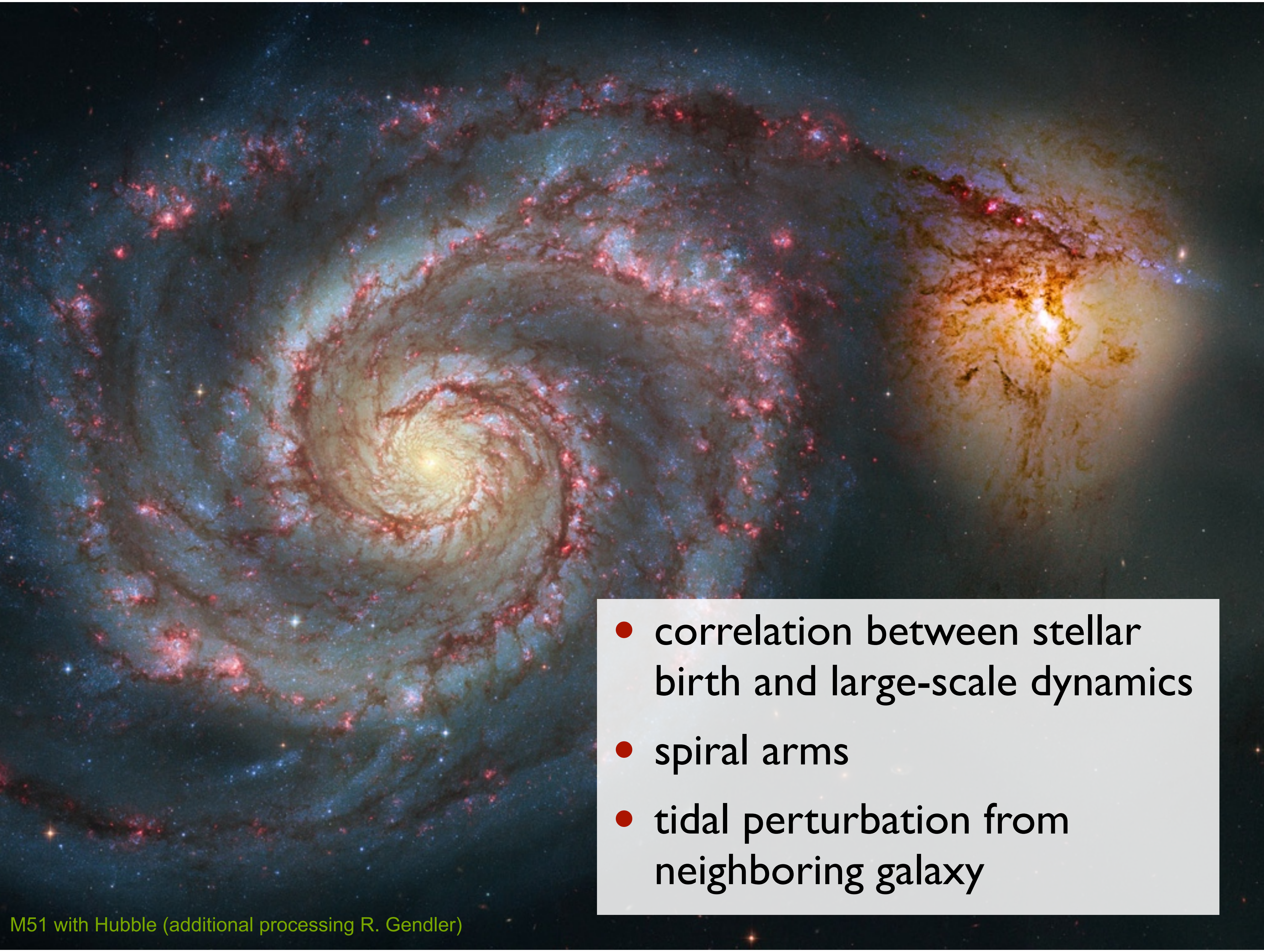
M51 with Hubble (additional processing R. Gendler)

- correlation between stellar birth and large-scale dynamics
- spiral arms
- tidal perturbation from neighboring galaxy

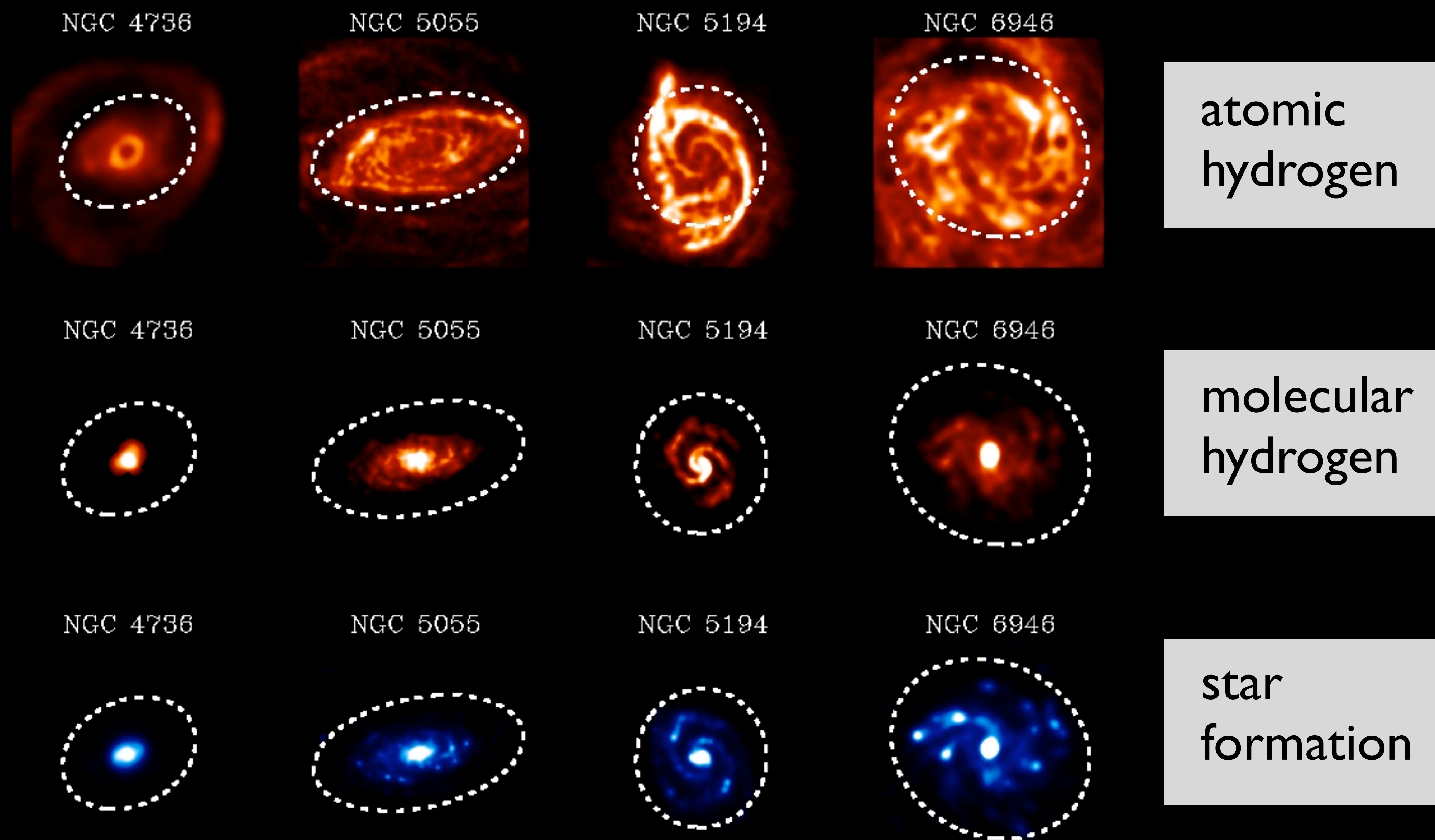

galaxies from THINGS and HERACLES survey
(images from Frank Bigiel, ZAH/ITA)

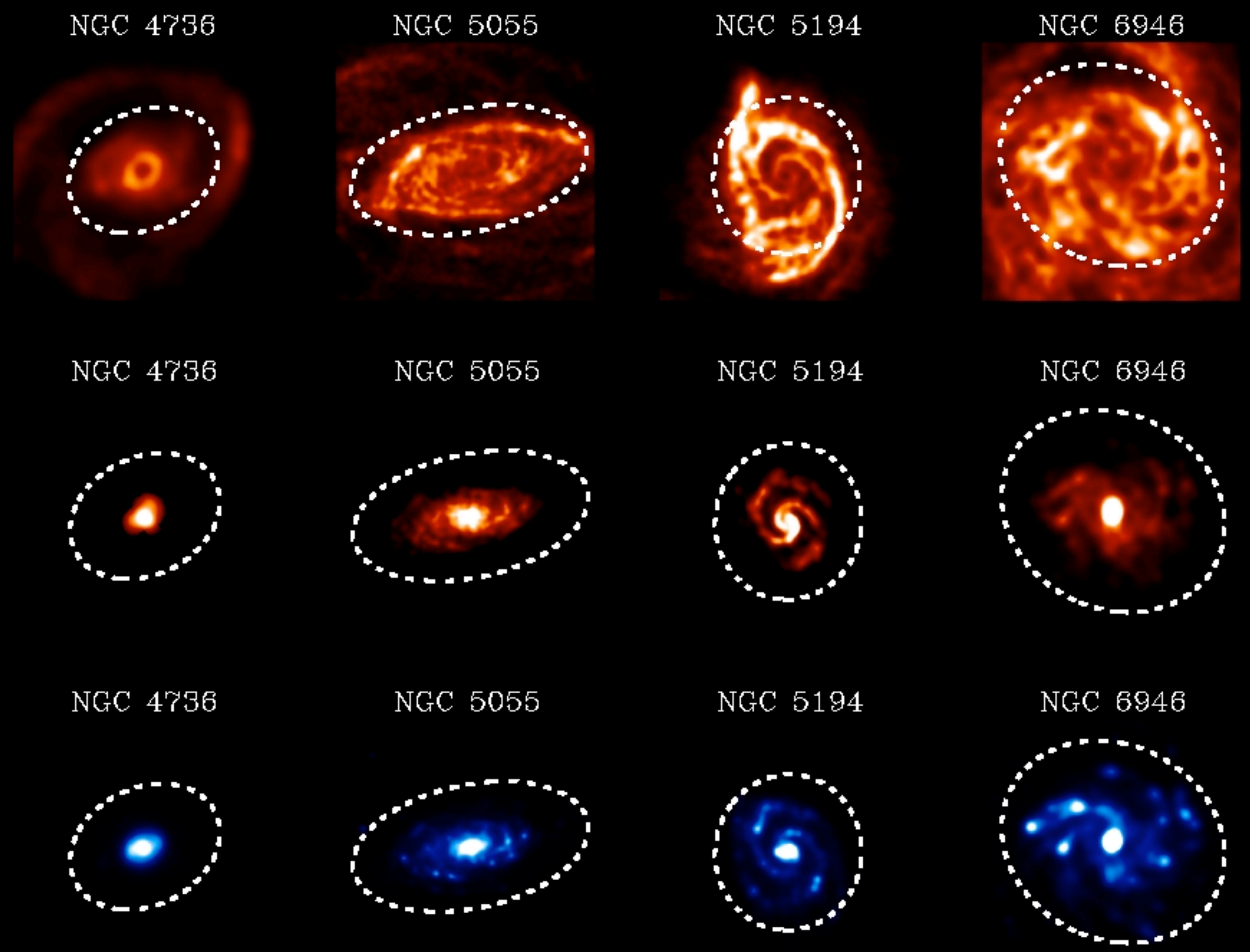

atomic hydrogen

molecular hydrogen

star formation

- HI gas more extended
- H2 and SF well correlated

galaxies from THINGS and HERACLES survey
(images from Frank Bigiel, ZAH/ITA)

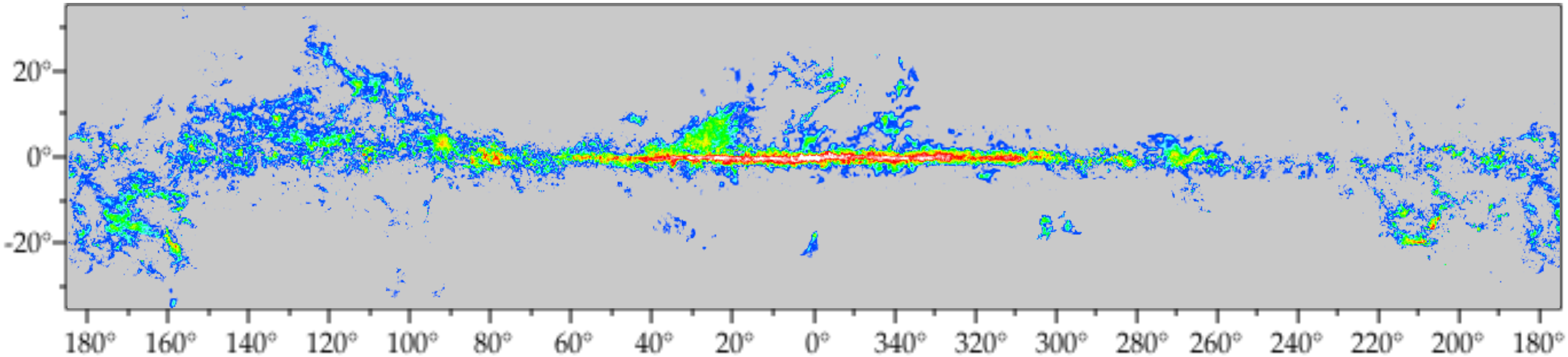

distribution of molecular gas in the Milky Way as traced by CO emission

data from T. Dame (CfA Harvard)

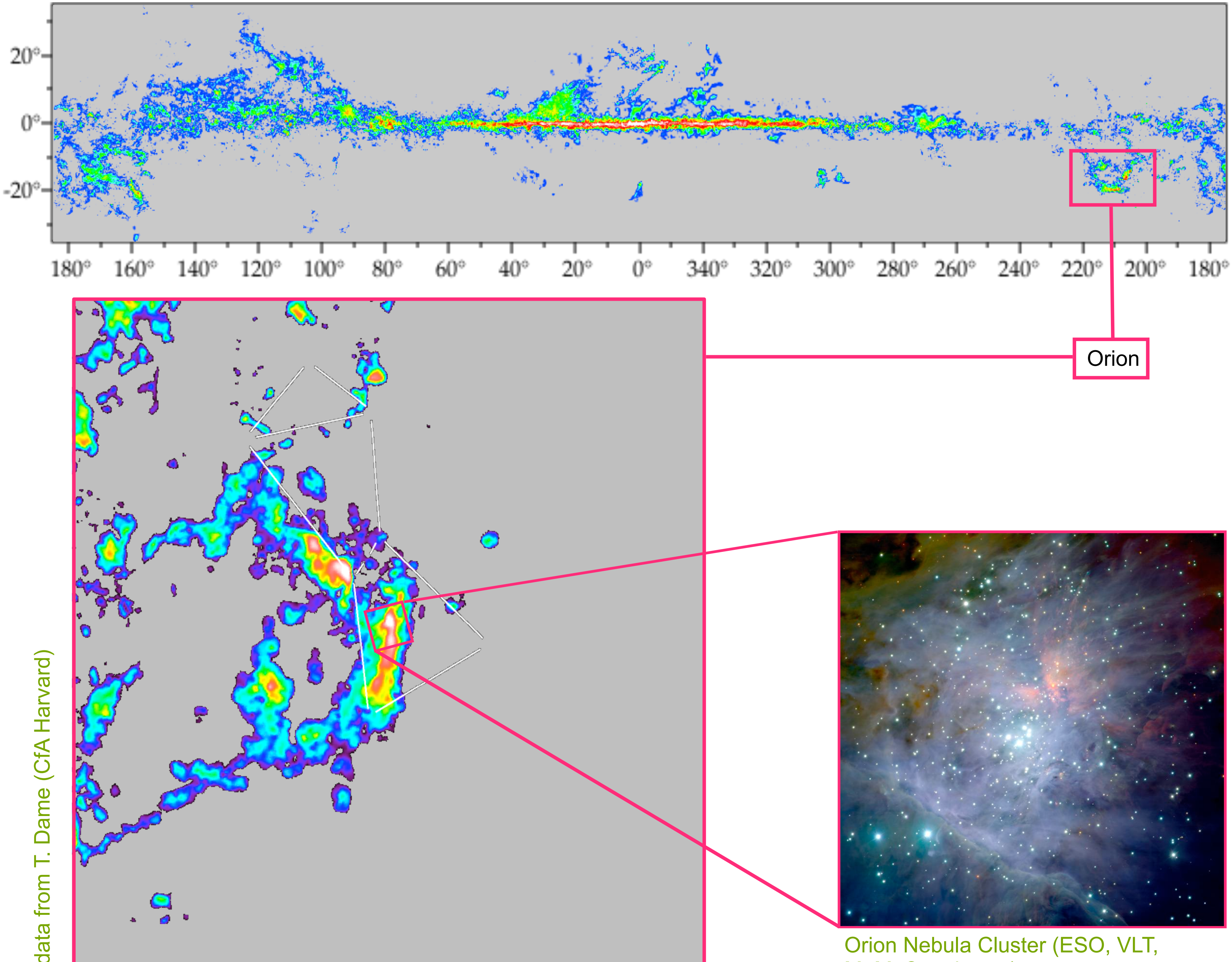

data from T. Dame (CfA Harvard)

Orion Nebula Cluster (ESO, VLT, M. McCaughrean)

Orion Nebula Cluster (ESO, VLT, M. McCaughrean)

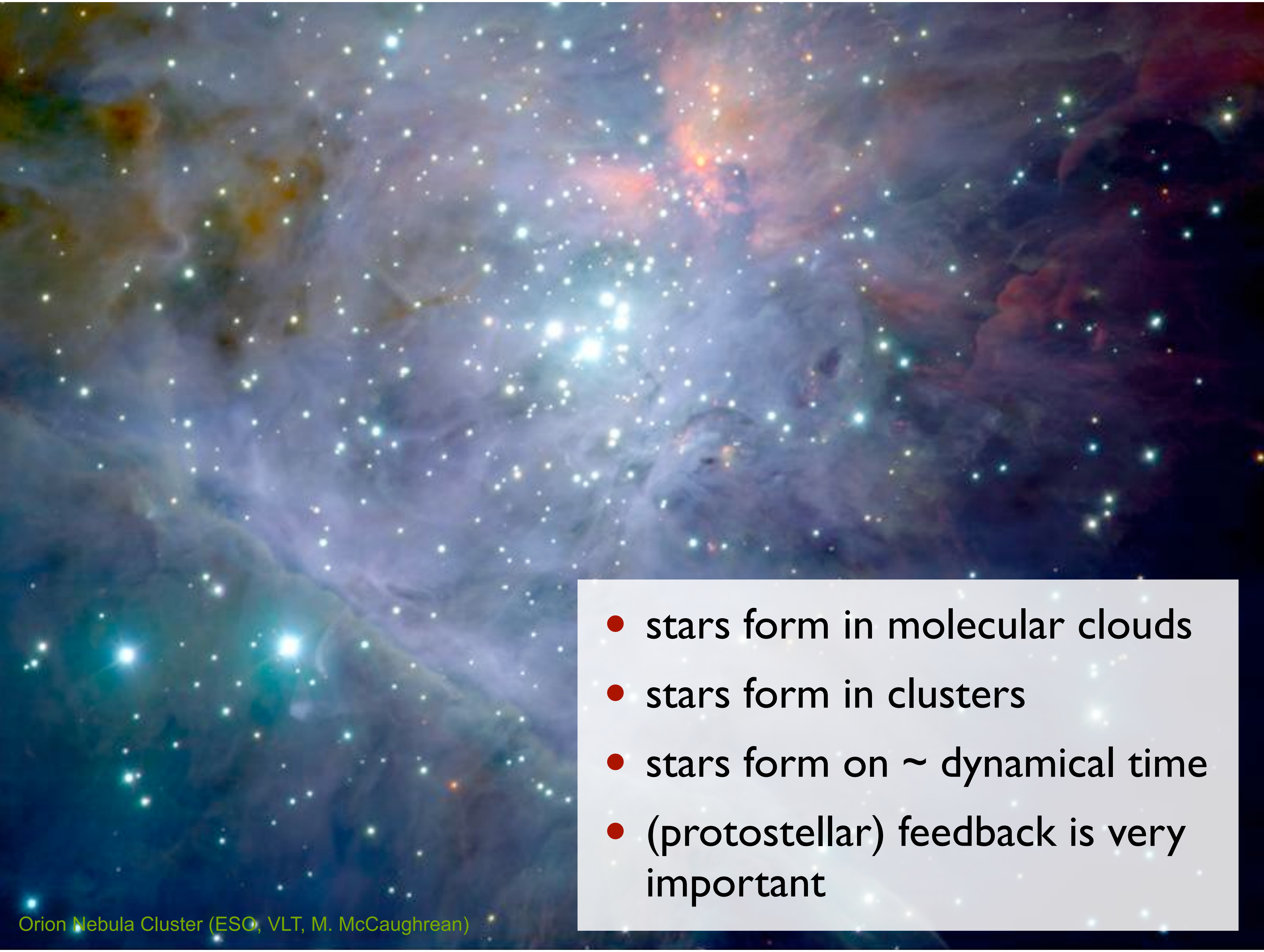

Orion Nebula Cluster (ESO, VLT, M. McCaughrean)

- stars form in molecular clouds
- stars form in clusters
- stars form on ~ dynamical time
- (protostellar) feedback is very important

Trapezium stars in the center of the ONC (HST, Johnstone et al. 1998)

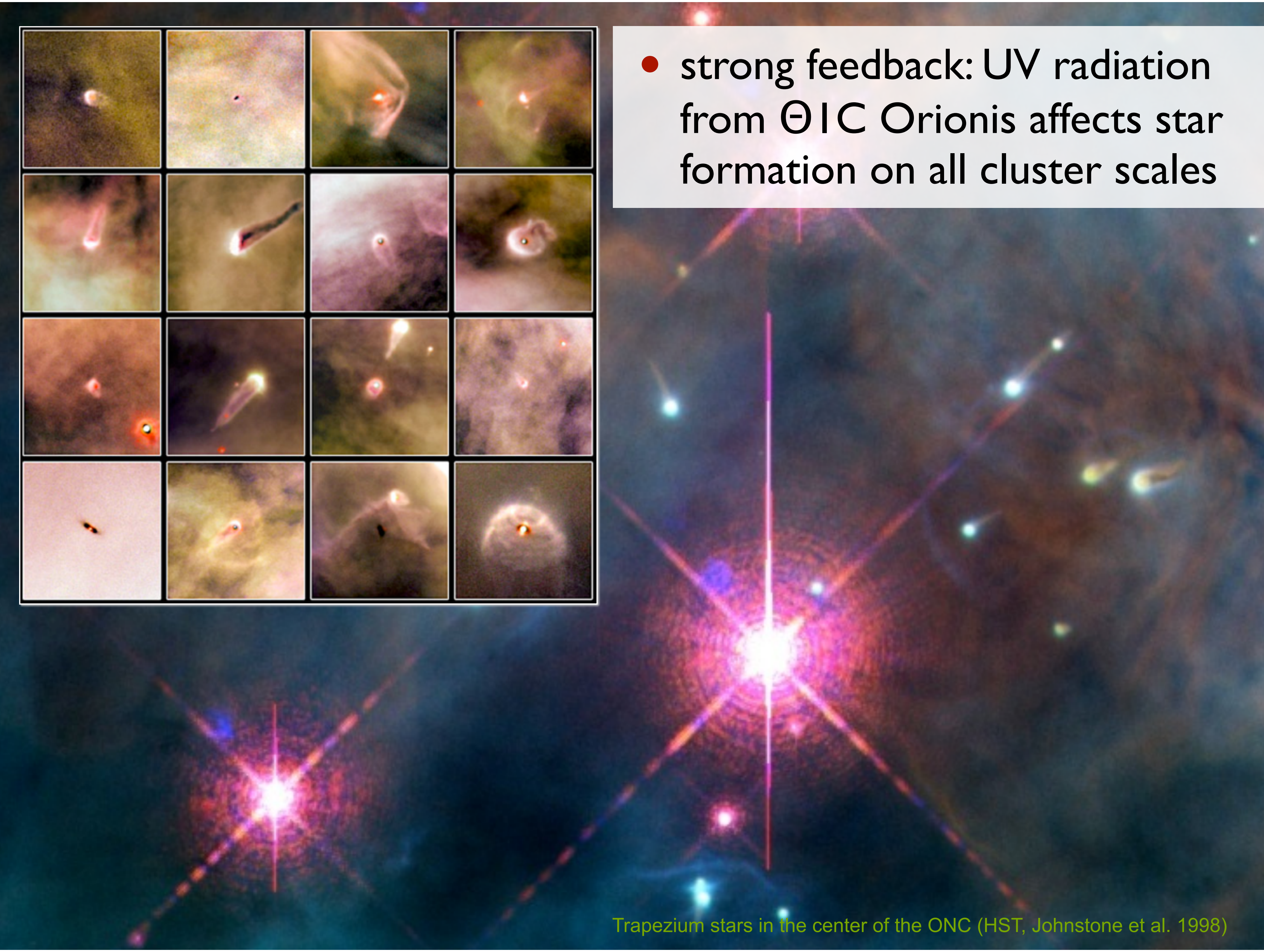

- strong feedback: UV radiation from Θ1C Orionis affects star formation on all cluster scales

Trapezium stars in the center of the ONC (HST, Johnstone et al. 1998)

Pleiades (DSS, Palomar Observatory Sky Survey) what is needed?

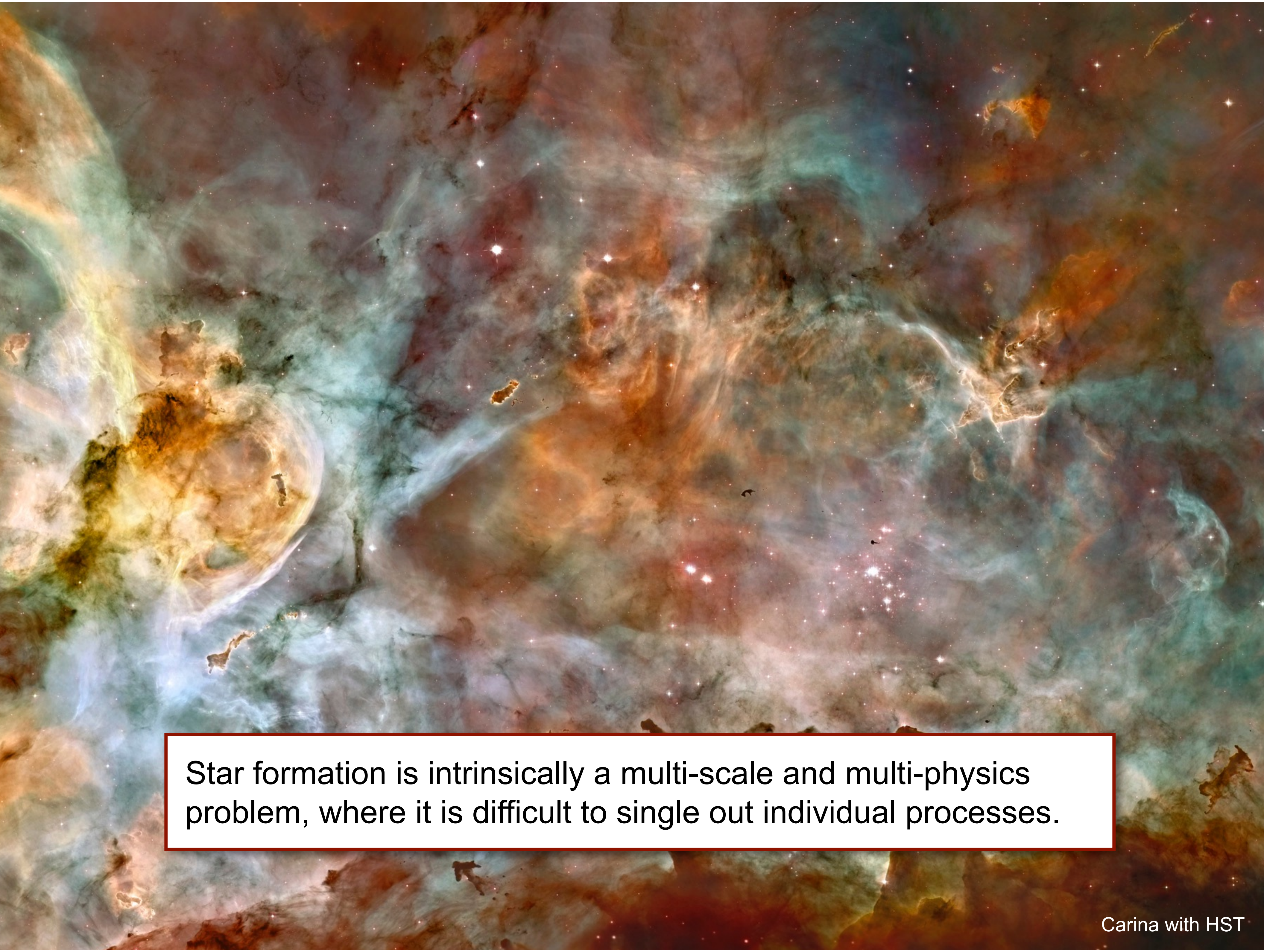

Star formation is intrinsically a multi-scale and multi-physics problem, where it is difficult to single out individual processes.

Carina with HST

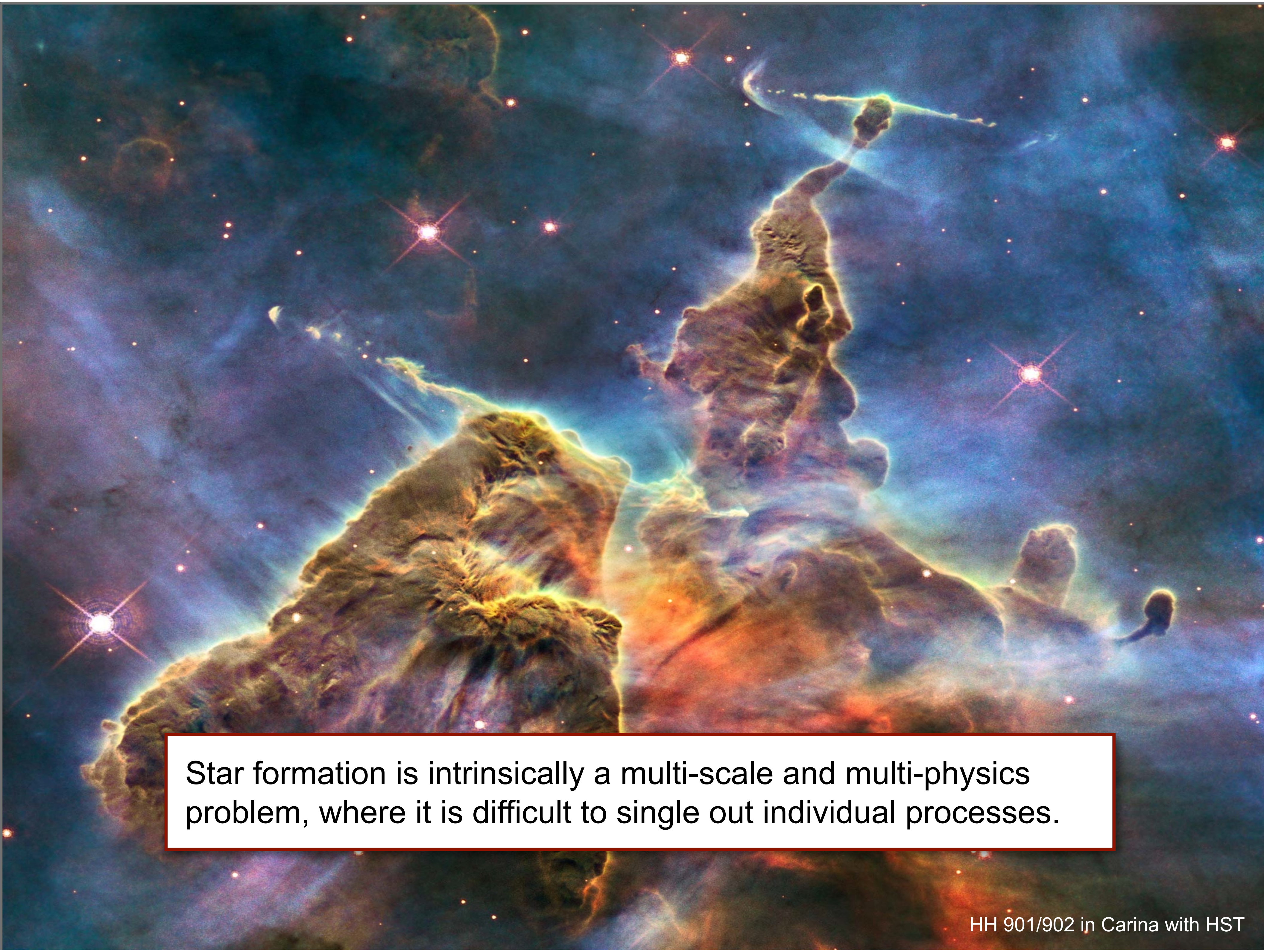

Star formation is intrinsically a multi-scale and multi-physics problem, where it is difficult to single out individual processes.

HH 901/902 in Carina with HST

examples

- large scales: Kennicutt-Schmidt type relations
  - how does star formation depend on galactic environment?
- intermediate scales: molecular cloud formation
  - how to connect ISM dynamics to galactic dynamics?
- small scales: filaments and star formation
  - what is the physical origin of the ISM?

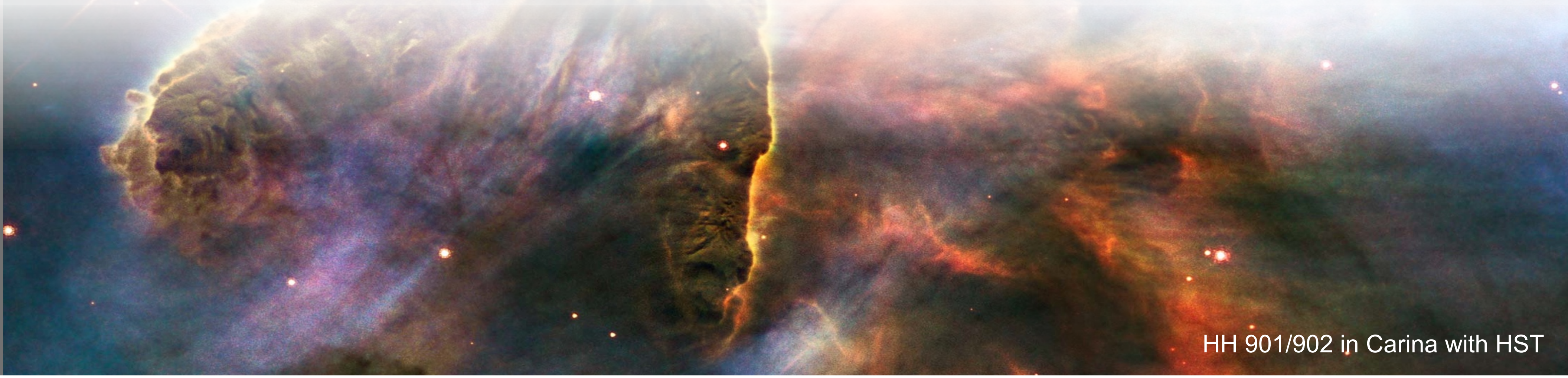

HH 901/902 in Carina with HST

global SF relations

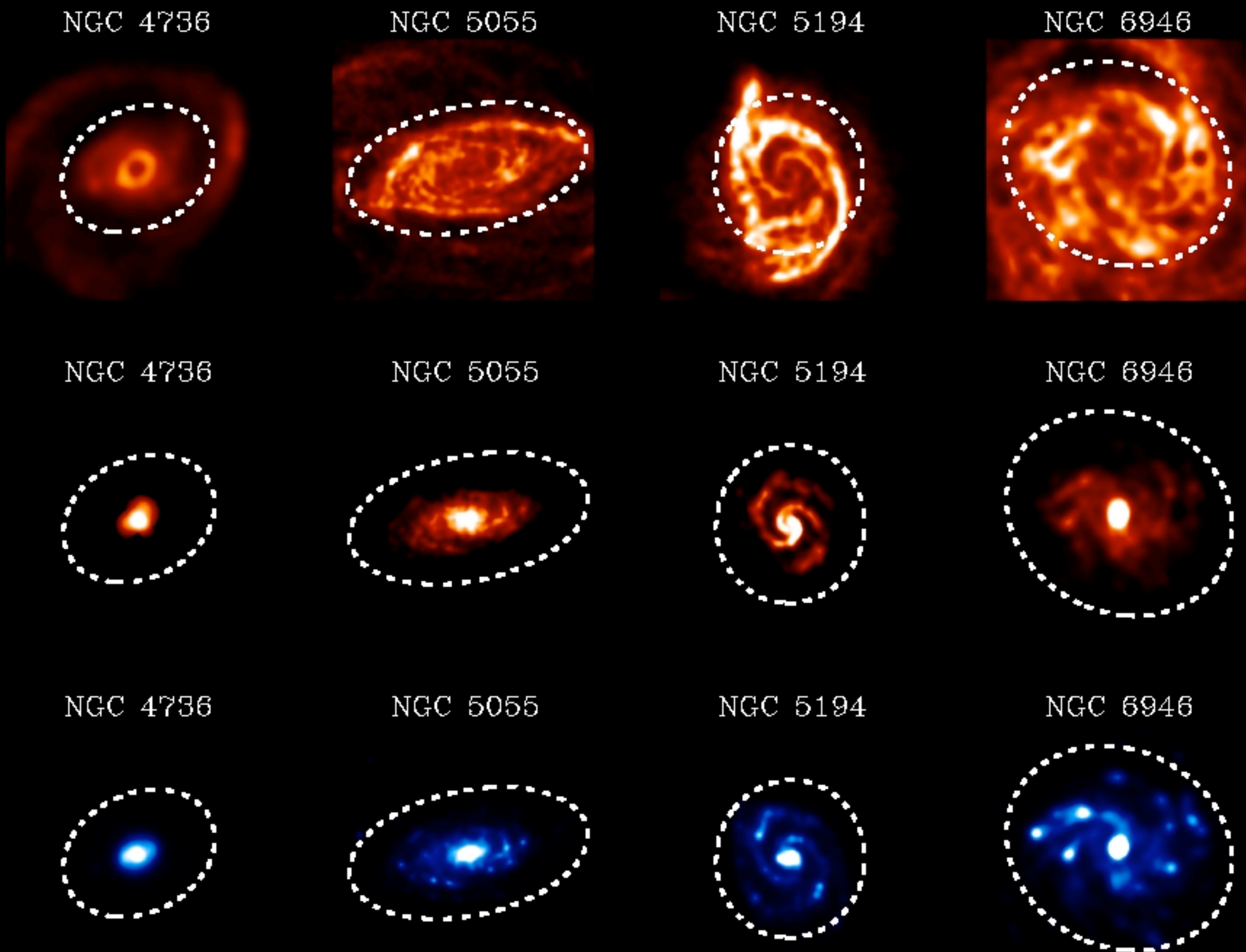

atomic hydrogen

molecular hydrogen

star formation

- HI gas more extended
- H2 and SF well correlated

galaxies from THINGS and HERACLES survey
(images from Frank Bigiel, ZAH/ITA)

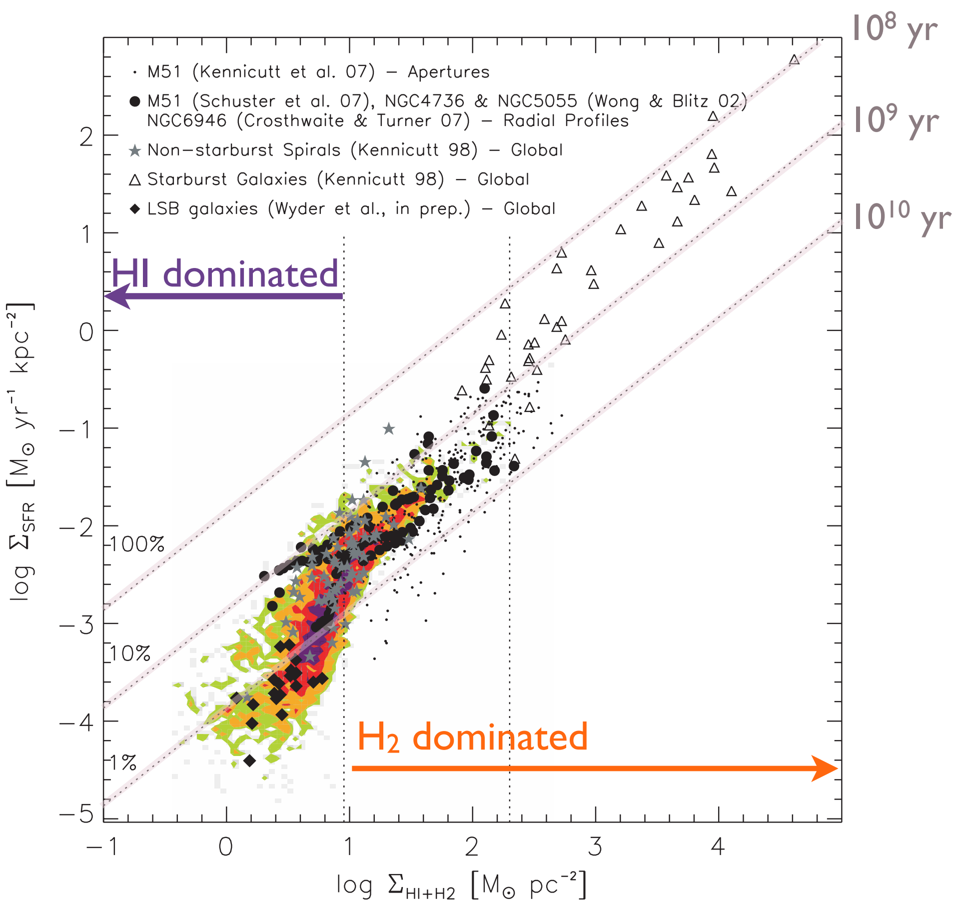

Bigiel et al. (2008, AJ, 136, 2846)

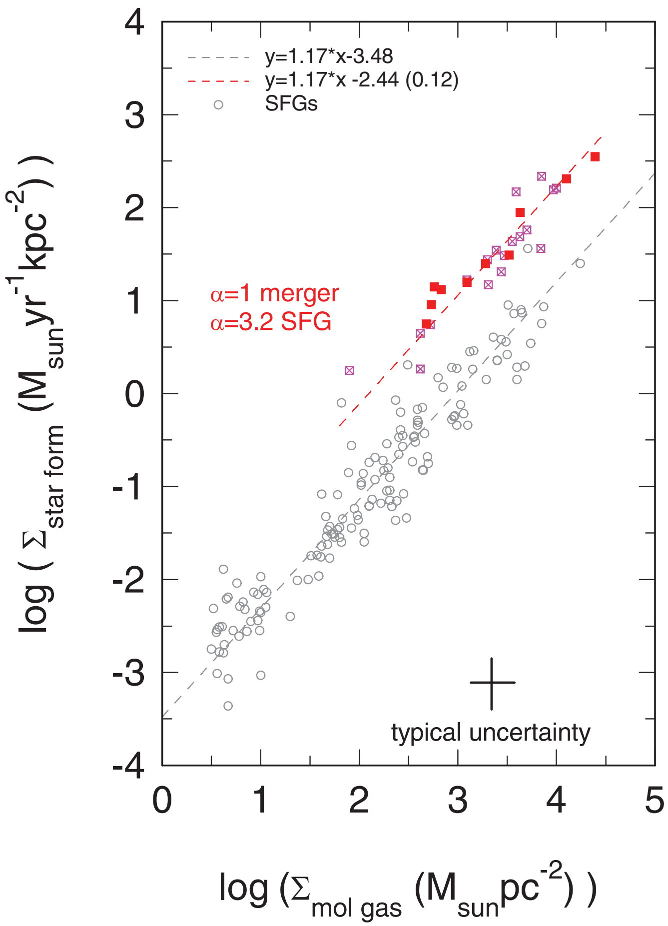

Genzel et al. (2010, MNRAS, AJ, 407, 2091)

- standard model: roughly linear relation between H
- standard model: roughly constant depletion time: few x 10
- super linear relation between total gas and SFR

data from STING survey (Rahman et al. 2011, 2012)

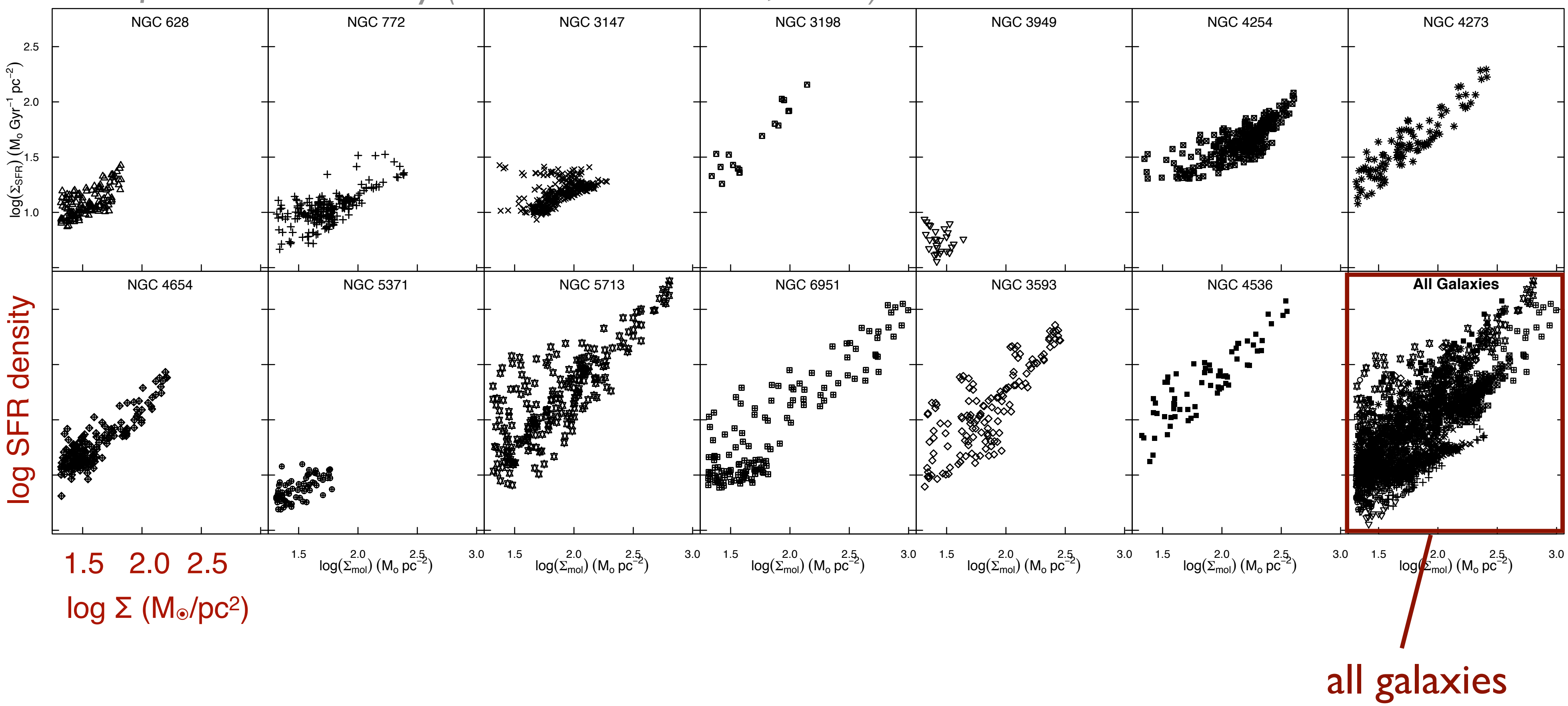

- QUIZ: do you see a universal

Shetty et al. (2014, MNRAS, 437, L61, see also Shetty, Kelly, Bigiel, 2013, MNRAS, 430, 288)

data from STING survey (Rahman et al. 2011, 2012)

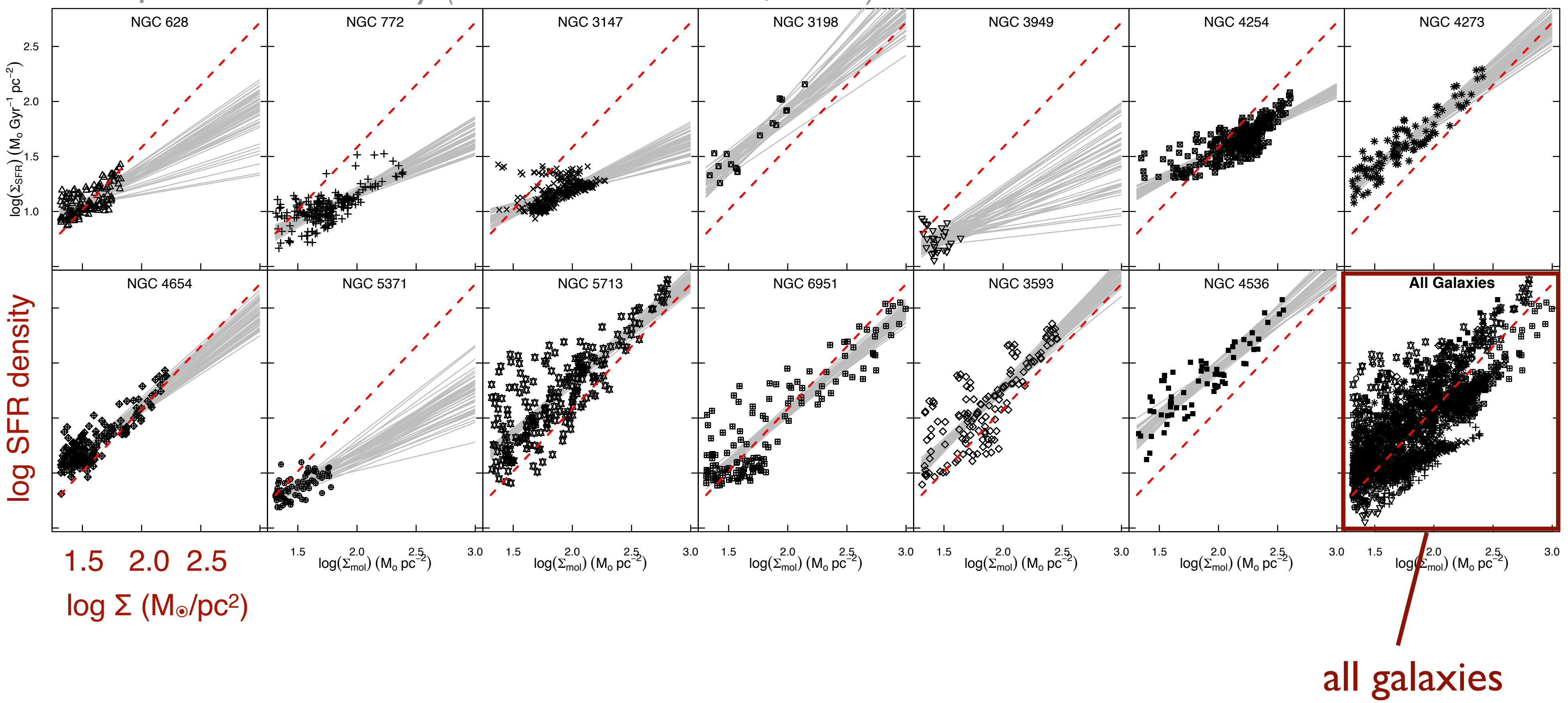

- QUIZ: do you see a universal
- ANSWER: - probably not
  - in addition, the relation often is sublinear

Shetty et al. (2014, MNRAS, 437, L61, see also Shetty, Kelly, Bigiel, 2013, MNRAS, 430, 288)

data from STING survey (Rahman et al. 2011, 2012)

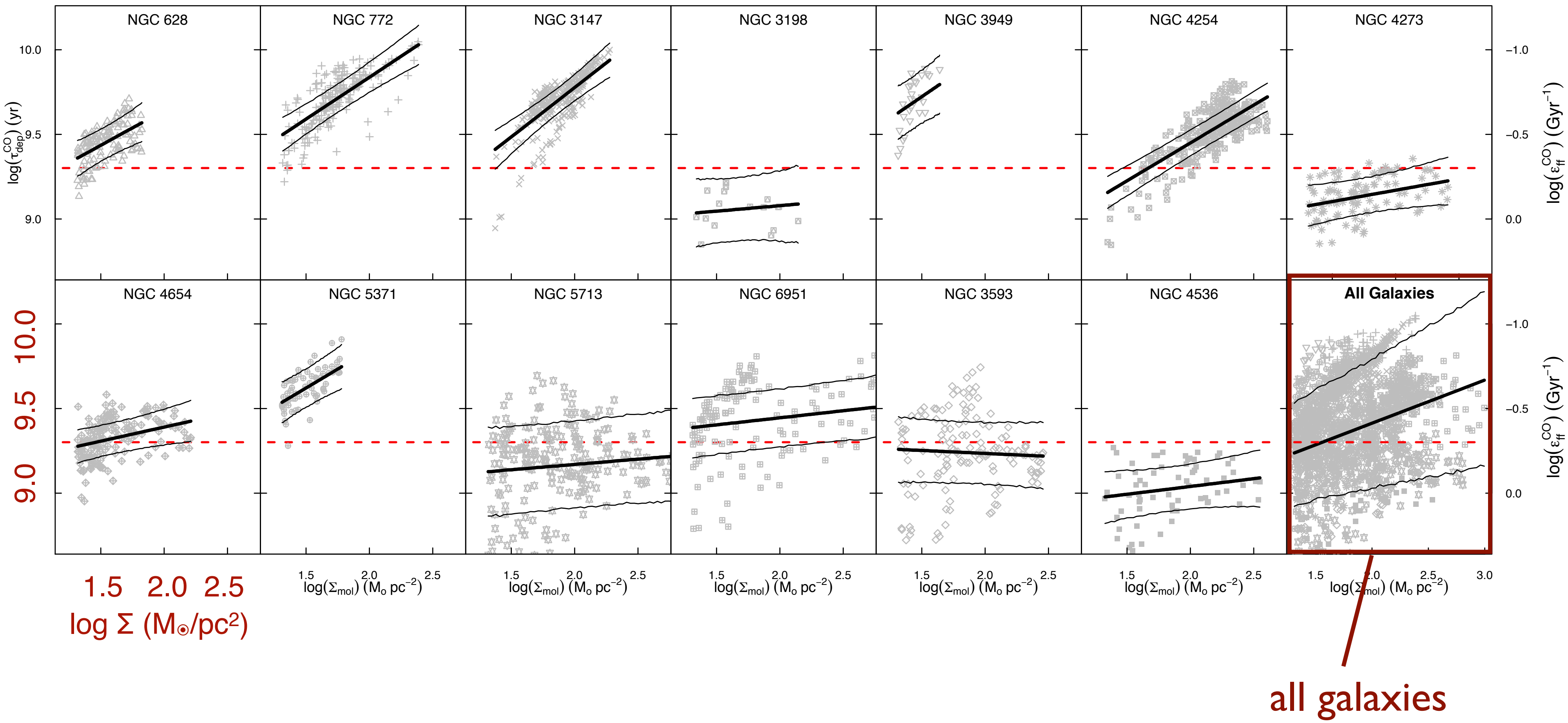

Hierarchical Bayesian model for STING galaxies indicate *varying depleting times.*

Shetty et al. (2014, MNRAS, 437, L61)

data from STING survey (Rahman et al. 2011, 2012)

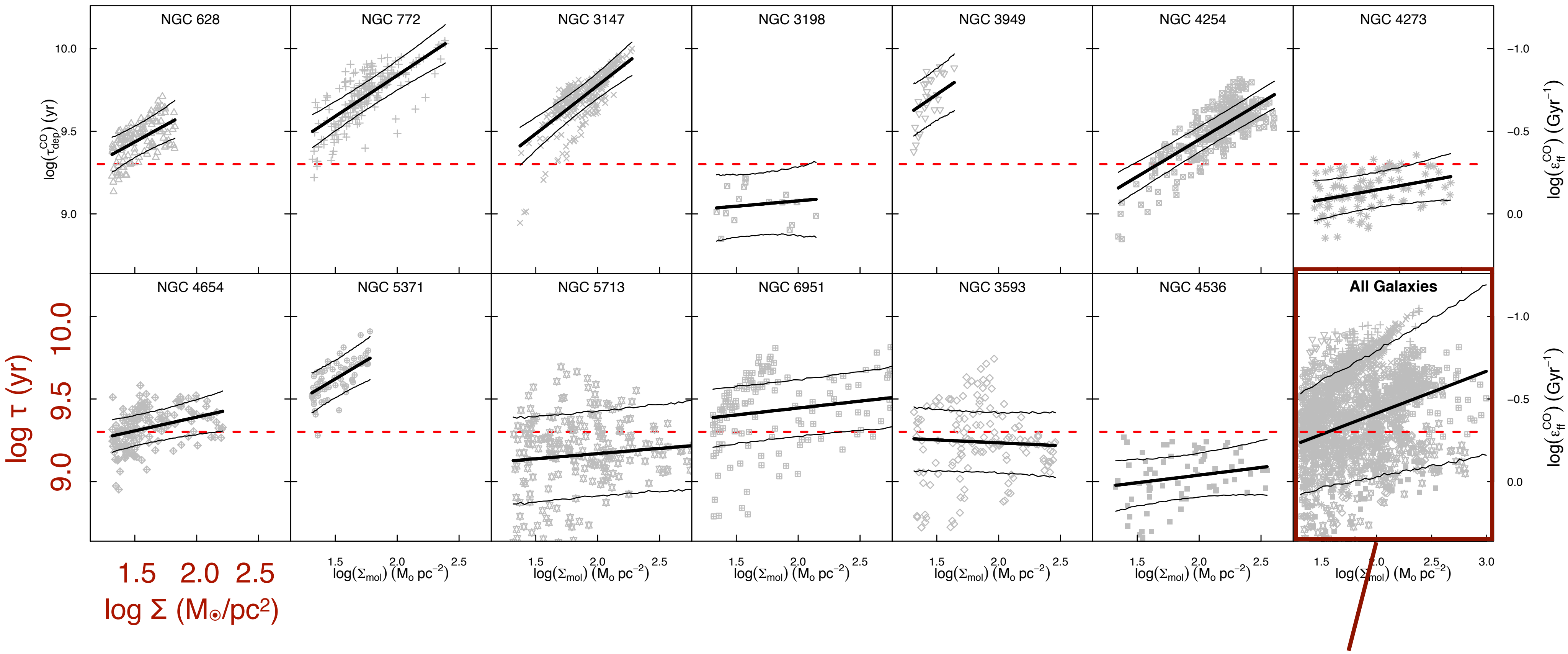

physical origin of this behavior?

- maybe strong shear in dense arms (example M51, Meidt et al. 2013)...
- maybe non-star forming H column densities (recall H

Shetty et al. (2013, MNRAS, 437, L61, see also Shetty, Kelly, Bigiel, 2013, MNRAS, 430, 288)

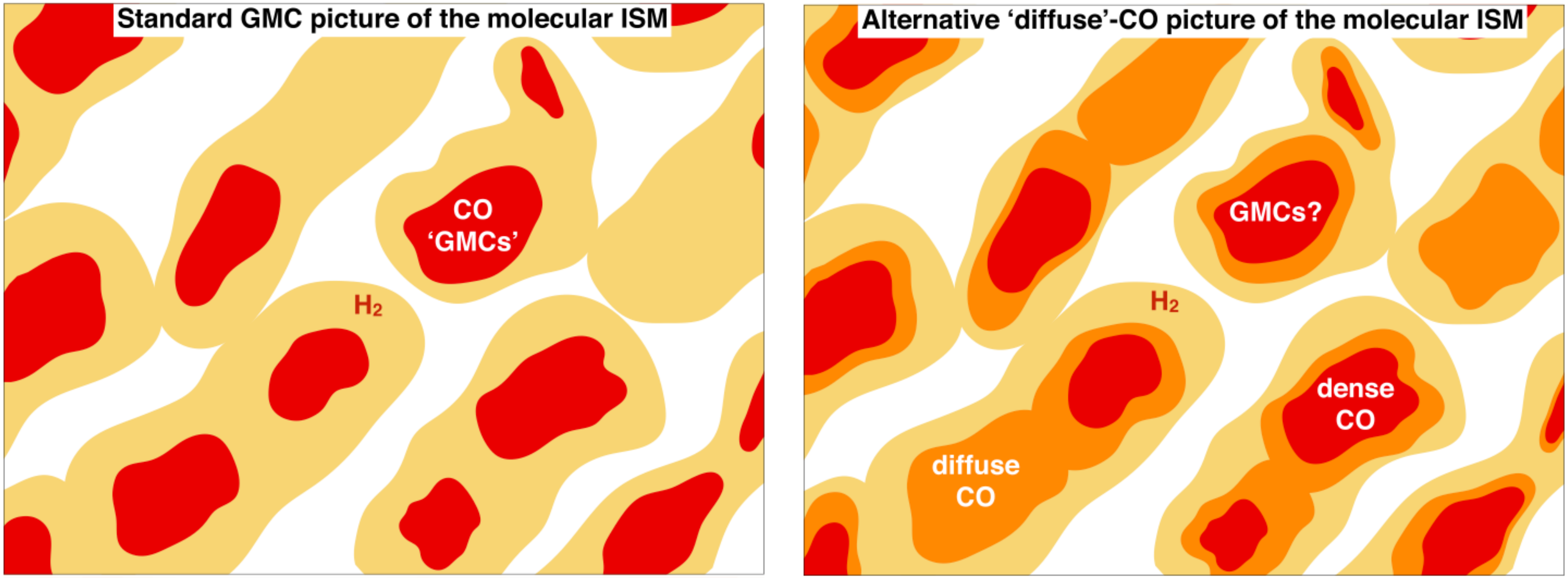

physical origin of this behavior?

- maybe strong shear in dense arms (example M51, Meidt et al. 2013)...
- maybe non-star forming H
  column densities (recall H

Shetty et al. (2014, MNRAS in press, arXiv:1404.5964) molecular cloud formation

molecular cloud formation

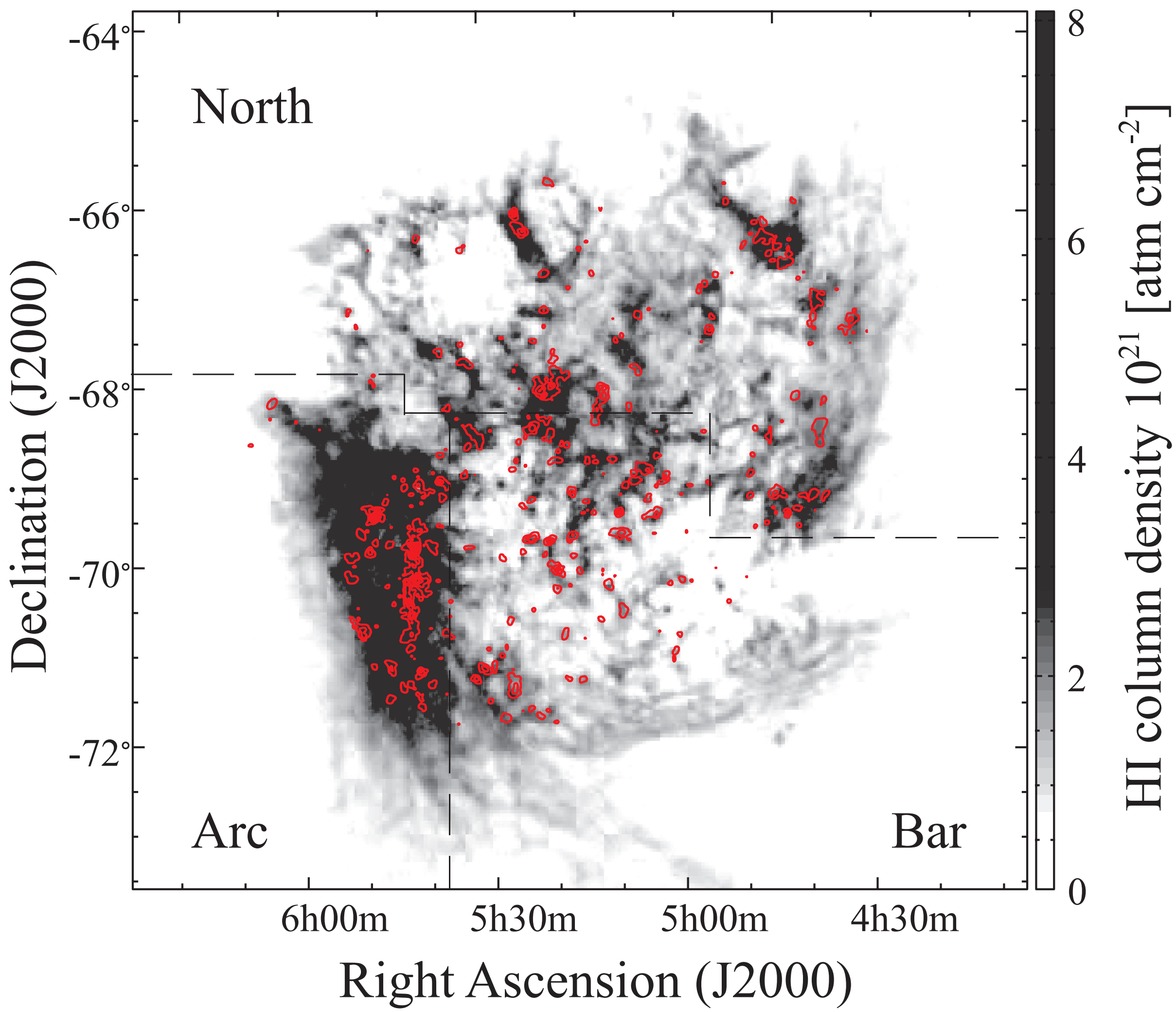

Idea:

Molecular clouds form at *stagnation points* of large-scale convergent flows, mostly triggered by global (or external) perturbations. Their internal turbulence is driven by accretion, i.e. by the process of cloud formation

- molecular clouds grow in mass
- this is inferred by looking at molecular clouds in different evolutionary phases in the LMC (Fukui et al. 2008, 2009)

Fukui et al. (2009)

correlation with large-scale perturbations

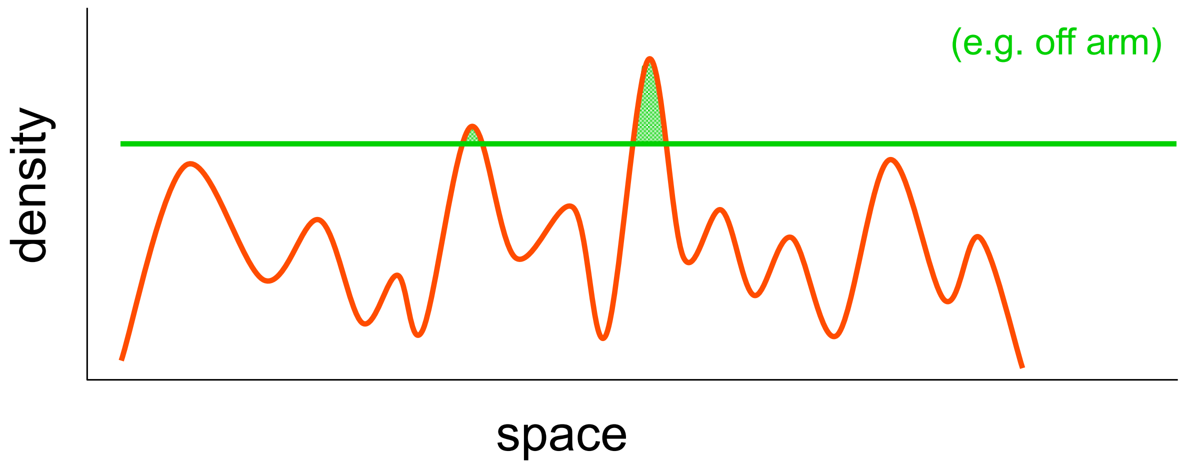

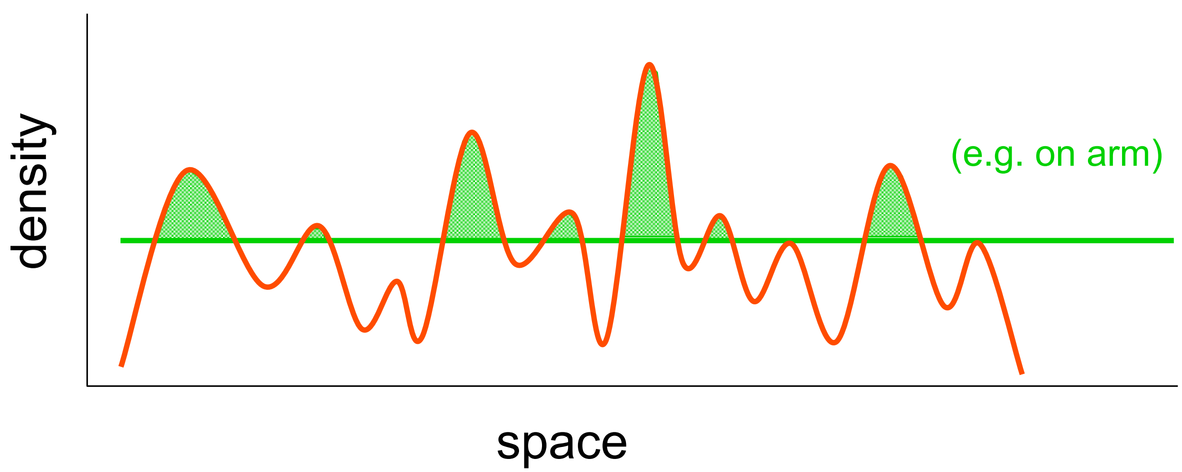

density/temperature fluctuations in warm atomar ISM are caused by *thermal/ gravitational instability* and/ or *supersonic turbulence*

some fluctuations are *dense* enough to *form H_2* within "*reasonable time*"
→ *molecular cloud*

external perturbuations (i.e. potential changes) *increase* likelihood

star formation on *global* scales

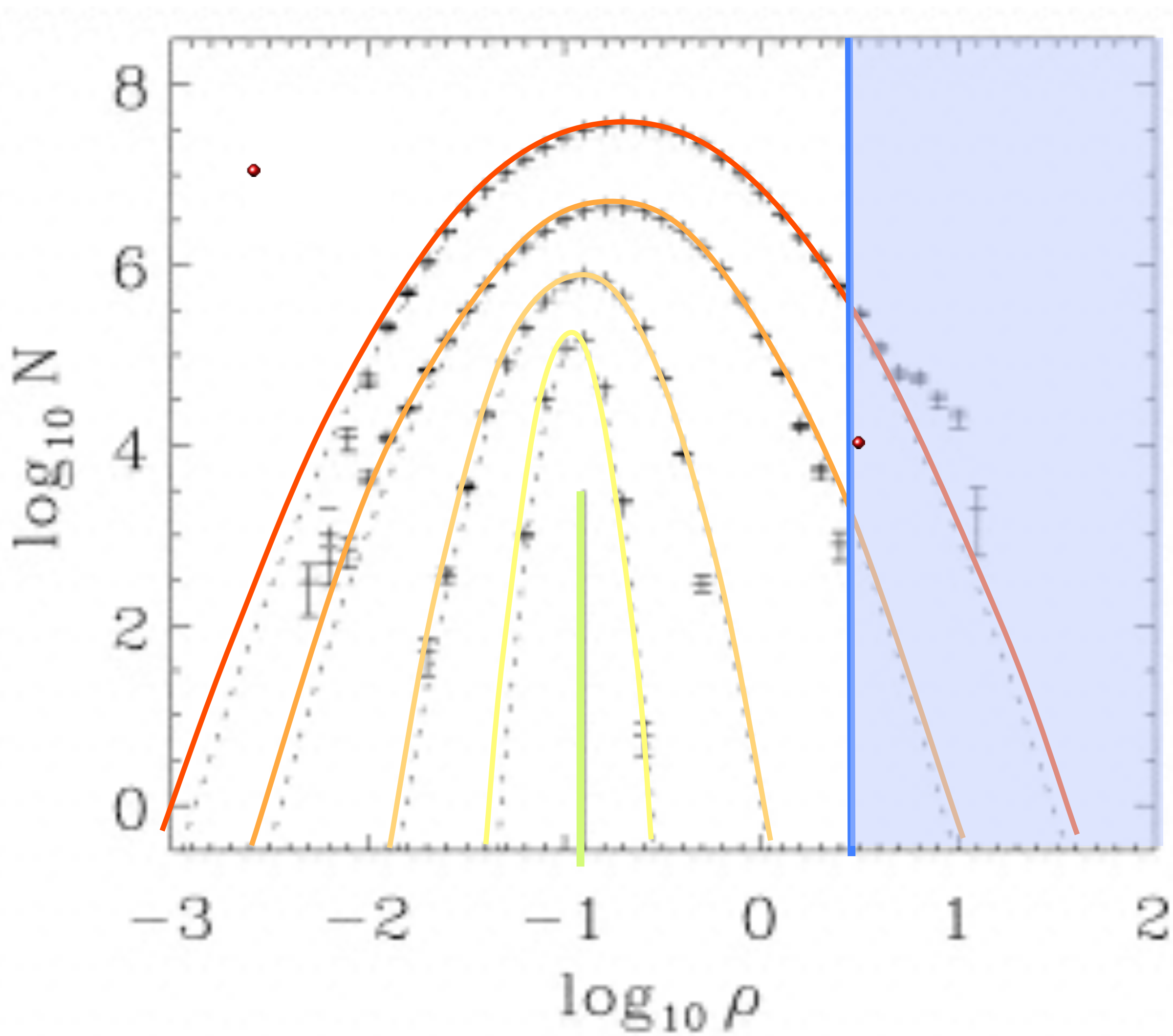

mass weighted ρ-pdf, each shifted by ΔlogN=1

(rate from Hollenback, Werner, & Salpeter 1971)

H_2 formation rate:

$$\boxed{\tau_{H_2} \approx \frac{1.5\,\mathrm{Gyr}}{n_H / 1\mathrm{cm}^{-3}}}$$

for $n_H \geq 100$ cm^{-3}, H_2 forms within 10 Myr, this is about the lifetime of typical MC's.

in turbulent gas, the H_2 fraction can become very high on short timescale

(for models with coupling between cloud dynamics and time-dependent chemistry, see Glover & Mac Low 2007a,b)

star formation on *global* scales

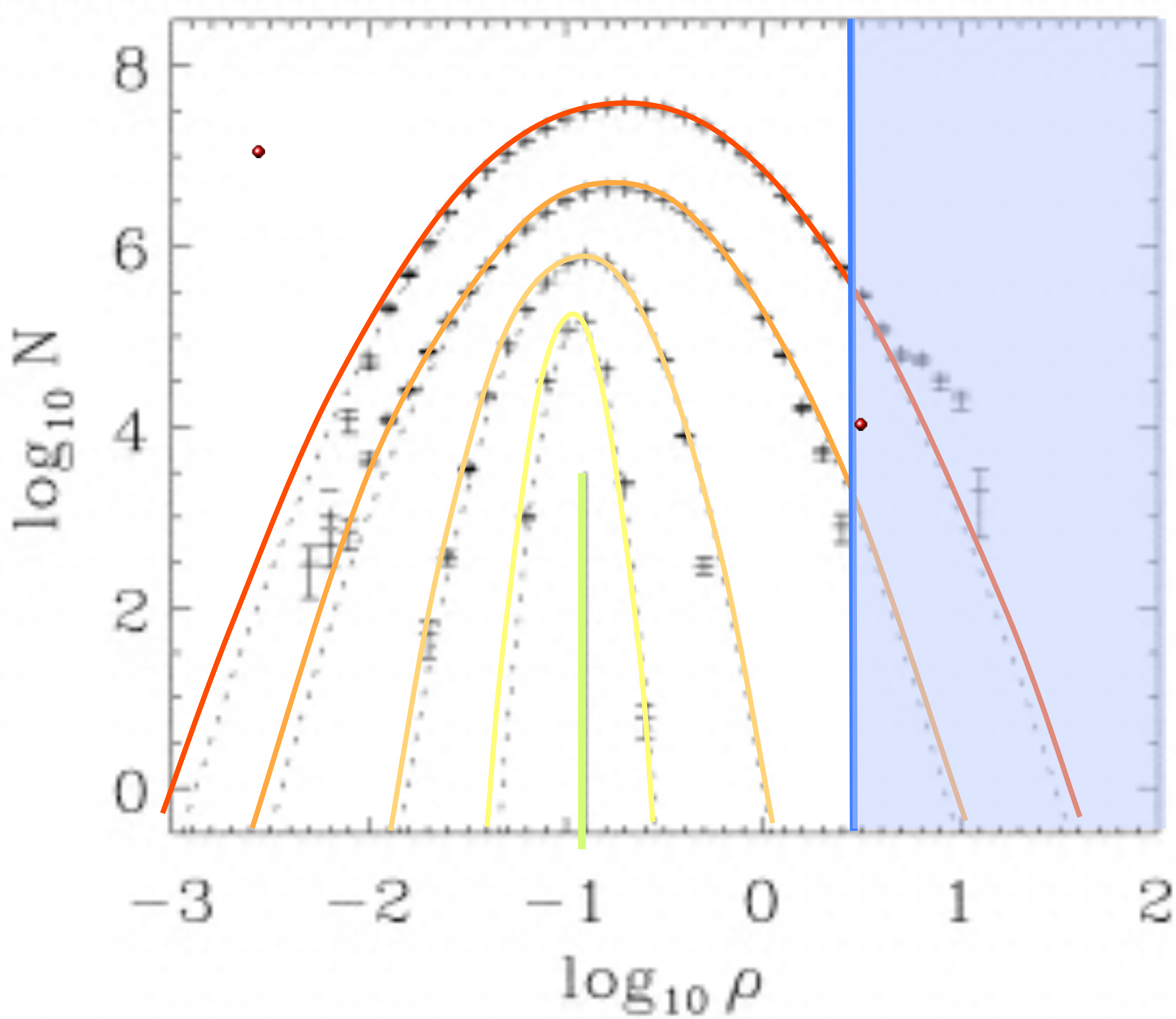

mass weighted ρ-pdf, each shifted by $\Delta \log N=1$

(rate from Hollenback, Werner, & Salpeter 1971)

BUT: *it doesn't work* (at least not so easy):

Chemistry has a memory effect!

H2 forms more quickly in high-density regions as it gets destroyed in low-density parts.

(for models with coupling between cloud dynamics and time-dependent chemistry, see Glover & Mac Low 2007a,b)

molecular cloud formation

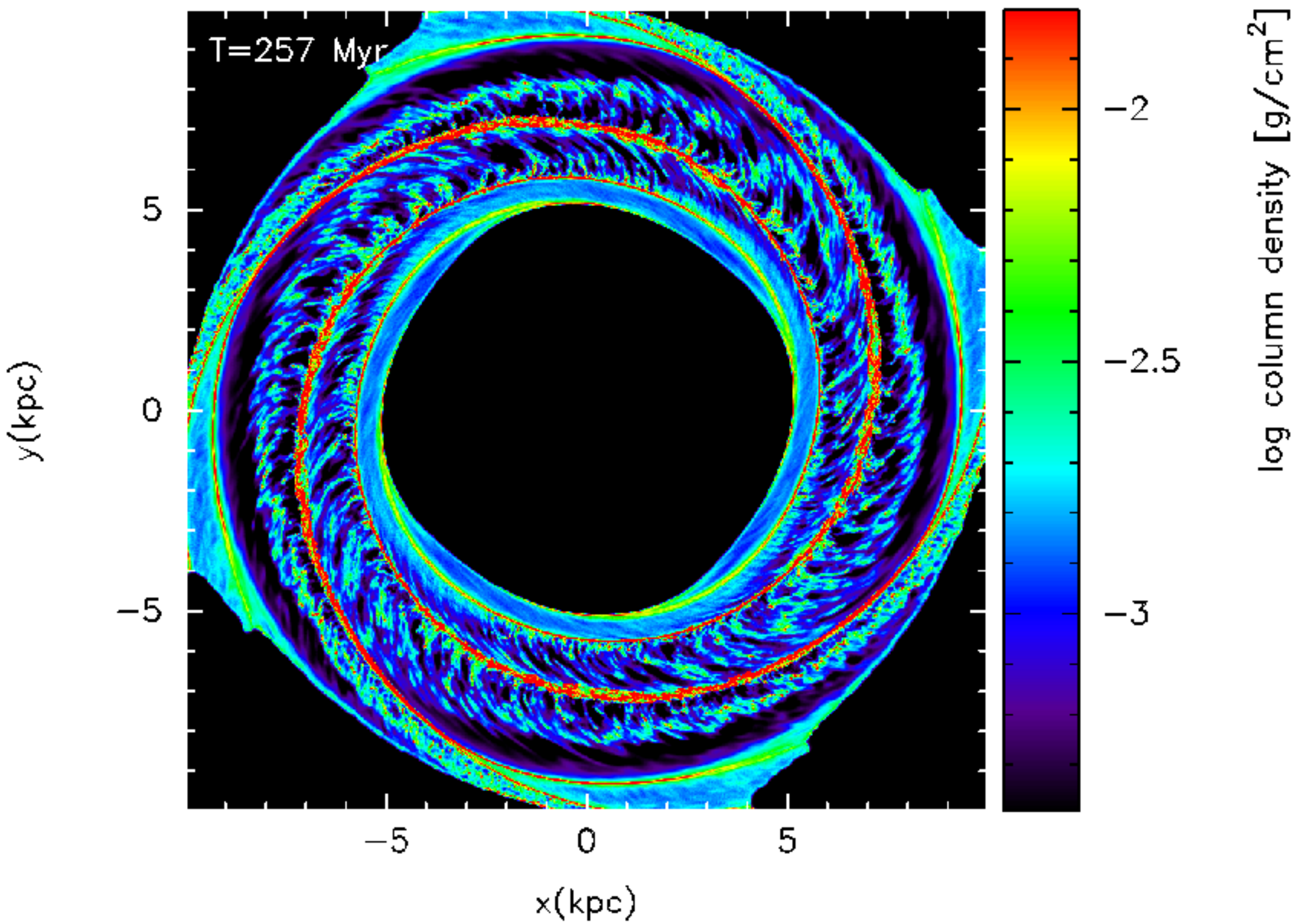

(from Dobbs et al. 2008)

molecular cloud formation

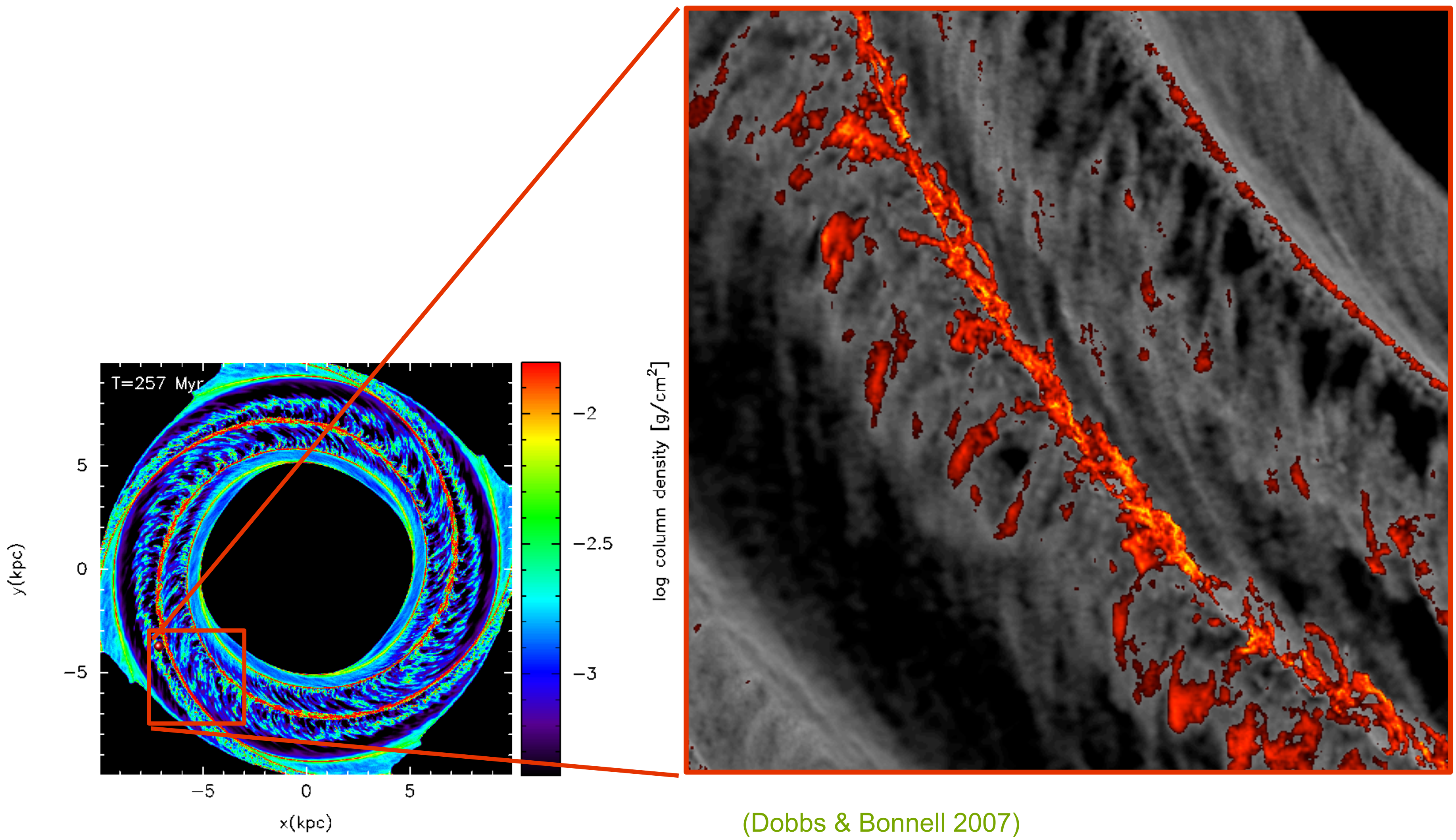

(Dobbs & Bonnell 2007)

molecular cloud formation

molecular gas fraction of fluid element as function of time

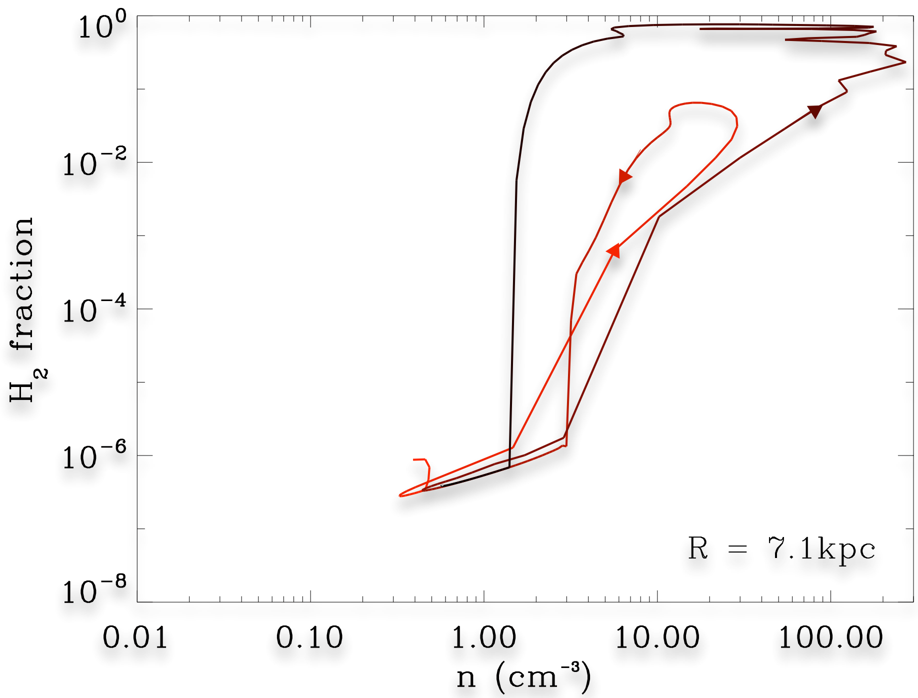

molecular gas fraction as function of density

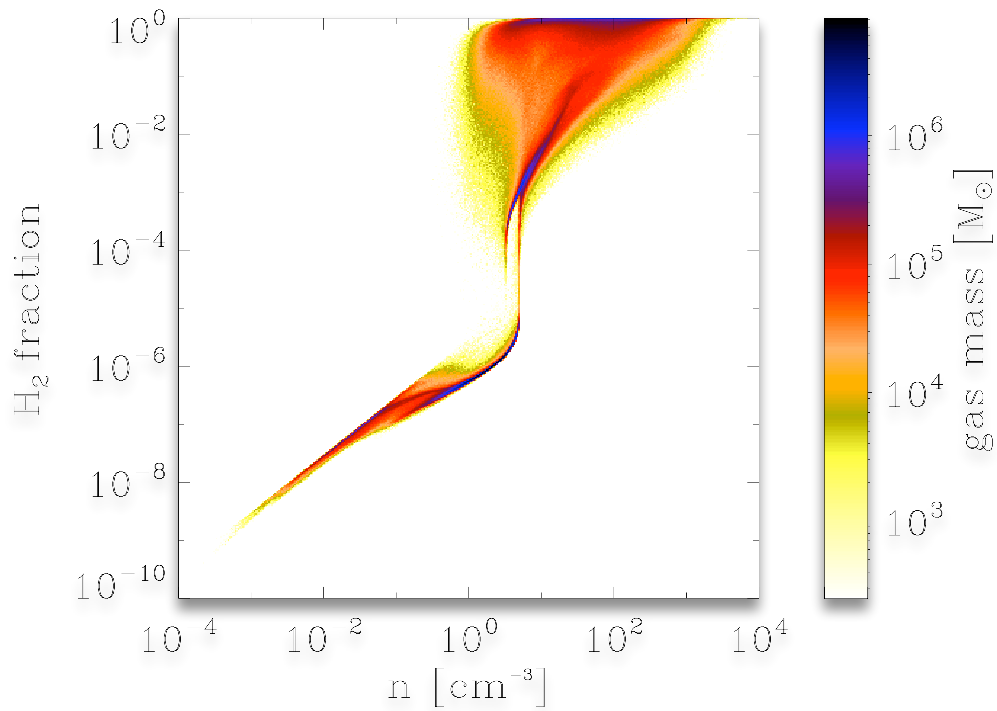

(Dobbs et al. 2008)

zooming in ...

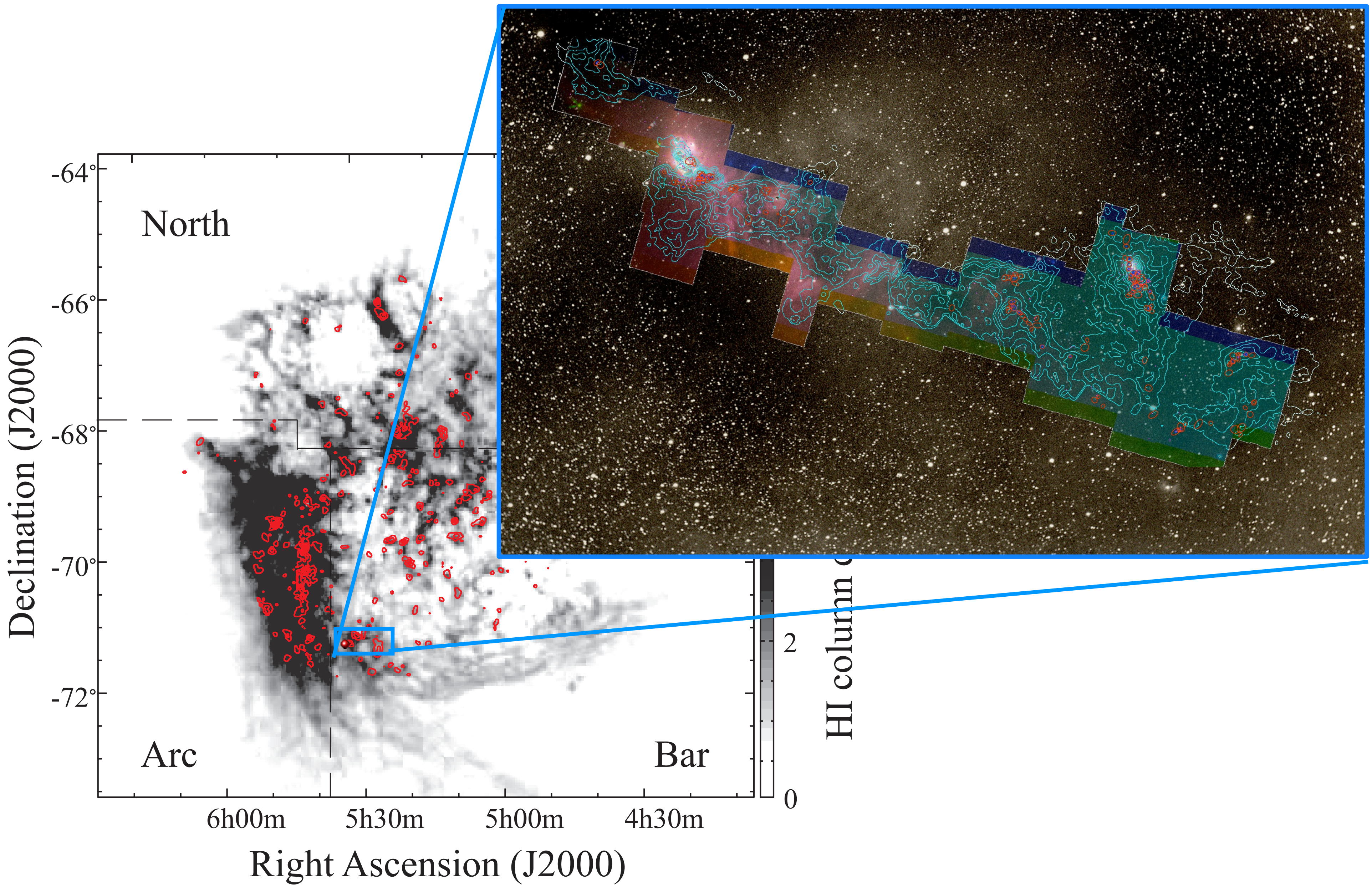

North
Arc
Bar
-64°
-66°
-68°
-70°
-72°
Declination (J2000)
6h00m
5h30m
5h00m
4h30m
Right Ascension (J2000)
2
0
HI column

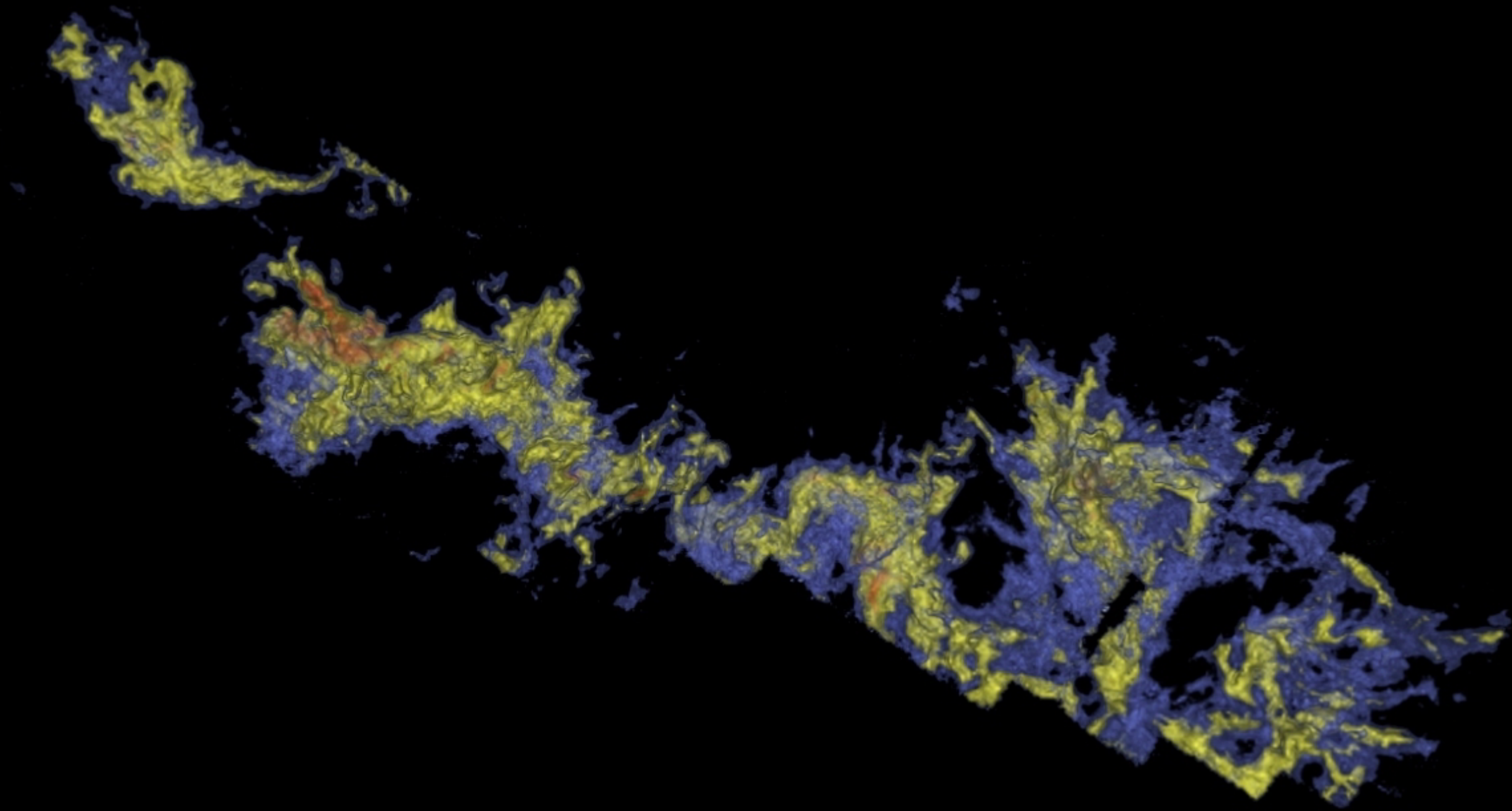

image from Alyssa Goodman: COMPLETE survey

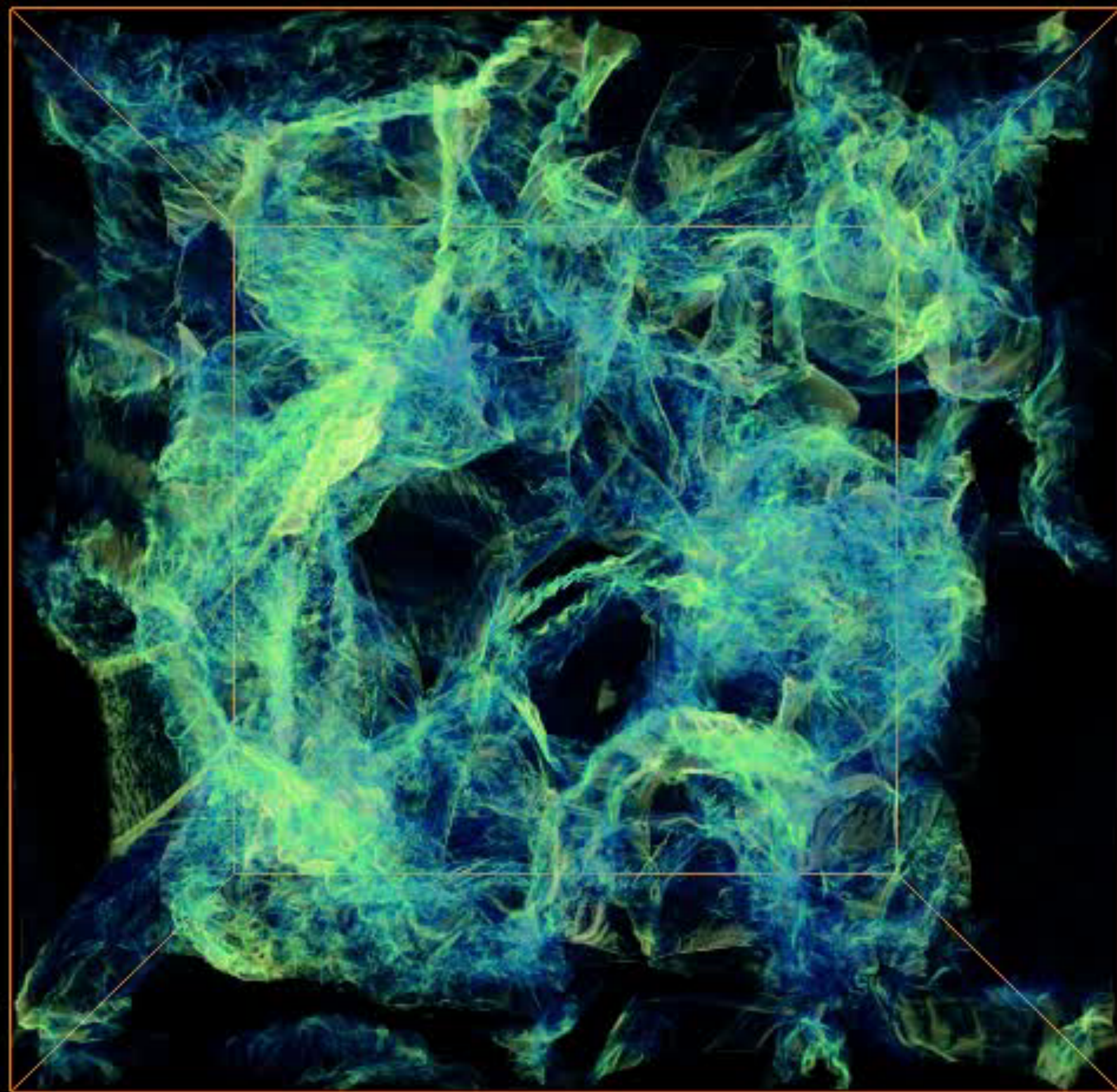

(movie from Christoph Federrath, see his talk tomorrow)

Large-eddy simulations

- We use ***LES*** to model the large-scale dynamics
- Principal problem: only large scale flow properties
  - Reynolds number: Re = LV/ν ***(Re$_{nature}$ >> Re$_{model}$)***
  - dynamic range much smaller than true physical one
  - need *subgrid model* (in our case simple: only dissipation)
  - but what to do for more complex when processes on subgrid scale determine large-scale dynamics (chemical reactions, nuclear burning, etc)
  - Turbulence is "space filling" --> difficulty for AMR (don't know what criterion to use for refinement)
- How *large* a Reynolds number do we need to catch basic dynamics right?

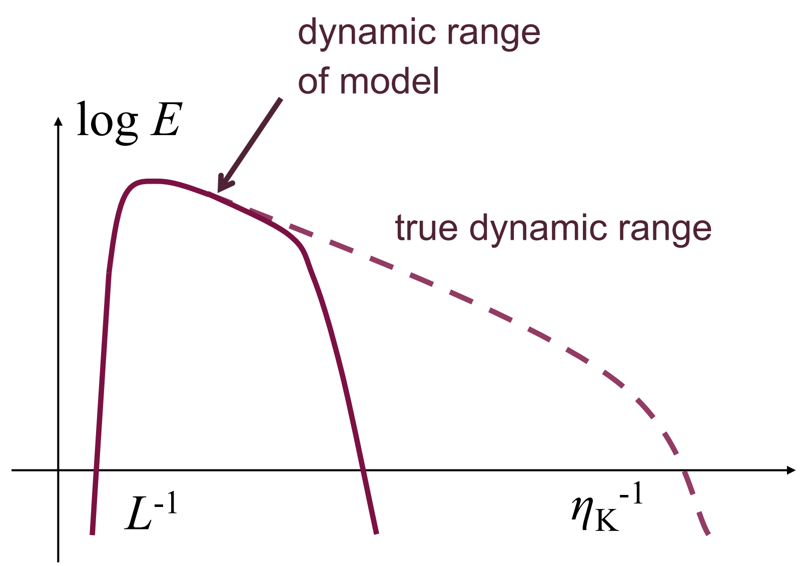

including detailed
chemistry

experimental set-up

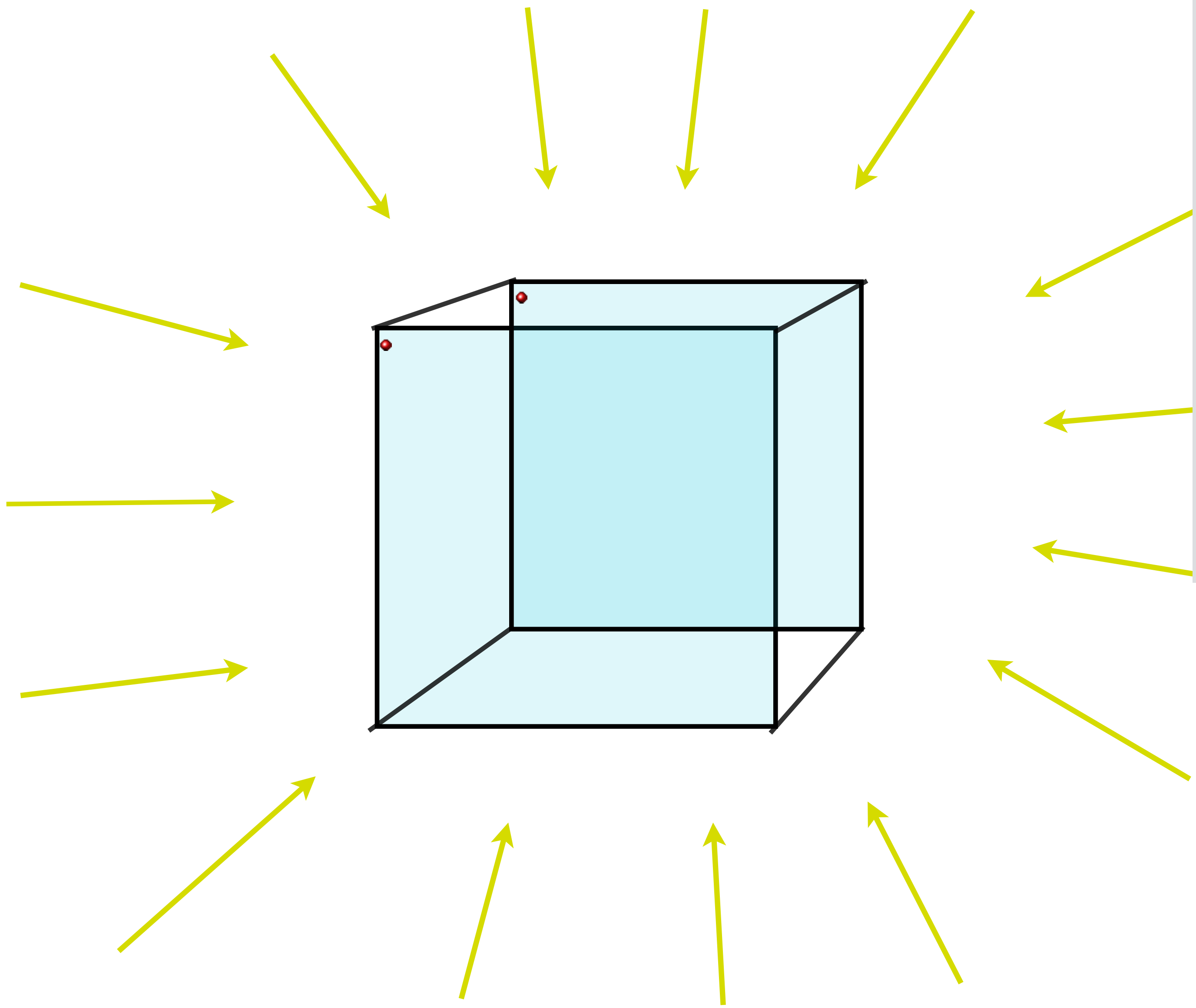

- Arepo and FLASH
- stochastic forcing (Ornstein-Uhlenbeck)
- self-gravity
- time-dependent chemistry (DVODE, standard variable-coefficient ordinary differential equation solver)
- cooling & heating processes
- gives you mathematically well defined boundary conditions
  --> good for statistical studies

external radiation with TreeCol (a new approximative scheme to calculate column densities from the gravity solver)

TreeCol

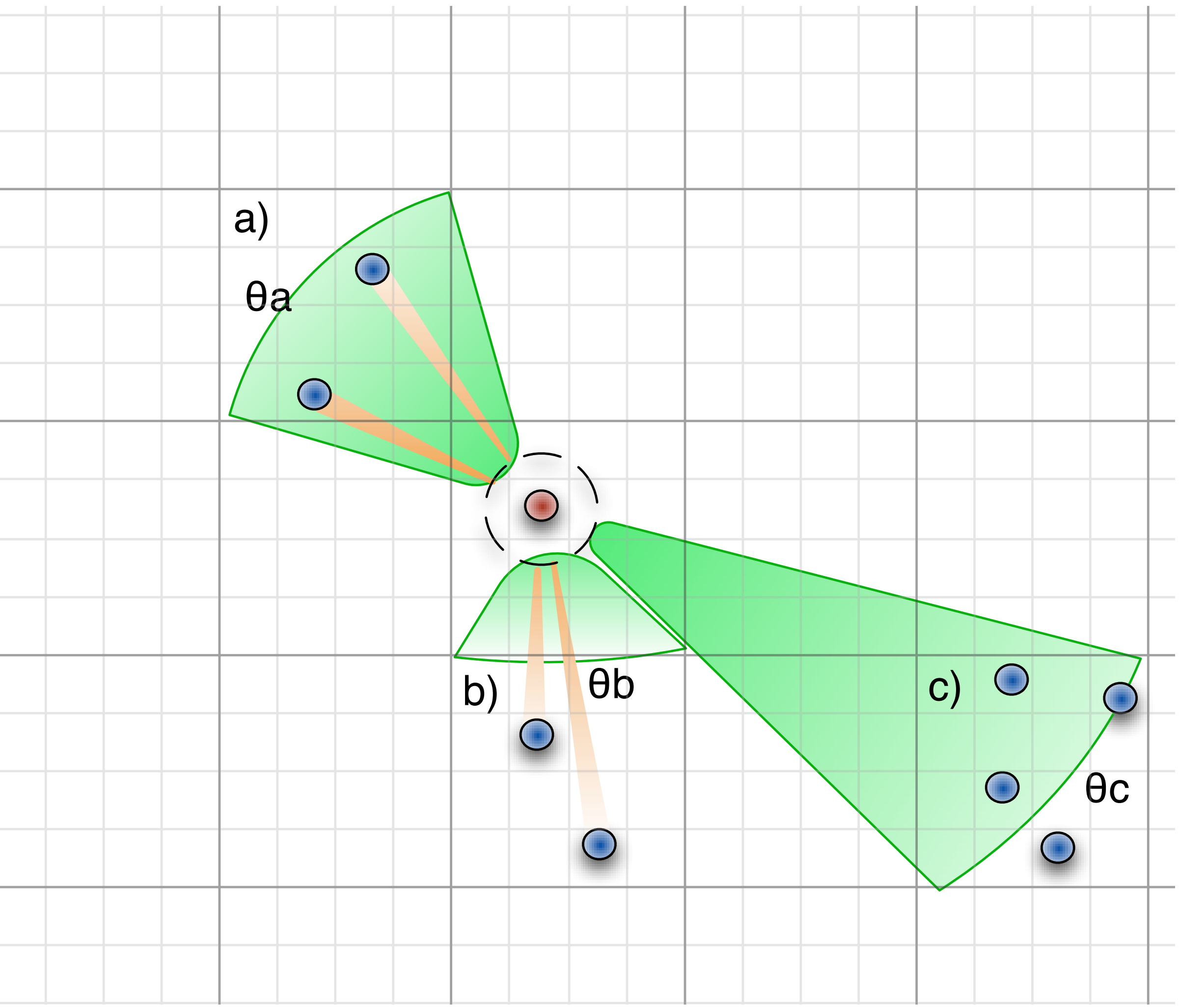

IDEA

- (gravitational) tree-walk
- calculated column densities
- accumulate on HEALPIX sphere

(Clark, Glover, Klessen, 2012, MNRAS, 420, 745)

TreeCol

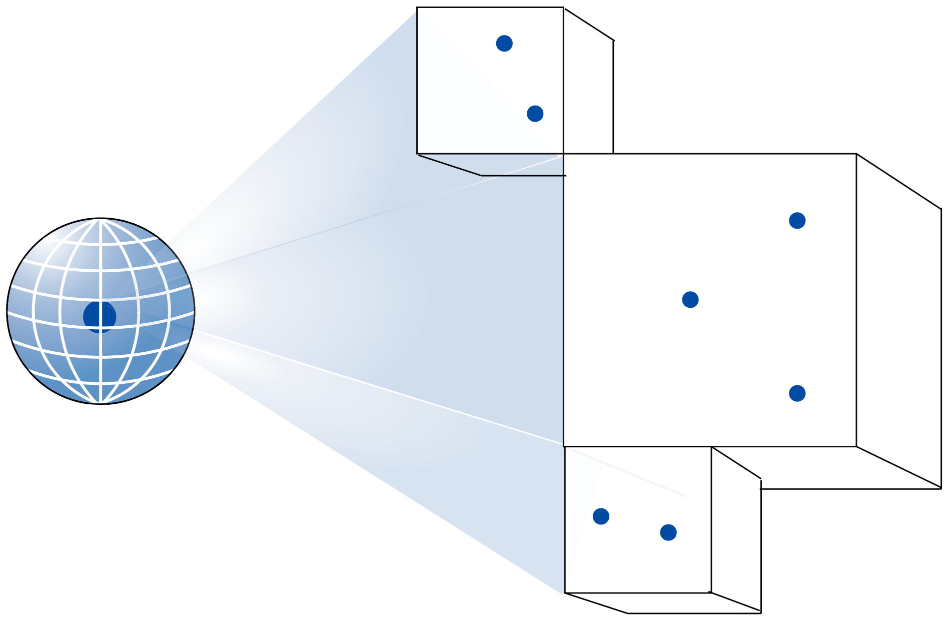

Figure 2. Schematic diagram illustrating the *TreeCol* concept. During the tree walk to obtain the gravitational forces, the projected column densities of the tree nodes (the boxes shown on the right) are mapped onto a spherical grid surrounding the particle for which the forces are being computed (the "target" particle, shown on the left). The tree already stores all of the information necessary to compute the column density of each node, the position of the node in the plane of the sky of the target particle, and the angular extent of the node. This information is used to compute the column density map at the same time that the tree is being walked to calculate the gravitational forces. Provided that the tree is already employed for the gravity calculation, the information required to create the 4π steradian map of the column densities can be obtained for minimal computational cost.

IDEA

- (gravitational) tree-walk
- calculated column densities
- accumulate on HEALPIX sphere

PERFORMANCE

- adds little computational overhead to gravitational tree-walk
- *but:* can add considerable memory overhead

(Clark, Glover, Klessen, 2012, MNRAS, 420, 745)

TreeCol

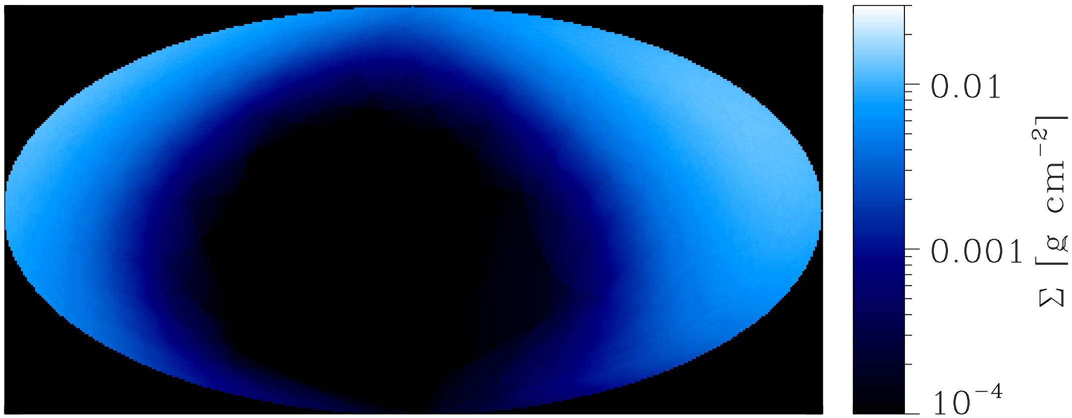

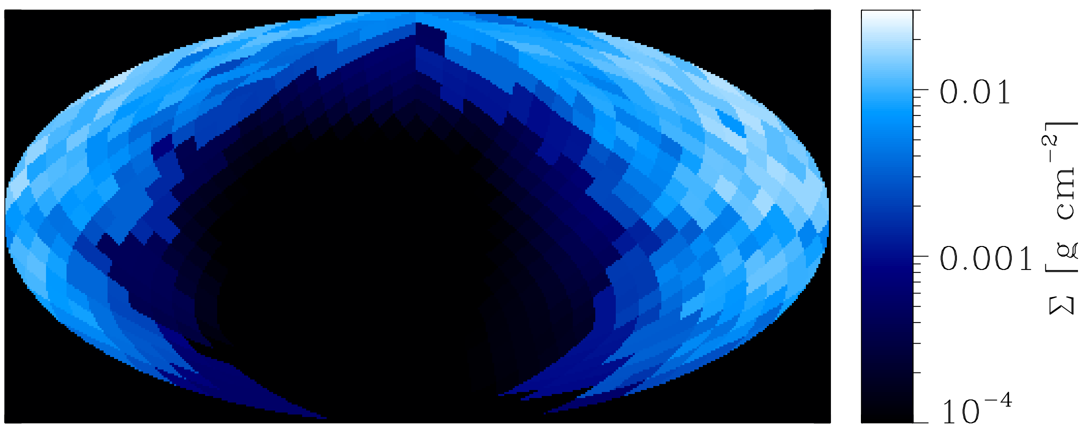

IDEA

- (gravitational) tree-walk
- calculated column densities
- accumulate on HEALPIX sphere

PERFORMANCE

- adds little computational overhead to gravitational tree-walk
- but: can add considerable memory overhead

- approximation usually good to a few percent!

(Clark, Glover, Klessen, 2012, MNRAS, 420, 745)

TreeCol

Model	N_{pix}	θ_{tol}	$\bar{\Sigma}$ [g cm^{-2}]	Error [%]
Spherical cloud			3.060×10^{-3}	
	48	0.3	3.234×10^{-3}	5.7
	48	0.5	3.274×10^{-3}	7.0
	192	0.3	3.205×10^{-3}	4.7
	192	0.5	3.239×10^{-3}	5.8
	768	0.3	3.192×10^{-3}	4.3
	768	0.5	3.226×10^{-3}	5.4
Turbulent cloud			1.151×10^{-2}	
	48	0.3	1.126×10^{-2}	2.2
	192	0.3	1.125×10^{-2}	2.3
	768	0.3	1.133×10^{-2}	1.6

(Clark, Glover, Klessen, 2012, MNRAS, 420, 745)

PERFORMANCE

- approximation usually good to a few percent!
- example: protostellar core, comparison with RADMC

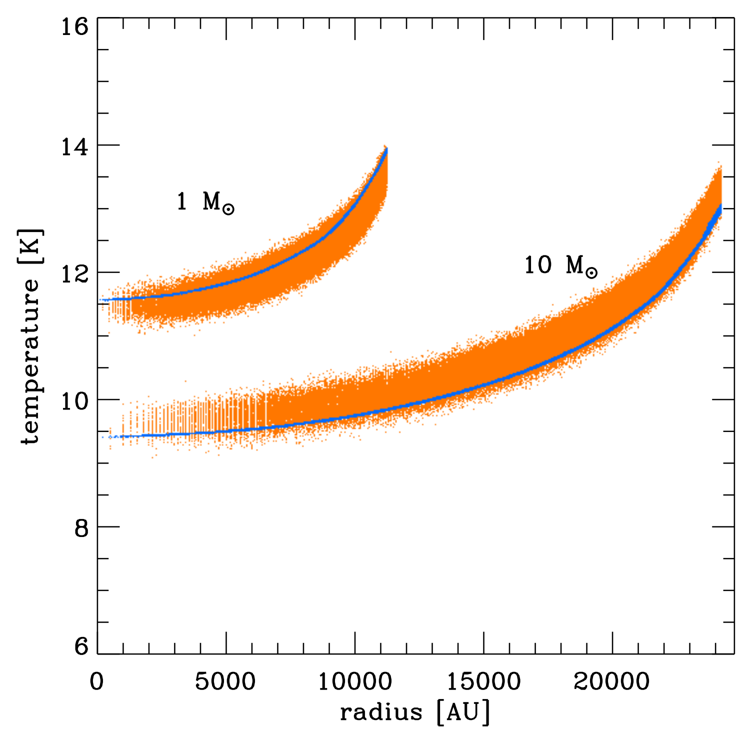

chemical model 0

- 32 chemical species
  - 17 in instantaneous equilibrium:

H^-, H_2^+, H_3^+, CH^+, CH_2^+, OH^+, H_2O^+, H_3O^+, CO^+, HOC^+, O^-, C^- and O_2^+

  - 19 full non-equilibrium evolution

e^-, H^+, H, H_2, He, He^+, C, C^+, O, O^+, OH, H_2O, CO,

C_2, O_2, HCO^+, CH, CH_2 and CH_3^+

- 218 reactions
- various heating and cooling processes

long series of publications by Simon Glover and collaborators, e.g. Glover & Mac Low (2007ab), Glover, Federrath, Mac Low, Klessen (2010), Glover & Clark (2012, 2013), Clark & Clover (2012, 2013)

chemical model 1

Process	Reference(s)
Cooling:	
C fine structure lines	Atomic data – Silva & Viegas (2002)
	Collisional rates (H) – Abrahamsson, Krems & Dalgarno (2007)
	Collisional rates (H_2) – Schroder et al. (1991)
	Collisional rates (e^-) – Johnson et al. (1987)
	Collisional rates (H^+) – Roueff & Le Bourlot (1990)
C^+ fine structure lines	Atomic data – Silva & Viegas (2002)
	Collisional rates (H_2) – Flower & Launay (1977)
	Collisional rates (H, $T < 2000$ K) – Hollenbach & McKee (1989)
	Collisional rates (H, $T > 2000$ K) – Keenan et al. (1986)
	Collisional rates (e^-) – Wilson & Bell (2002)
O fine structure lines	Atomic data – Silva & Viegas (2002)
	Collisional rates (H) – Abrahamsson, Krems & Dalgarno (2007)
	Collisional rates (H_2) – see Glover & Jappsen (2007)
	Collisional rates (e^-) – Bell, Berrington & Thomas (1998)
	Collisional rates (H^+) – Pequignot (1990, 1996)
H_2 rovibrational lines	Le Bourlot, Pineau des Forêts & Flower (1999)
CO and H_2O rovibrational lines	Neufeld & Kaufman (1993); Neufeld, Lepp & Melnick (1995)
OH rotational lines	Pavlovski et al. (2002)
Gas-grain energy transfer	Hollenbach & McKee (1989)
Recombination on grains	Wolfire et al. (2003)
Atomic resonance lines	Sutherland & Dopita (1993)
H collisional ionization	Abel et al. (1997)
H_2 collisional dissociation	See Table B1
Compton cooling	Cen (1992)
Heating:	
Photoelectric effect	Bakes & Tielens (1994); Wolfire et al. (2003)
H_2 photodissociation	Black & Dalgarno (1977)
UV pumping of H_2	Burton, Hollenbach & Tielens (1990)
H_2 formation on dust grains	Hollenbach & McKee (1989)
Cosmic ray ionization	Goldsmith & Langer (1978)

(Glover, Federrath, Mac Low, Klessen, 2010, MNRS, 404, 2)

chemical model 2

(Glover, Federrath, Mac Low, Klessen, 2010, MNRAS, 404, 2)

Table B2. List of photochemical reactions included in our chemical model

No.	Reaction	Optically thin rate (s^{-1})	γ	Ref.
166	$H^- + \gamma \rightarrow H + e^-$	$R_{166} = 7.1 \times 10^{-7}$	0.5	1
167	$H_2^+ + \gamma \rightarrow H + H^+$	$R_{167} = 1.1 \times 10^{-9}$	1.9	2
168	$H_2 + \gamma \rightarrow H + H$	$R_{168} = 5.6 \times 10^{-11}$	See §2.2	3
169	$H_3^+ + \gamma \rightarrow H_2 + H^+$	$R_{169} = 4.9 \times 10^{-13}$	1.8	4
170	$H_3^+ + \gamma \rightarrow H_2^+ + H$	$R_{170} = 4.9 \times 10^{-13}$	2.3	4
171	$C + \gamma \rightarrow C^+ + e^-$			
172	$C^- + \gamma \rightarrow$			
173	$CH + \gamma \rightarrow$			
174	$CH + \gamma \rightarrow$			
175	$CH^+ + \gamma$			
176	$CH_2 + \gamma$			
177	$CH_2 + \gamma$			
178	$CH_2^+ + \gamma$			
179	$CH_3^+ + \gamma$			
180	$CH_3^+ + \gamma$			
181	$C_2 + \gamma \rightarrow$			
182	$O^- + \gamma \rightarrow$			
183	$OH + \gamma \rightarrow$			
184	$OH + \gamma \rightarrow$			
185	$OH^+ + \gamma$			
186	$H_2O + \gamma$			
187	$H_2O + \gamma$			
188	$H_2O^+ +$			
189	$H_2O^+ +$			
190	$H_2O^+ +$			
191	$H_2O^+ +$			
192	$H_3O^+ +$			
193	$H_3O^+ +$			
194	$H_3O^+ +$			
195	$H_3O^+ +$			
196	$O_2 + \gamma \rightarrow$			
197	$O_2 + \gamma \rightarrow O + O$	$R_{197} = 7.0 \times 10^{-10}$	1.8	7
198	$CO + \gamma \rightarrow C + O$	$R_{198} = 2.0 \times 10^{-10}$	See §2.2	13

Table B3. List of reactions included in our chemical model that involve cosmic rays or cosmic-ray induced UV emission

No.	Reaction	Rate ($s^{-1} \zeta_H^{-1}$)	Ref.
199	$H + c.r. \rightarrow H^+ + e^-$	$R_{199} = 1.0$	—
200	$He + c.r. \rightarrow He^+ + e^-$	$R_{200} = 1.1$	1
201	$H_2 + c.r. \rightarrow H^+ + H + e^-$	$R_{201} = 0.037$	1
202	$H_2 + c.r. \rightarrow H + H$	$R_{202} = 0.22$	1
203	$H_2 + c.r. \rightarrow H^+ + H^-$	$R_{203} = 6.5 \times 10^{-4}$	1
204	$H_2 + c.r. \rightarrow H_2^+ + e^-$	$R_{204} = 2.0$	1
205	$C + c.r. \rightarrow C^+ + e^-$	$R_{205} = 3.8$	1
206	$O + c.r. \rightarrow O^+ + e^-$	$R_{206} = 5.7$	1
207	$CO + c.r. \rightarrow CO^+ + e^-$	$R_{207} = 6.5$	1
208	$C + \gamma_{c.r.} \rightarrow C^+ + e^-$	$R_{208} = 2800$	2
209	$CH + \gamma_{c.r.} \rightarrow C + H$	$R_{209} = 4000$	3
210	$CH^+ + \gamma_{c.r.} \rightarrow C^+ + H$	$R_{210} = 960$	3
211	$CH_2 + \gamma_{c.r.} \rightarrow CH_2^+ + e^-$	$R_{211} = 2700$	1
212	$CH_2 + \gamma_{c.r.} \rightarrow CH + H$	$R_{212} = 2700$	1
213	$C_2 + \gamma_{c.r.} \rightarrow C + C$	$R_{213} = 1300$	3
214	$OH + \gamma_{c.r.} \rightarrow O + H$	$R_{214} = 2800$	3
215	$H_2O + \gamma_{c.r.} \rightarrow OH + H$	$R_{215} = 5300$	3
216	$O_2 + \gamma_{c.r.} \rightarrow O + O$	$R_{216} = 4100$	3
217	$O_2 + \gamma_{c.r.} \rightarrow O_2^+ + e^-$	$R_{217} = 640$	3
218	$CO + \gamma_{c.r.} \rightarrow C + O$	$R_{218} = 0.21 T^{1/2} x_{H_2} x_{CO}^{-1/2}$	4

HI to H2 conversion rate

H2 forms rapidly in shocks / transient density fluctuations / H2 gets destroyed slowly in low density regions / *result: turbulence greatly enhances H2-formation rate*

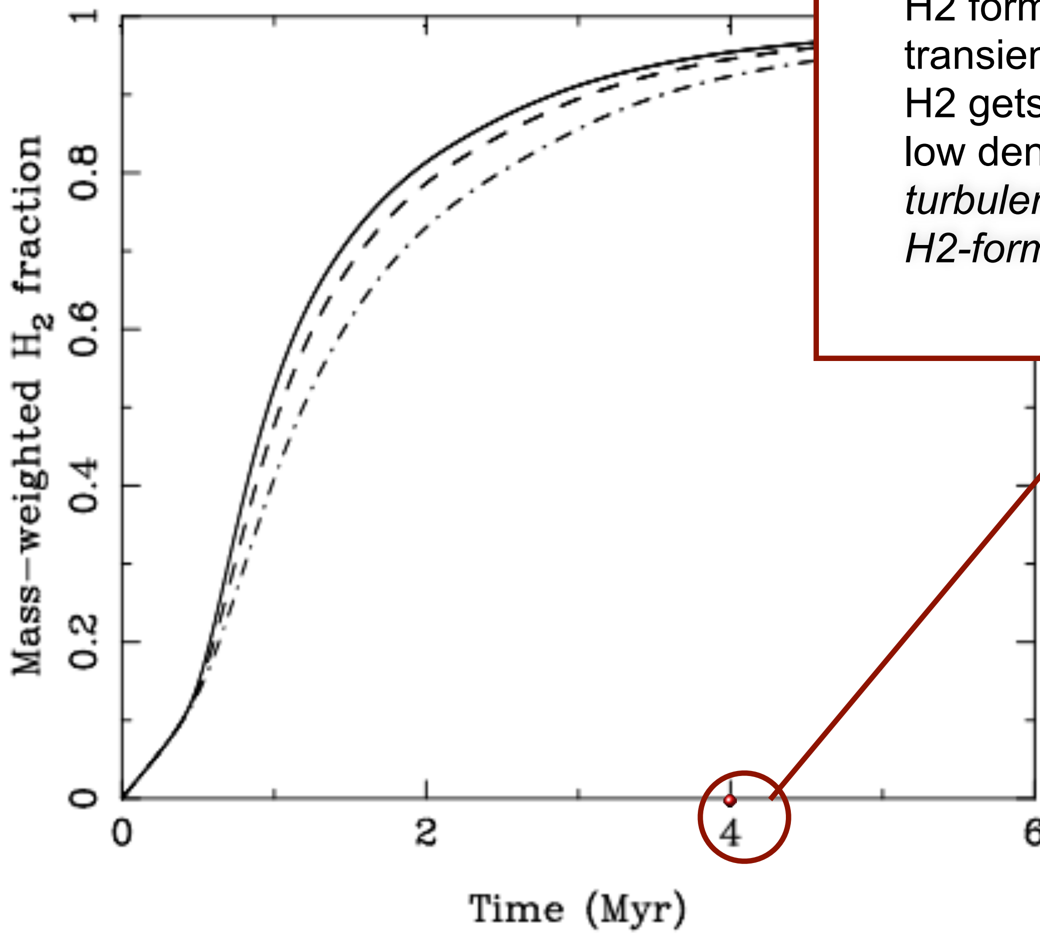

Figure 4. Time evolution of the mass-weighted H_2 abundance in simulations R1, R2 and R3, which have numerical resolutions of 64^3 zones (dot-dashed), 128^3 zones (dashed) and 256^3 zones (solid), respectively.

(Glover et al. 2010)

CO, C$^+$ formation rates

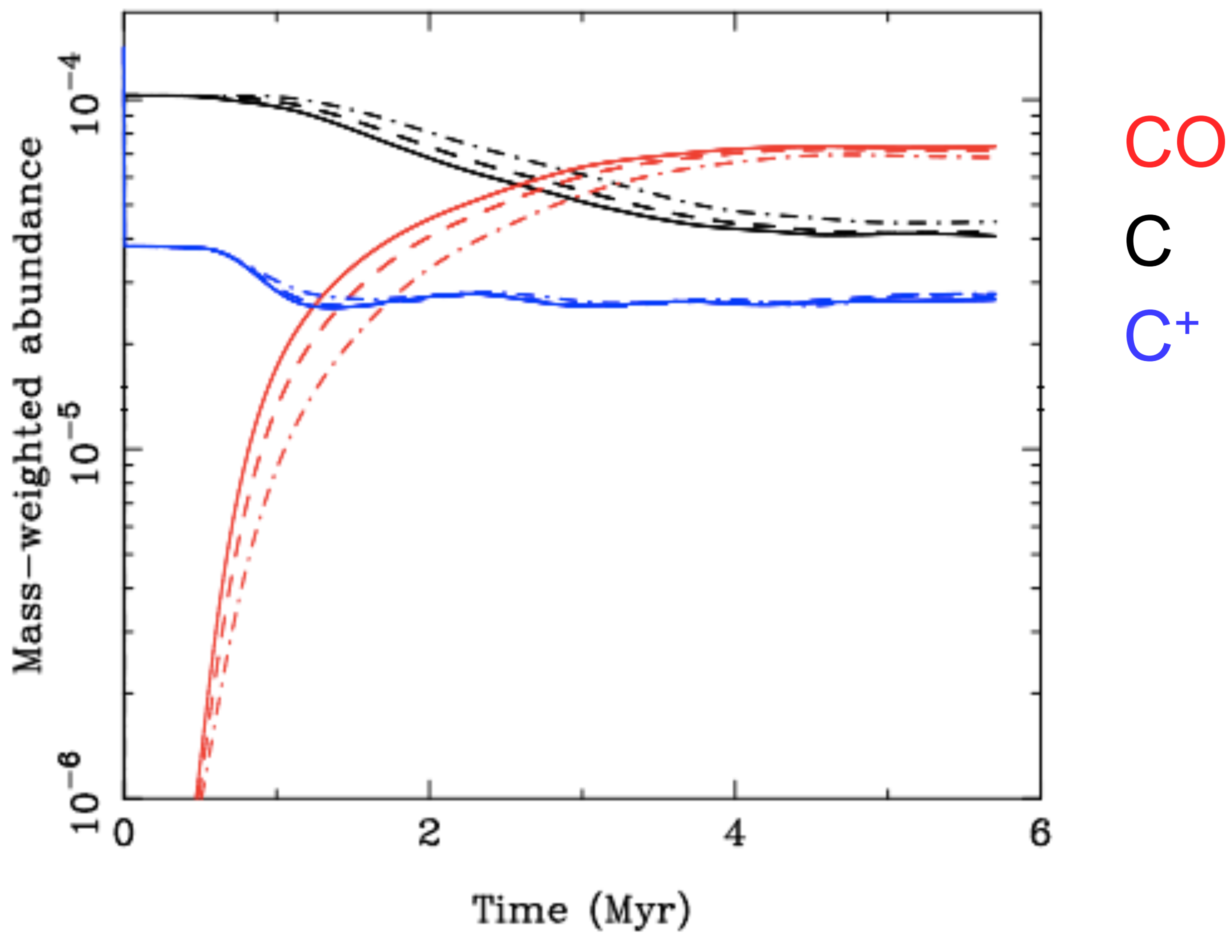

Figure 5. Time evolution of the mass-weighted abundances of atomic carbon (black lines), CO (red lines), and C$^+$ (blue lines) in simulations with numerical resolutions of 64^3 zones (dot-dashed), 128^3 zones (dashed) and 256^3 zones (solid).

(Glover et al. 2010)

effects of chemistry

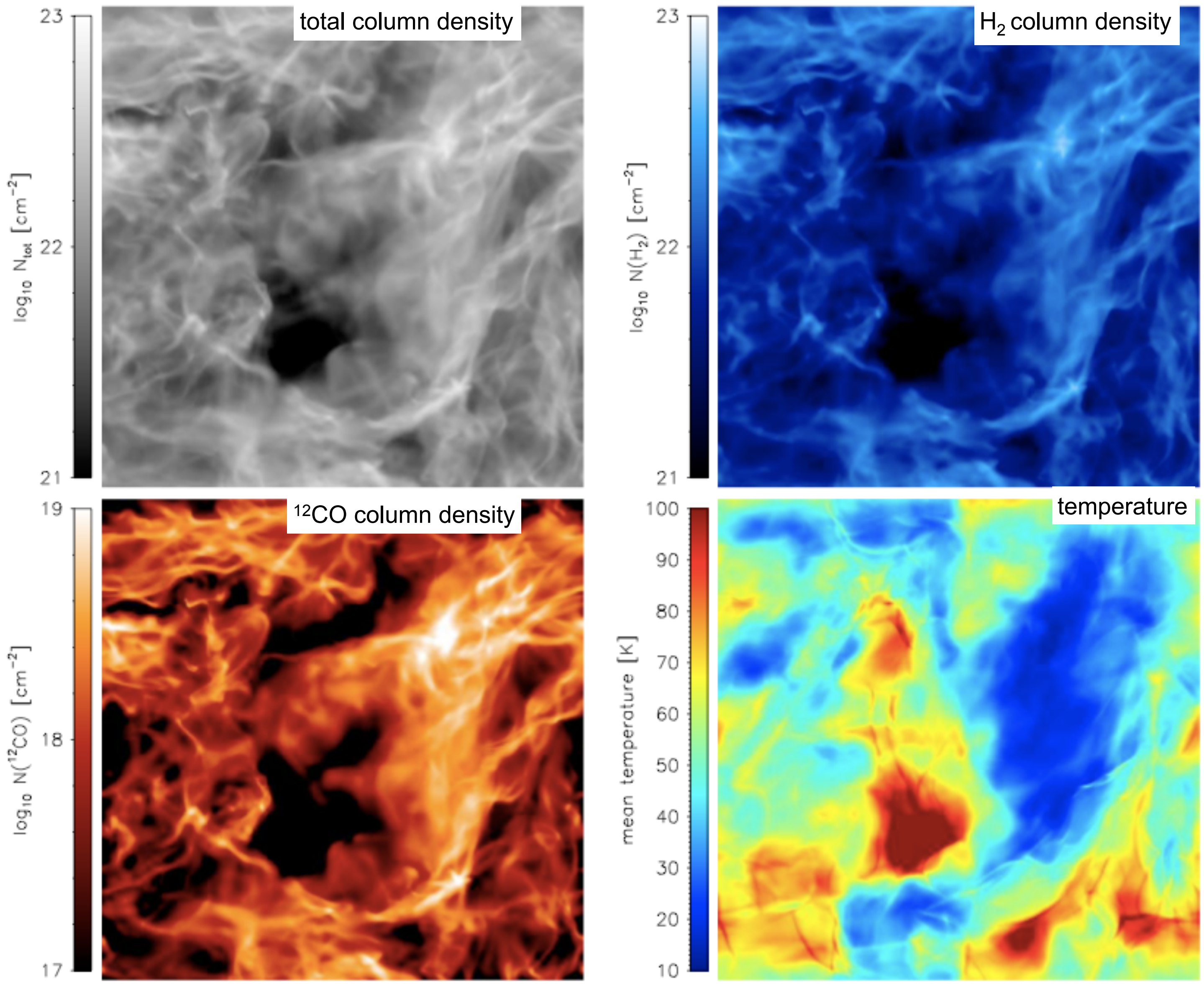

(Glover et al. 2010)

effects of chemistry

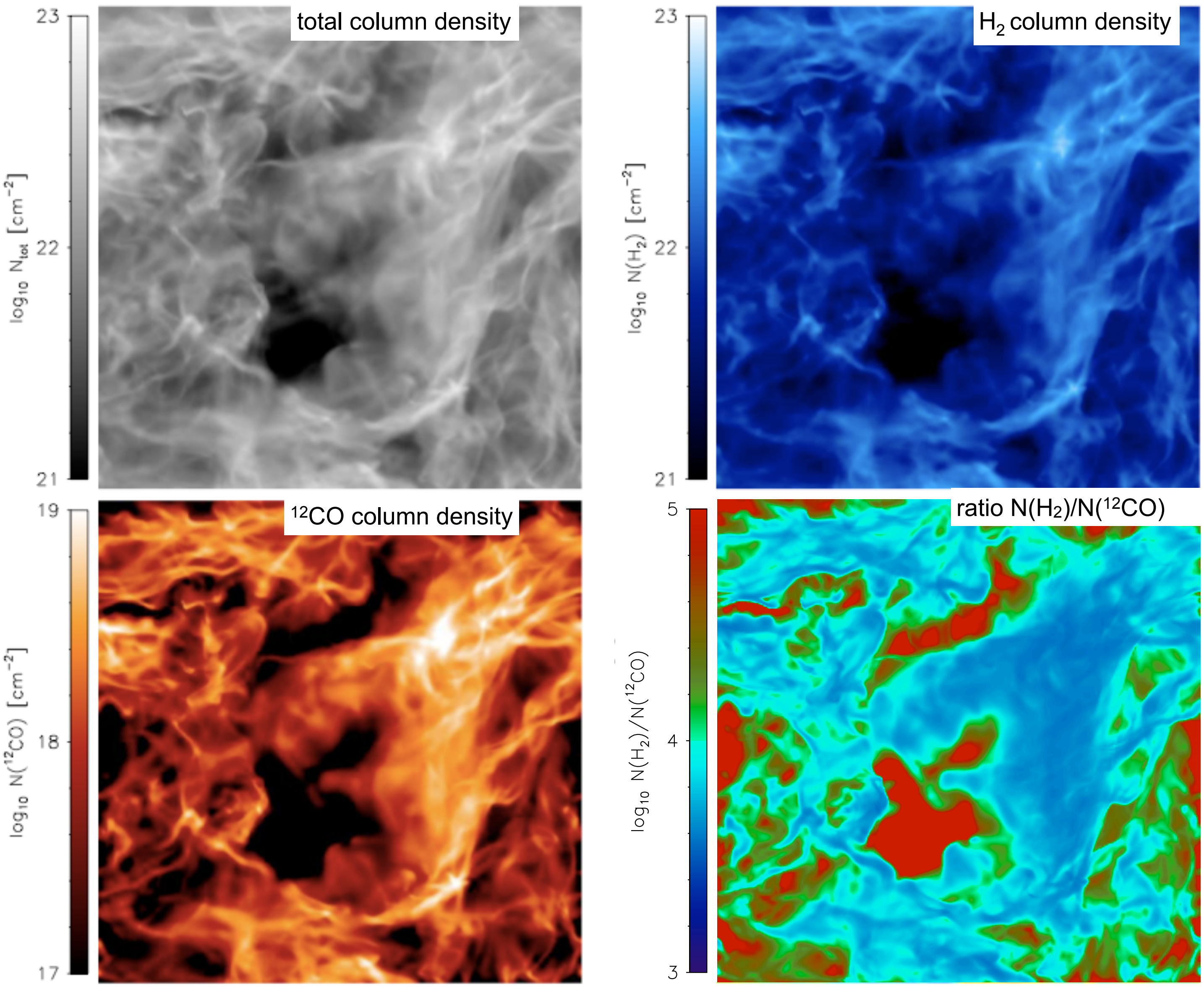

(Glover et al. 2010)

molecular cloud
formation with
Arepo

molecular cloud formation

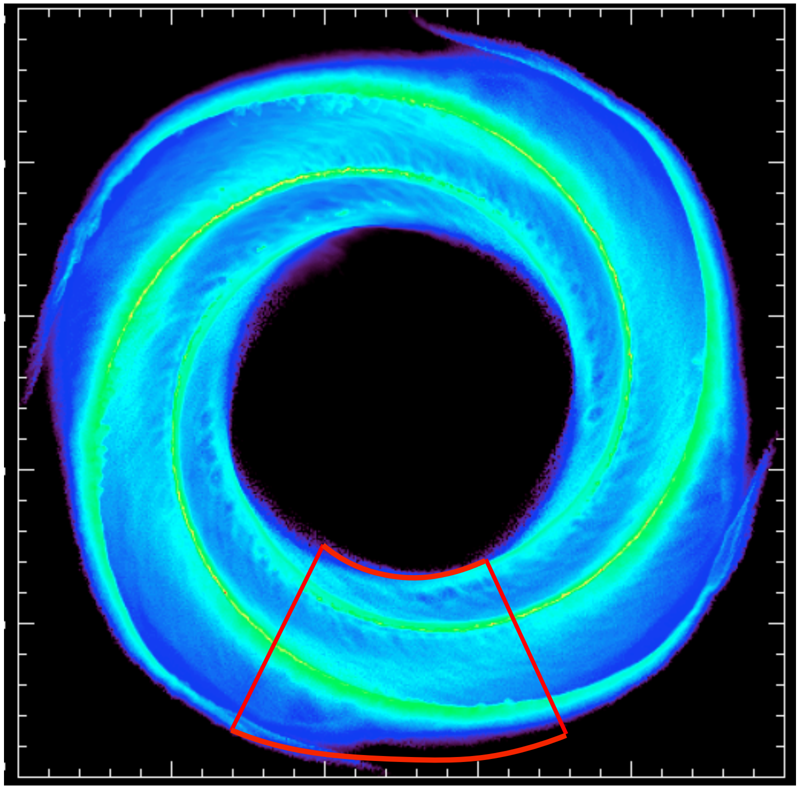

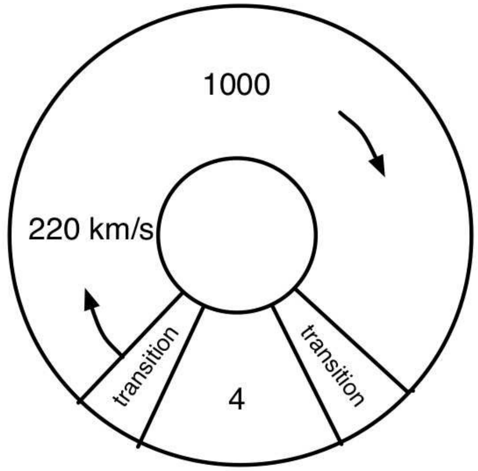

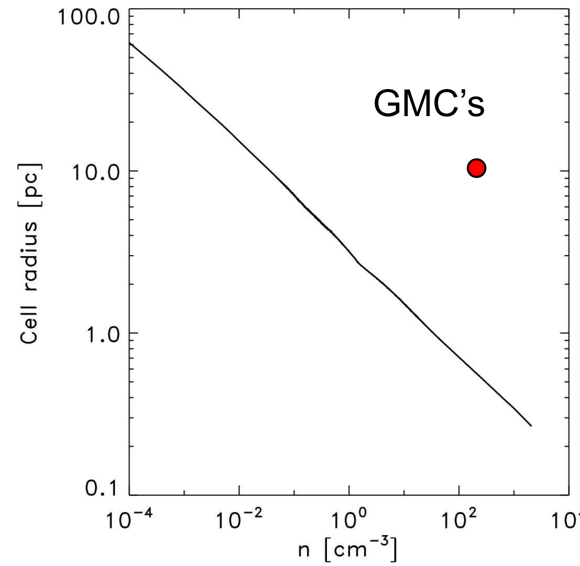

Simulation	Surface Density $M_\odot$ pc^{-2}	Radiation Field G_0
Milky Way	10	1
Low Density	4	1
Strong Field	10	10
Low & Weak	4	0.1

(Smith et al., 2014, MNRAS, 441, 1628)

- Arepo moving mesh code *(Springel 2010)*
- time dependent chemistry *(Glover et al. 2007)* gives heating & cooling in a 2 phase medium
- two layers of refinement with mass resolution down to 4 $M_\odot$ in full Galaxy simulation
- UV field and cosmic rays
- TreeCol *(Clark et al. 2012)*
- external spiral potential *(Dobbs & Bonnell 2006)*
- no gas self-gravity, SN, or magnetic fields yet

numerical method

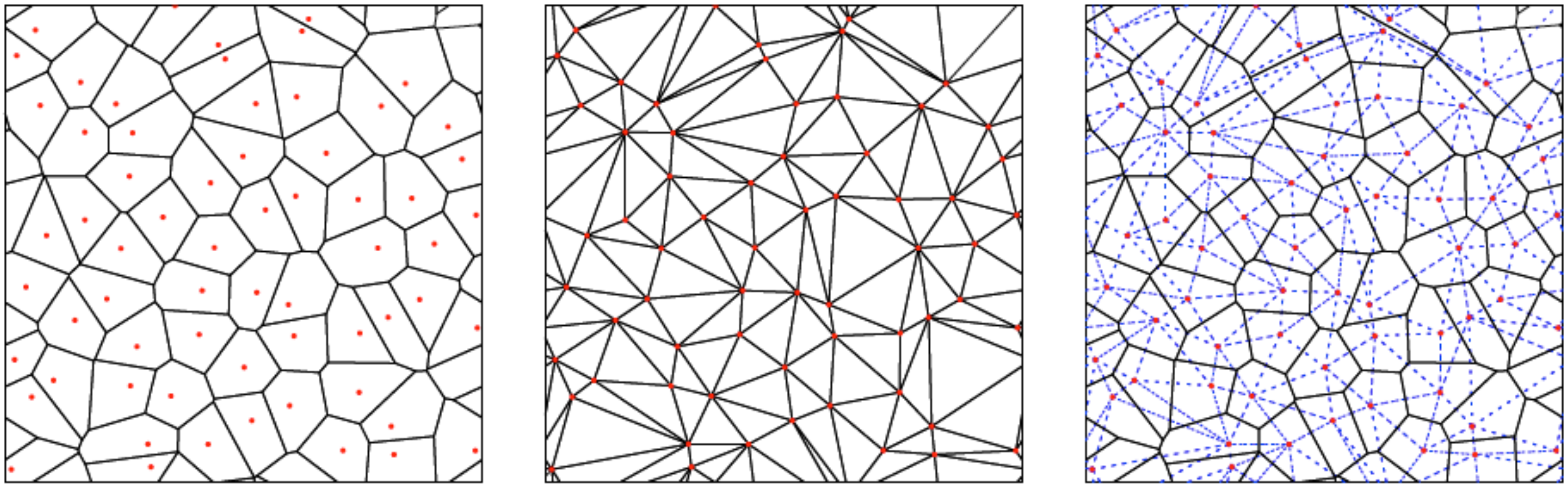

*moving mesh code **Arepo**:*

- semi-Lagrangian
- flexible refinement
- fluid instabilities and no artificial clumping
  (Agertz et al. 2007)
- can also handle sub-sonic turbulence
  (Bauer & Springel 2012)
- no preferred geometry

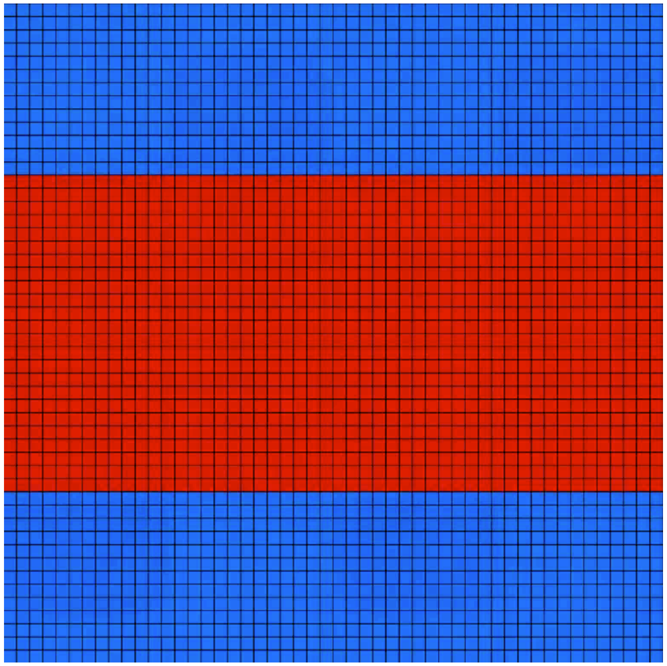

Springel (2010, MNRAS, 401, 791)

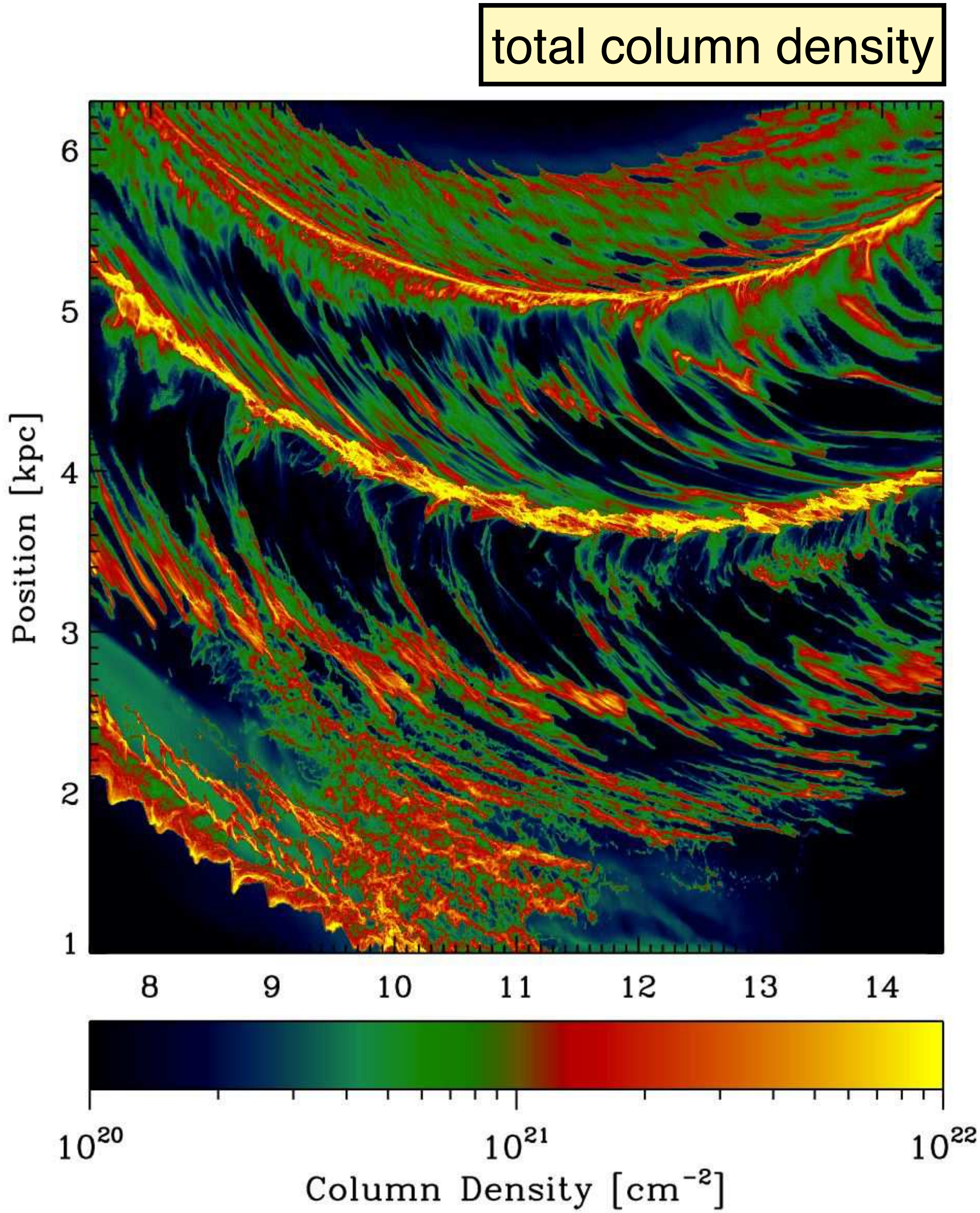

(Smith et al., 2014, MNRAS, 441, 1628)

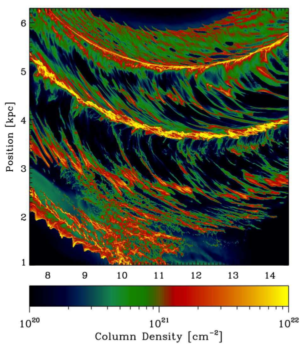

HI column density

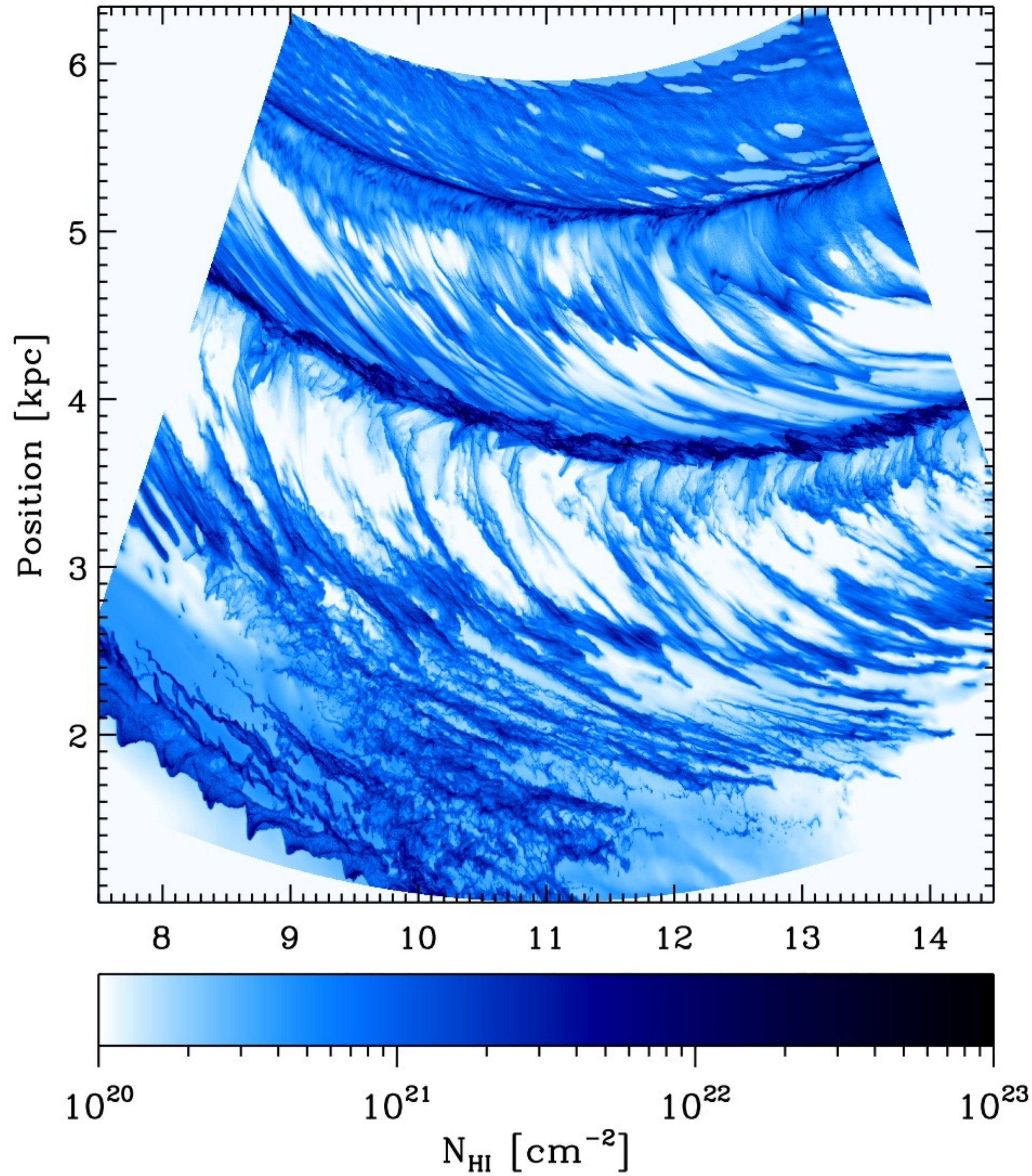

(Smith et al., 2014, MNRAS, 441, 1628)

preliminary image from THOR Galactic plane survey (PI H. Beuther): continuum emission around 21 cm

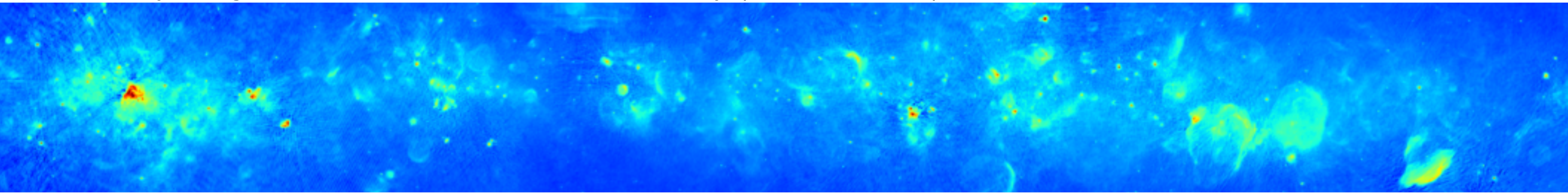

next step: produce all sky maps at various positions in the model galaxy (use RADMC-3D)

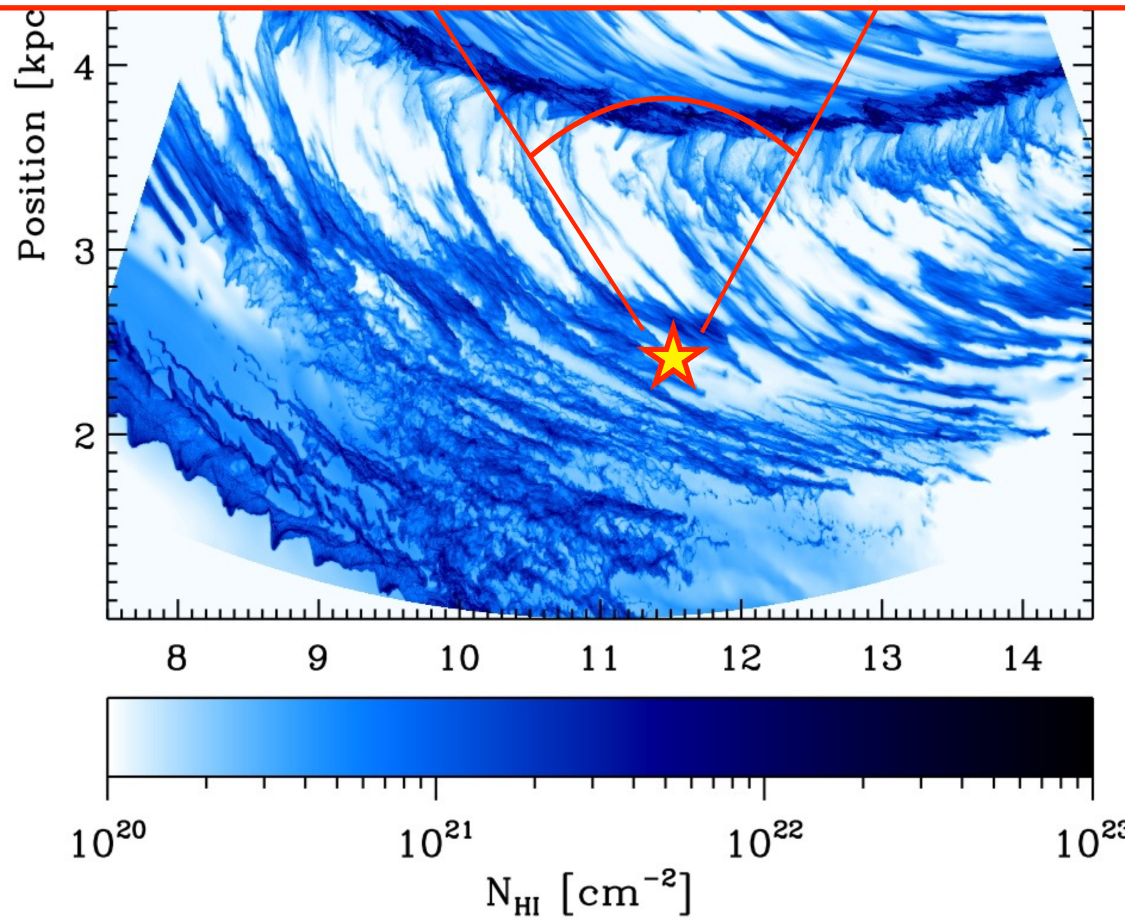

(Smith et al., 2014, MNRAS, 441, 1628)

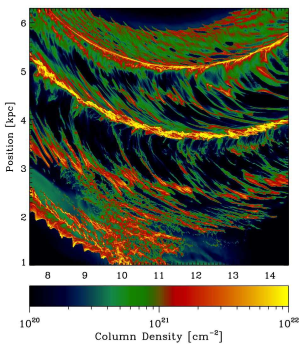

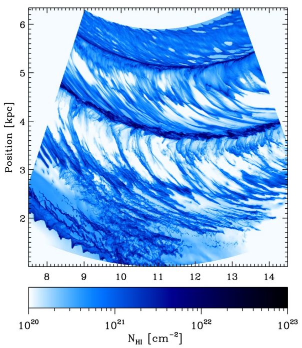

H_2 column density

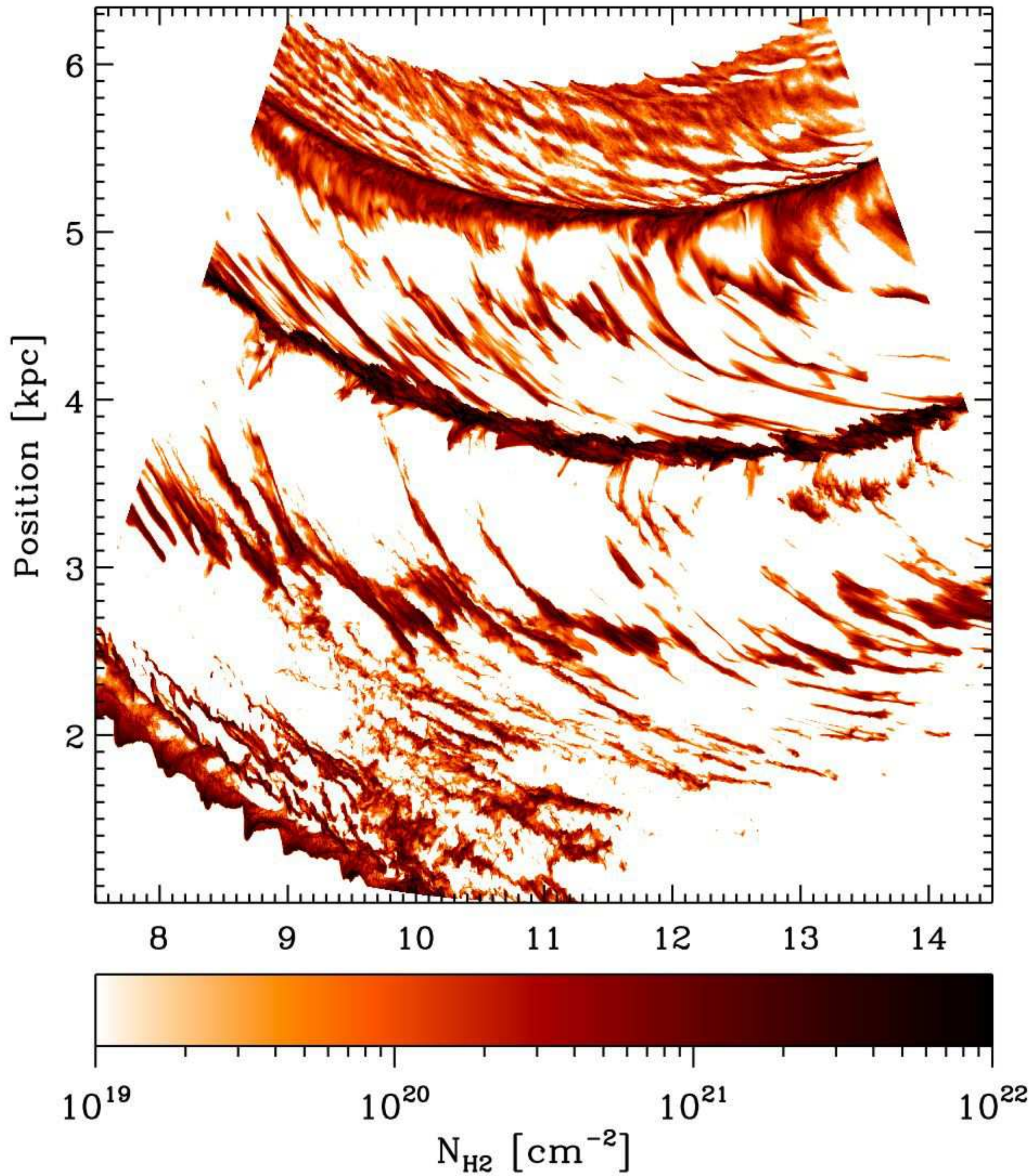

(Smith et al., 2014, MNRAS, 441, 1628)

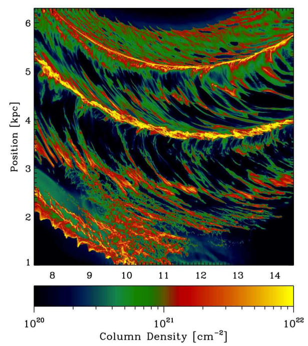

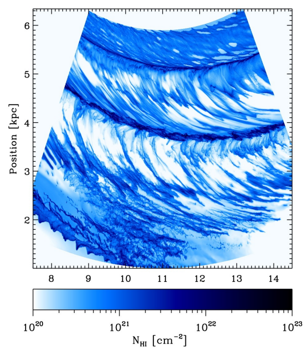

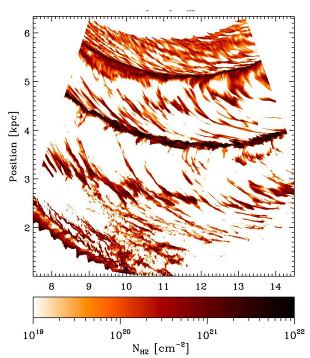

CO column density

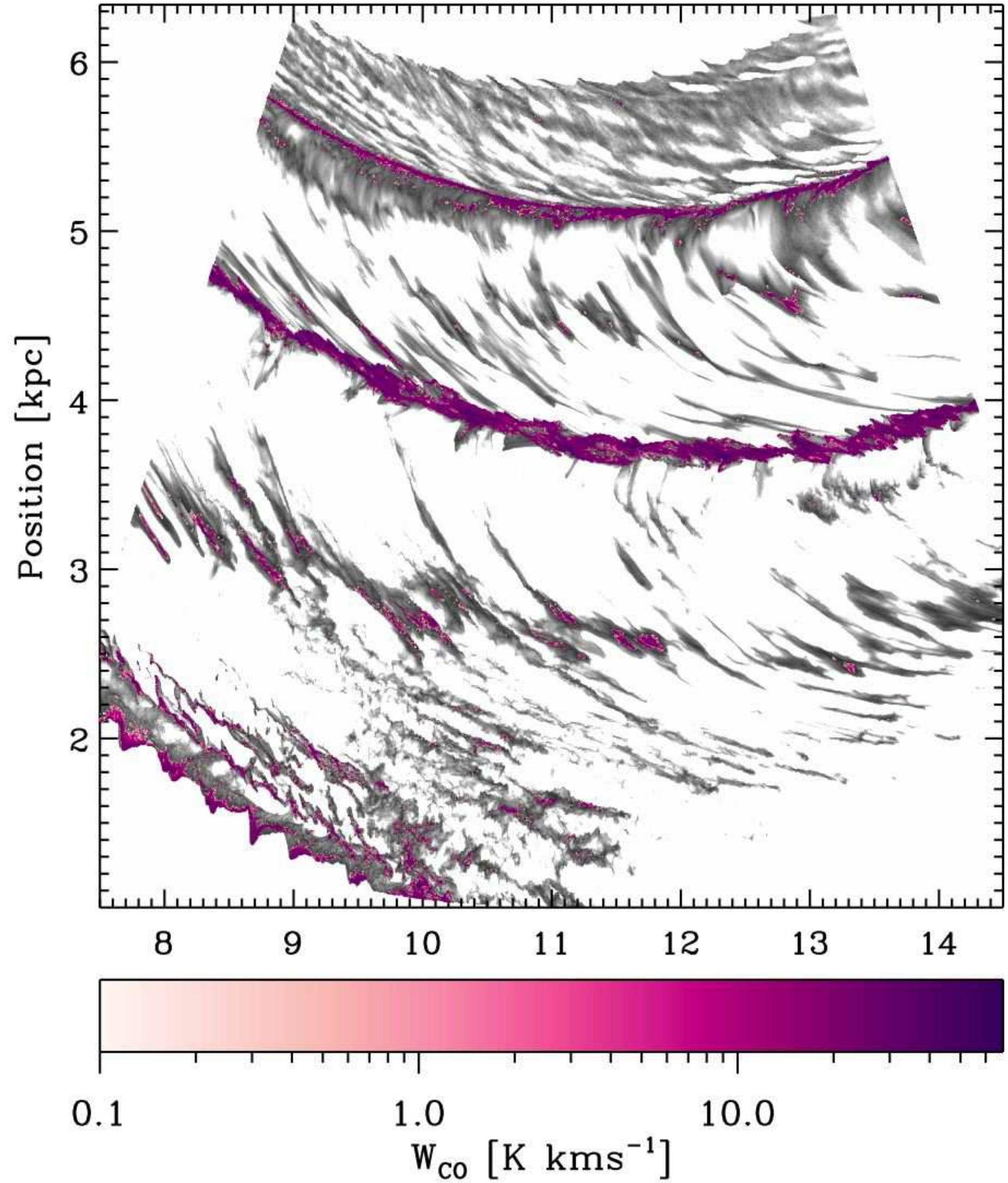

(Smith et al., 2014, MNRAS, 441, 1628)

H₂ fraction vs. column density N

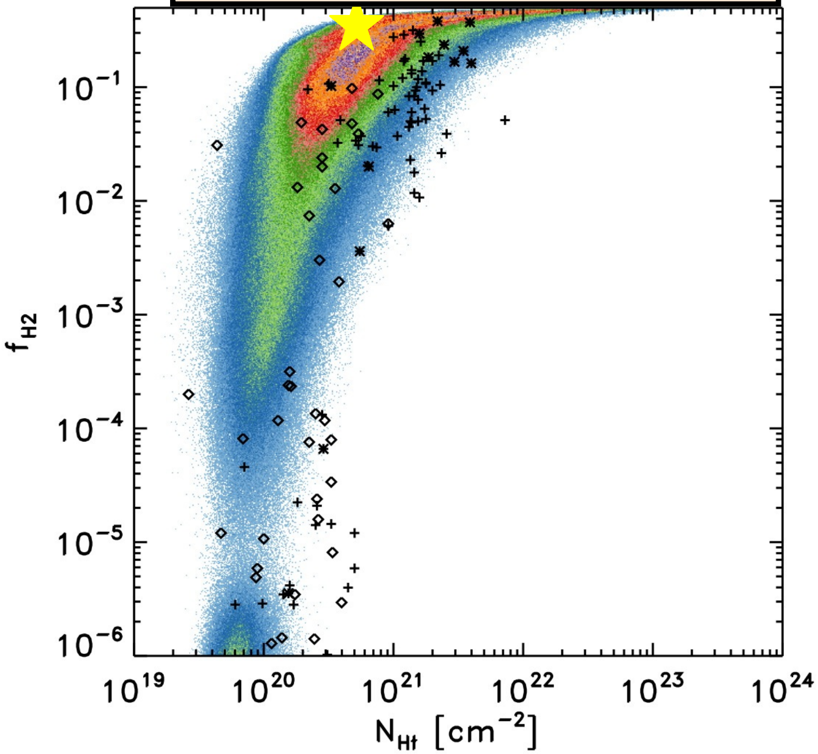

CO col. density vs. H₂ col. density

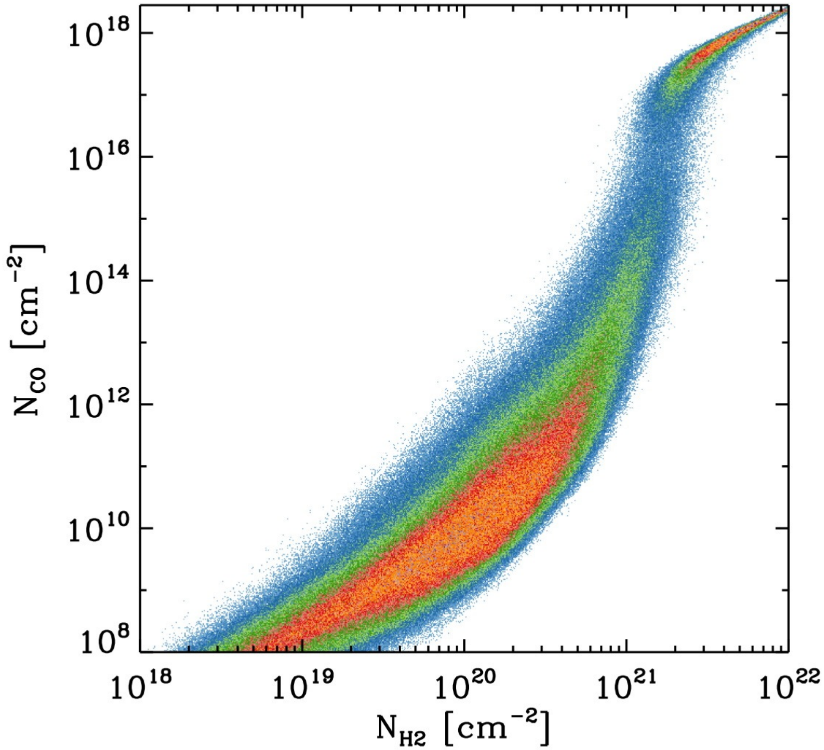

H_2 forms above column densities of 10^{20} cm^{-2}

CO columns jump after $N_{H2} \sim 10^{21}$ cm^{-2}

$$log(Z_{CO}[cm^{-2}]) = -18.1 log(N_{CO}[cm^{-2}]) + 0.8.$$

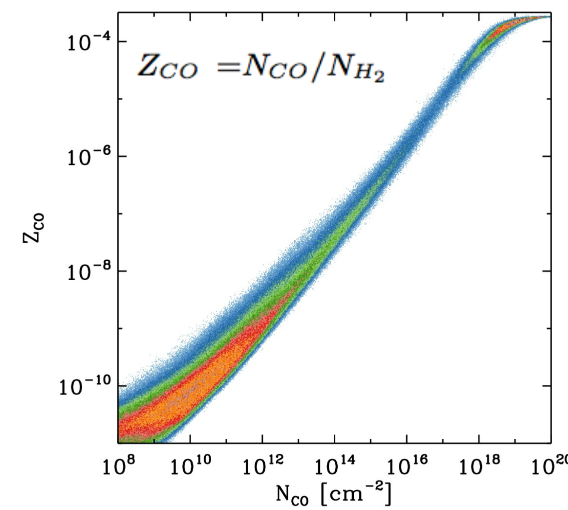

(Smith et al., 2014, MNRAS, 441, 1628)

details of CO emission

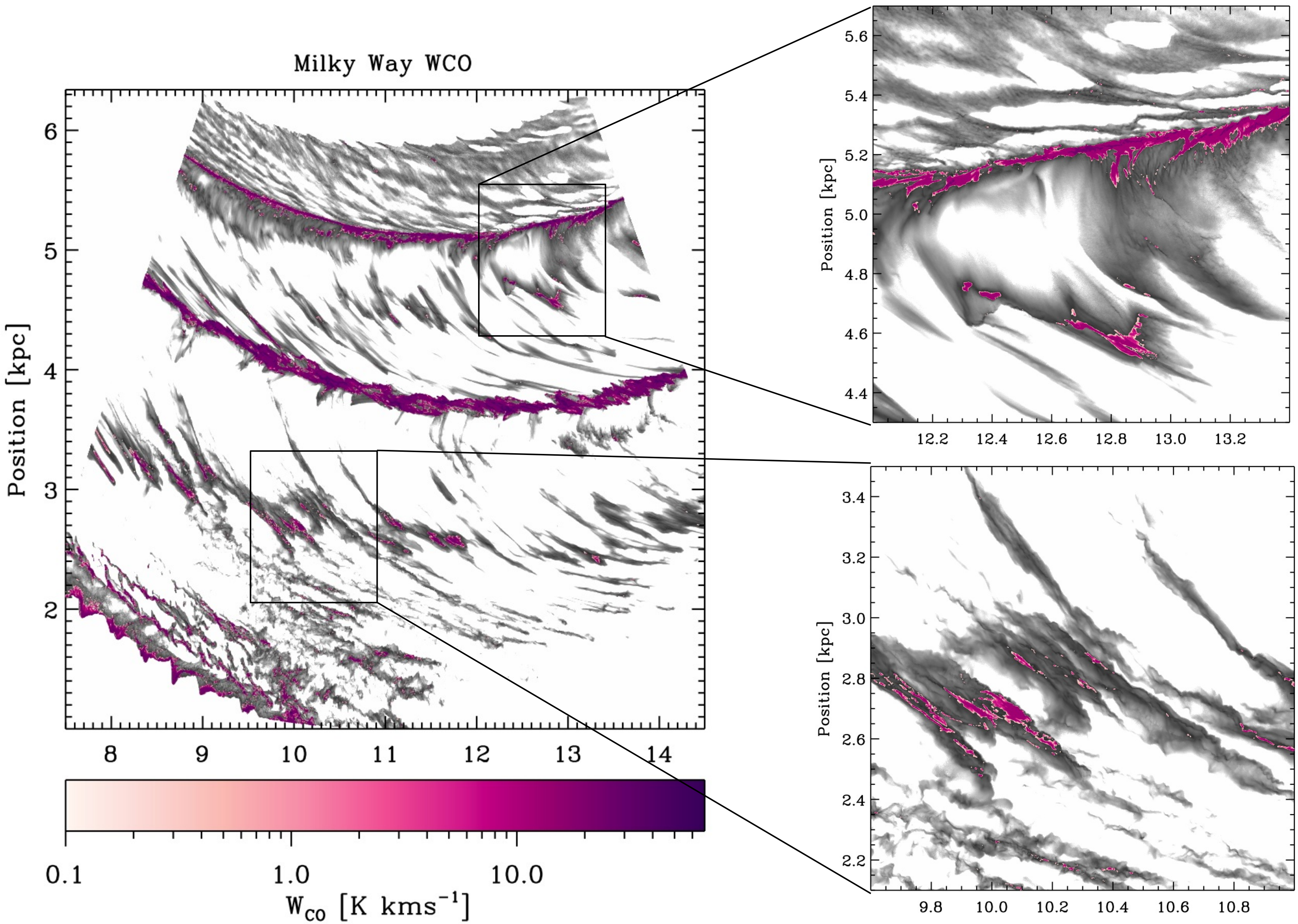

(Smith et al., 2014, MNRAS, 441, 1628)

relation between CO and H_2

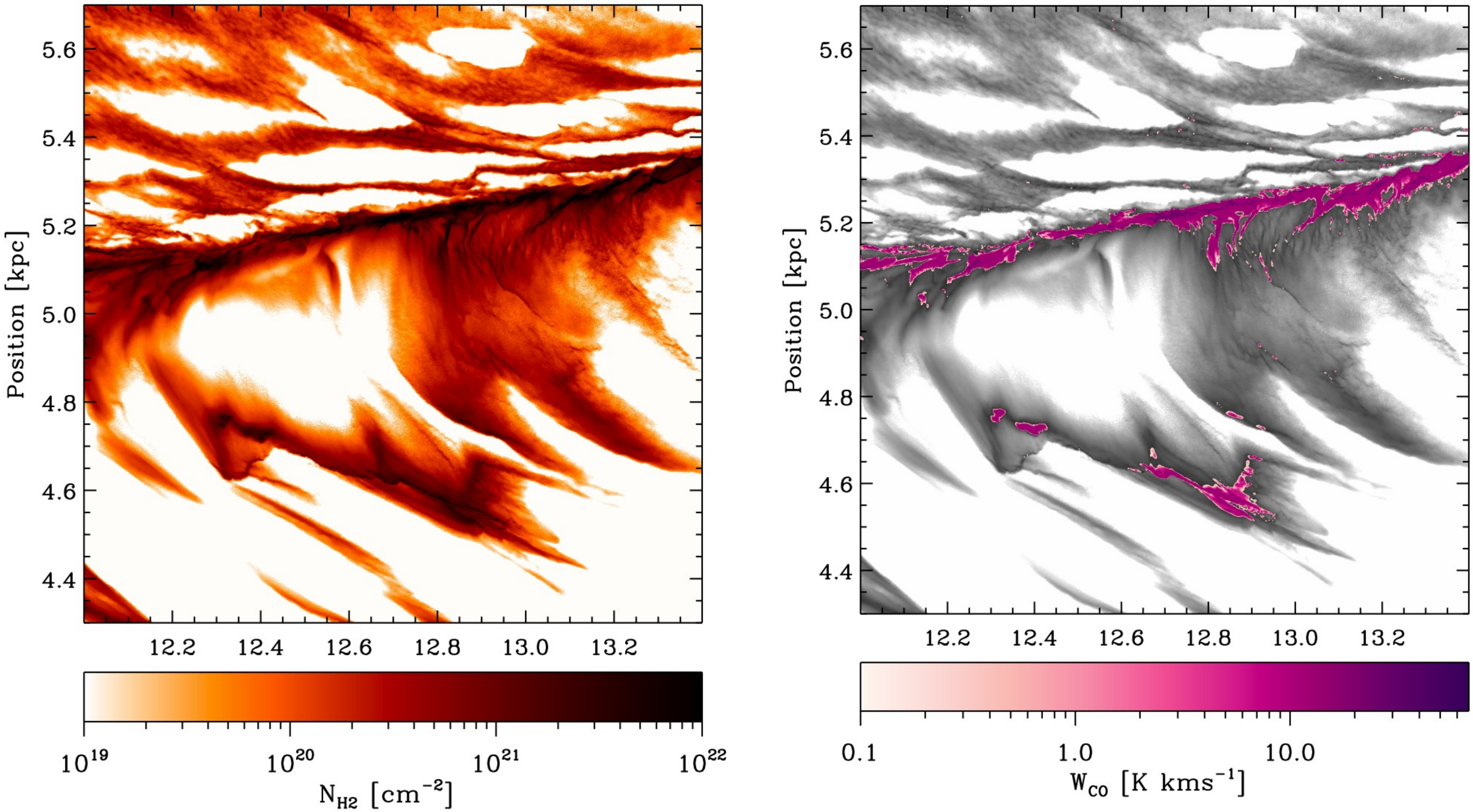

(Smith et al., 2014, MNRAS, 441, 1628)

relation between CO and H_2

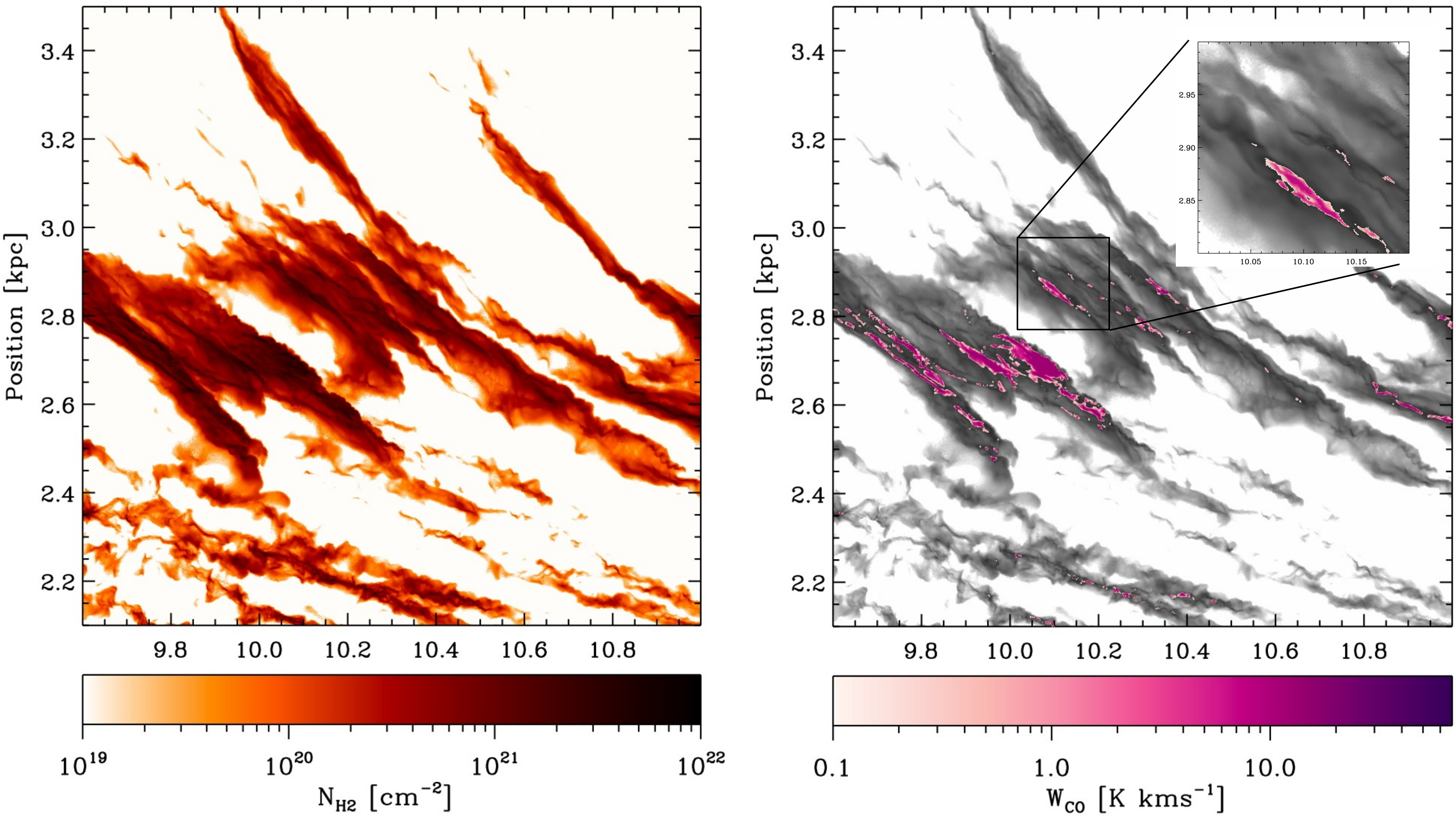

Filamentary molecular clouds in inter-arm regions are likely only the observable parts of much larger structures.

dark gas fraction

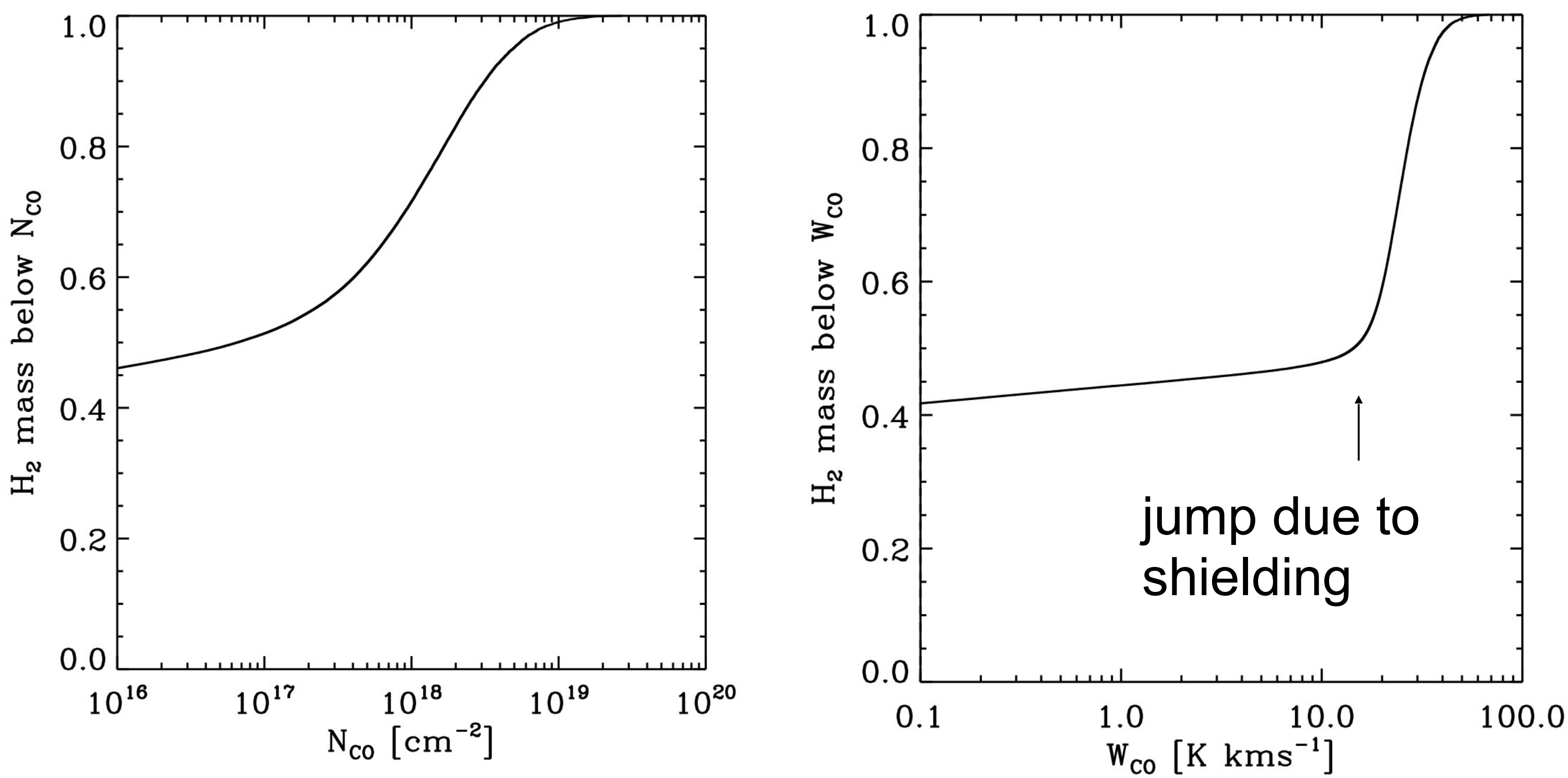

46% molecular gas below CO column densities of 10^{16} cm^{-2}

42% has an integrated CO emission of less than 0.1 K kms^{-1}

$f_{DG} = 0.42$ $\quad$ $X_{CO}=2.2 \times 10^{20}\ cm^{-2}K^{-1}km^{-1}s$

(Smith et al., 2014, MNRAS, 441, 1628)

dark gas fraction

Observational estimates:

Grenier et al. 2005 f_{DG} = 0.33-0.5

Planck collaboration 2011* f_{DG} = 0.54

Paradis et al. 2012* f_{DG} = 0.62

inner f_{DG} = 0.71, outer f_{DG} = 0.43

Pineda et al. 2013 f_D= 0.3

* dust methods have large uncertainties.

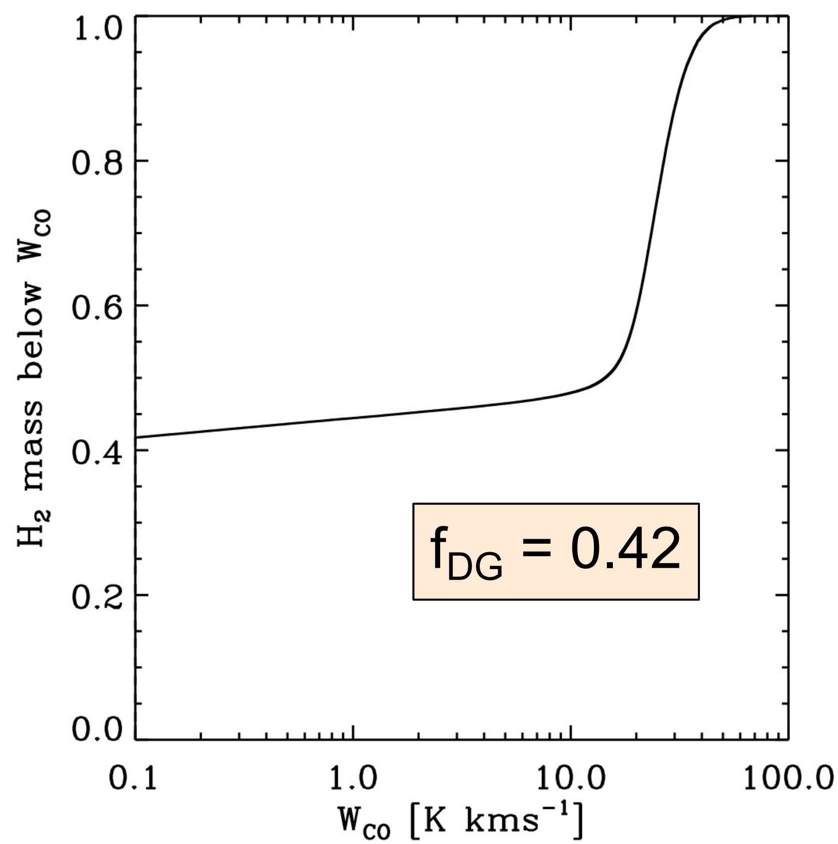

(Smith et al., 2014, MNRAS, 441, 1628)

other simulations

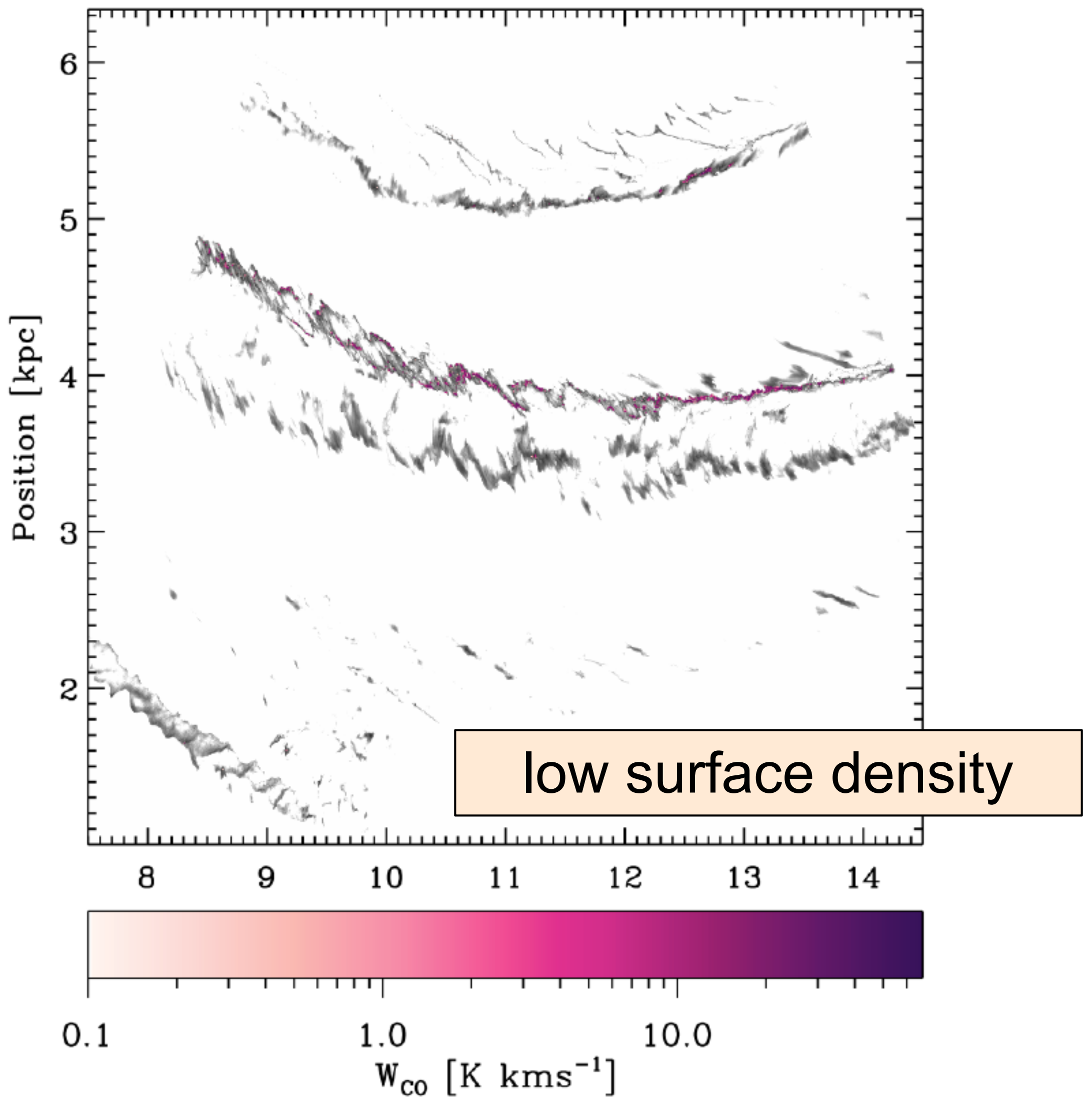

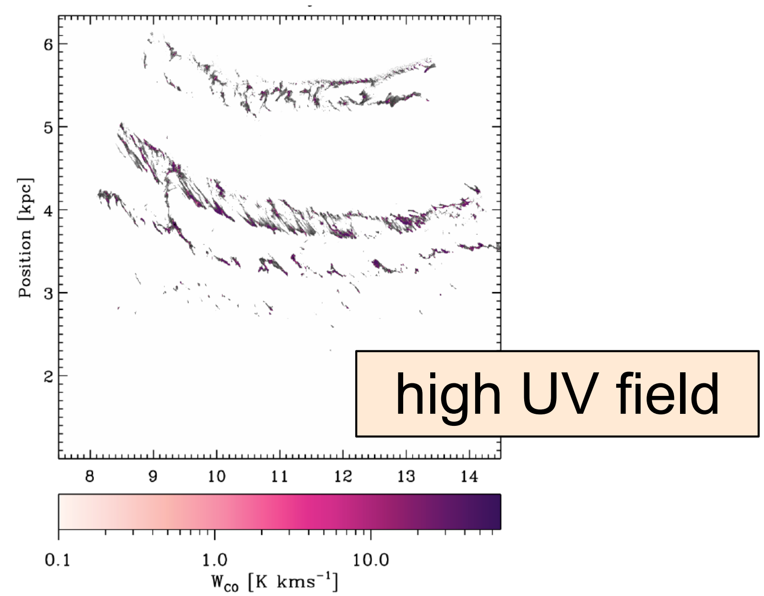

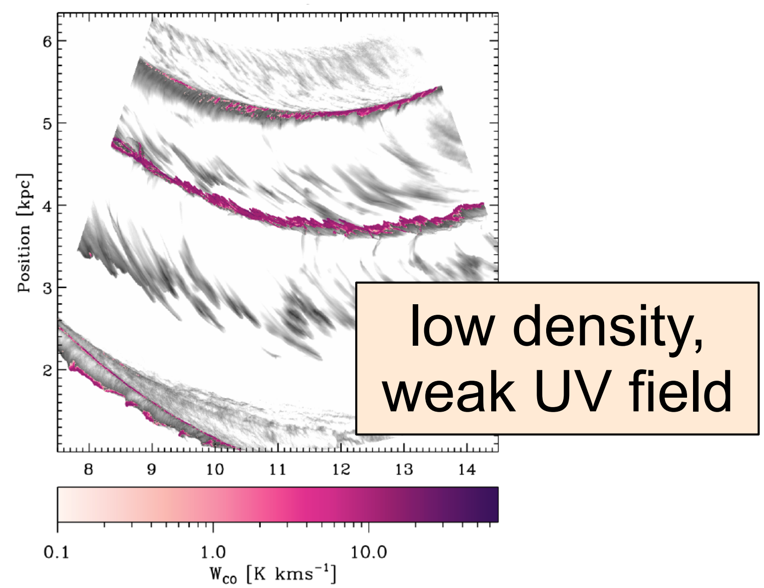

(Smith et al., 2014, MNRAS, 441, 1628)

dependence on UV field

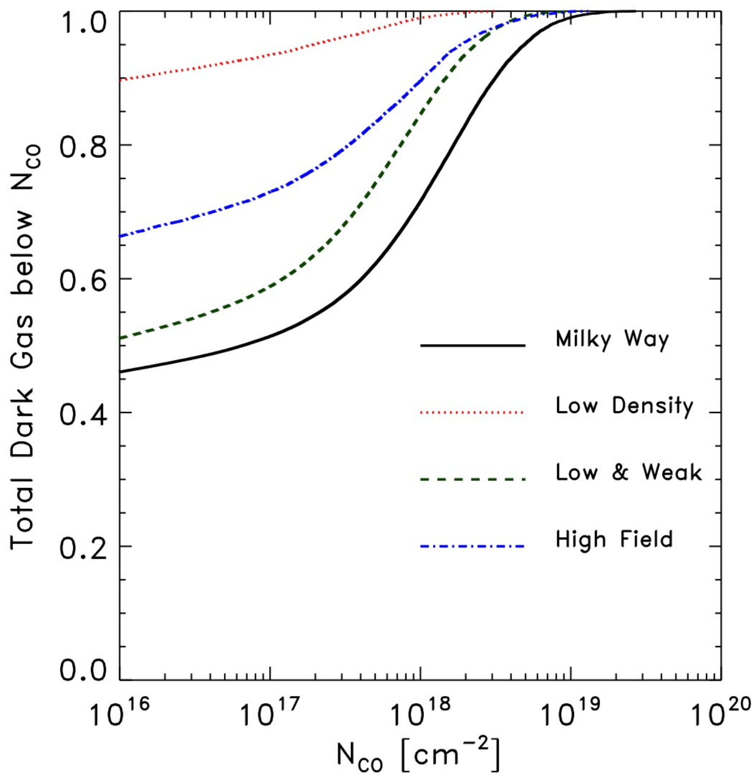

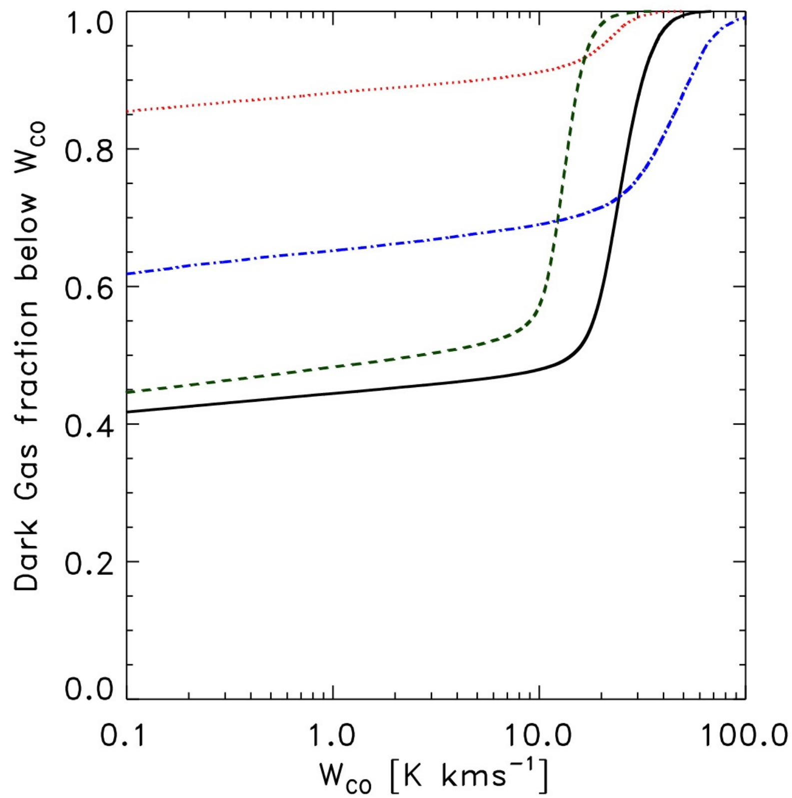

Simulation	Dark Gas @ $N_{CO} = 10^{16}$	Dark Gas @ W_{CO} =0.1	X_{CO}
Milky Way	46%	42%	2.28×10^{20}
Low Density	90%	85%	1.92×10^{20}
Strong Field	66%	62%	1.48×10^{20}
Low & Weak	51%	45%	2.20×10^{20}

in other galaxies the dark gas fraction is likely to be higher.

(Smith et al., 2014, MNRAS, 441, 1628)

further evidence form detailed colliding flow calculations

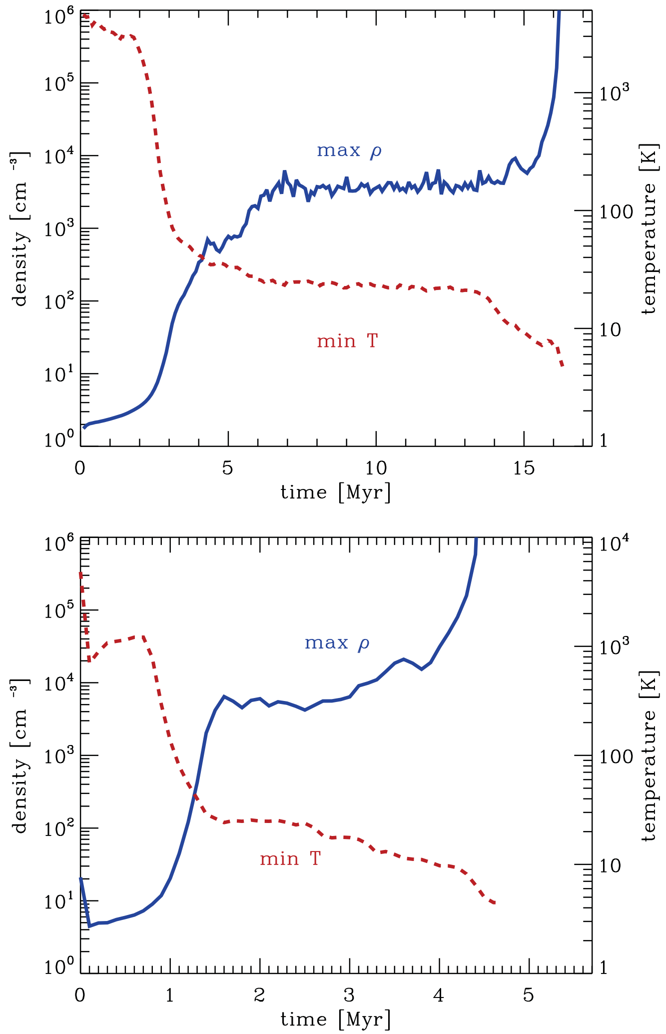

Figure 3. Evolution with time of the maximum density (blue, solid line) and minimum temperature (red, dashed line) in the slow flow (top panel) and the fast flow (bottom panel). Note that at any given instant, the coldest SPH particle is not necessarily the densest, and so the lines plotted are strictly independent of one another.

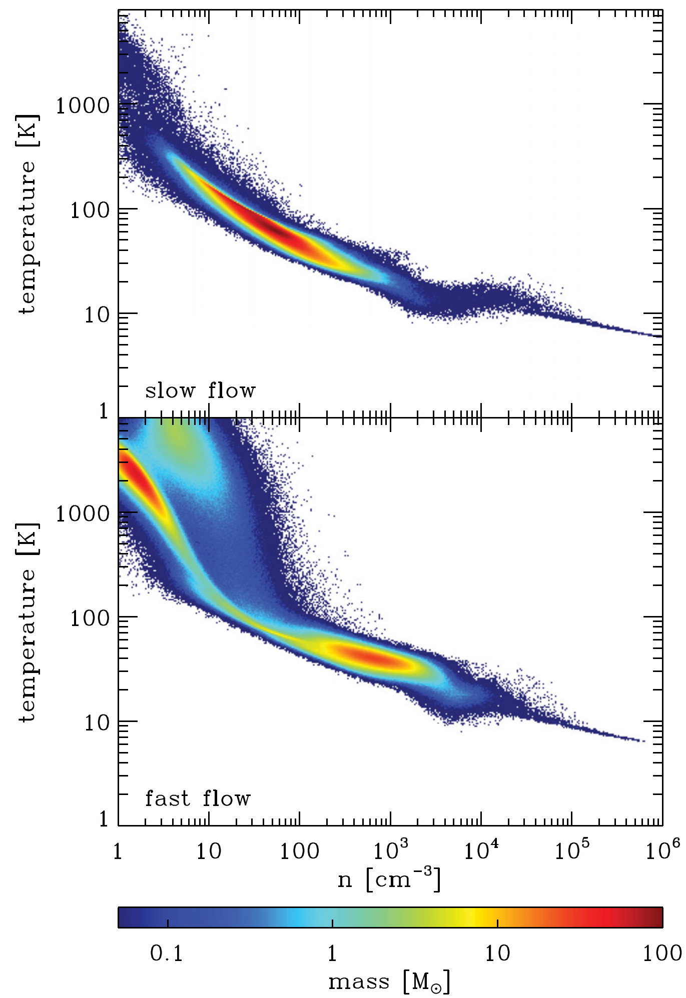

slow flow

fast flow

Figure 5. The gas temperature–density distribution in the flows at the onset of star formation.

Clark et al. (2012,MNRAS, 424, 2599)

see also Pringle, Allen, Lubov (2001), Hosokawa & Inutsuka (2007)

further evidence form detailed colliding flow calculations

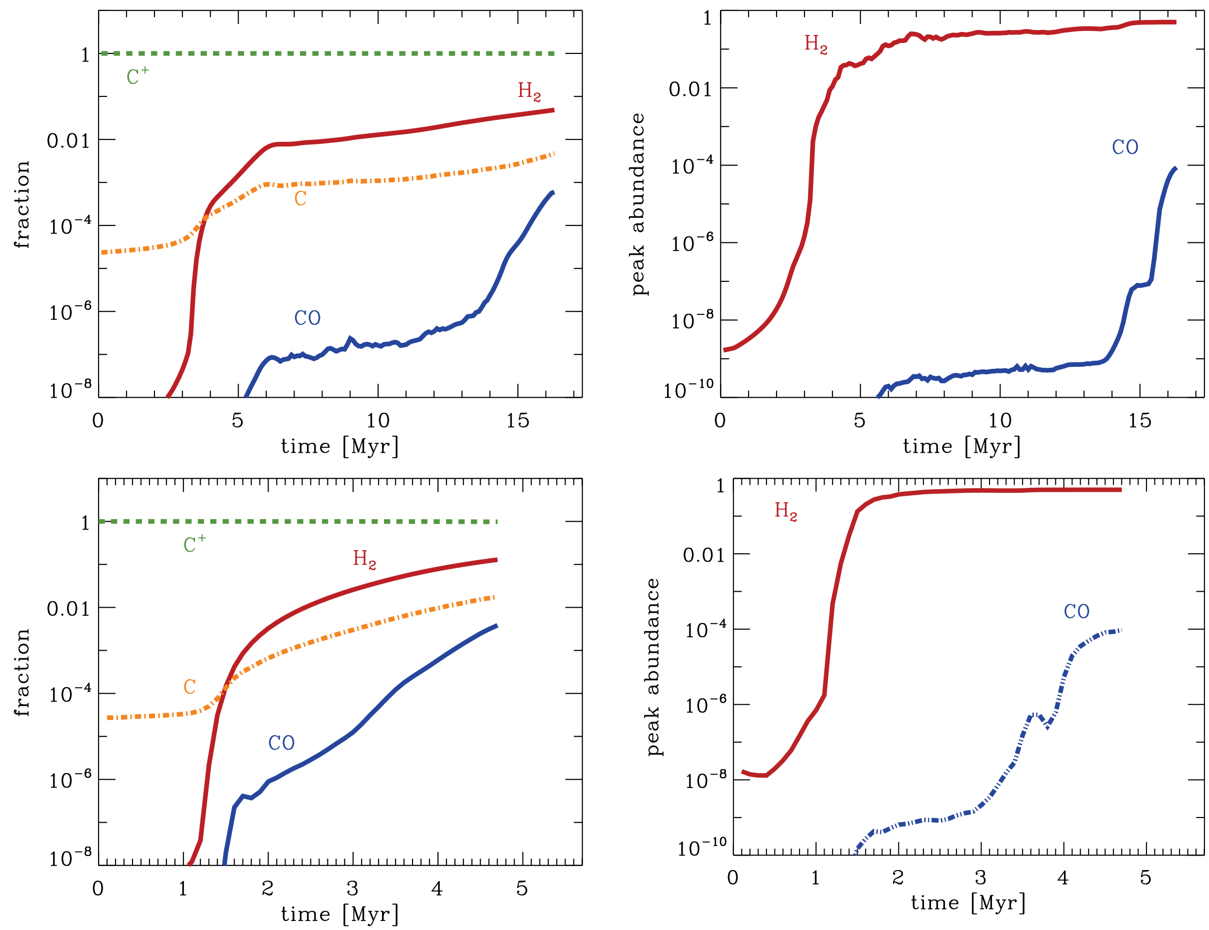

slow flow

fast flow

Figure 6. Chemical evolution of the gas in the flow. In the left-hand column, we show the time evolution of the fraction of the total mass of hydrogen that is in the form of H_2 (red solid line) for the 6.8 km s^{-1} flow (upper panel) and the 13.6 km s^{-1} flow (lower panel). We also show the time evolution of the fraction of the total mass of carbon that is in the form of C^+ (green dashed line), C (orange dot–dashed line) and CO (blue double-dot–dashed line). In the right-hand column, we show the peak values of the fractional abundances of H_2 and CO. These are computed relative to the total number of hydrogen nuclei, and so the maximum fractional abundances of H_2 and CO are 0.5 and 1.4×10^{-4}, respectively. Again, we show results for the 6.8 km s^{-1} flow in the upper panel and the 13.6 km s^{-1} flow in the lower panel. Note that the scale of the horizontal axis differs between the upper and lower panels.

Clark et al. (2012,MNRAS, 424, 2599)

see also Pringle, Allen, Lubov (2001), Hosokawa & Inutsuka (2007)

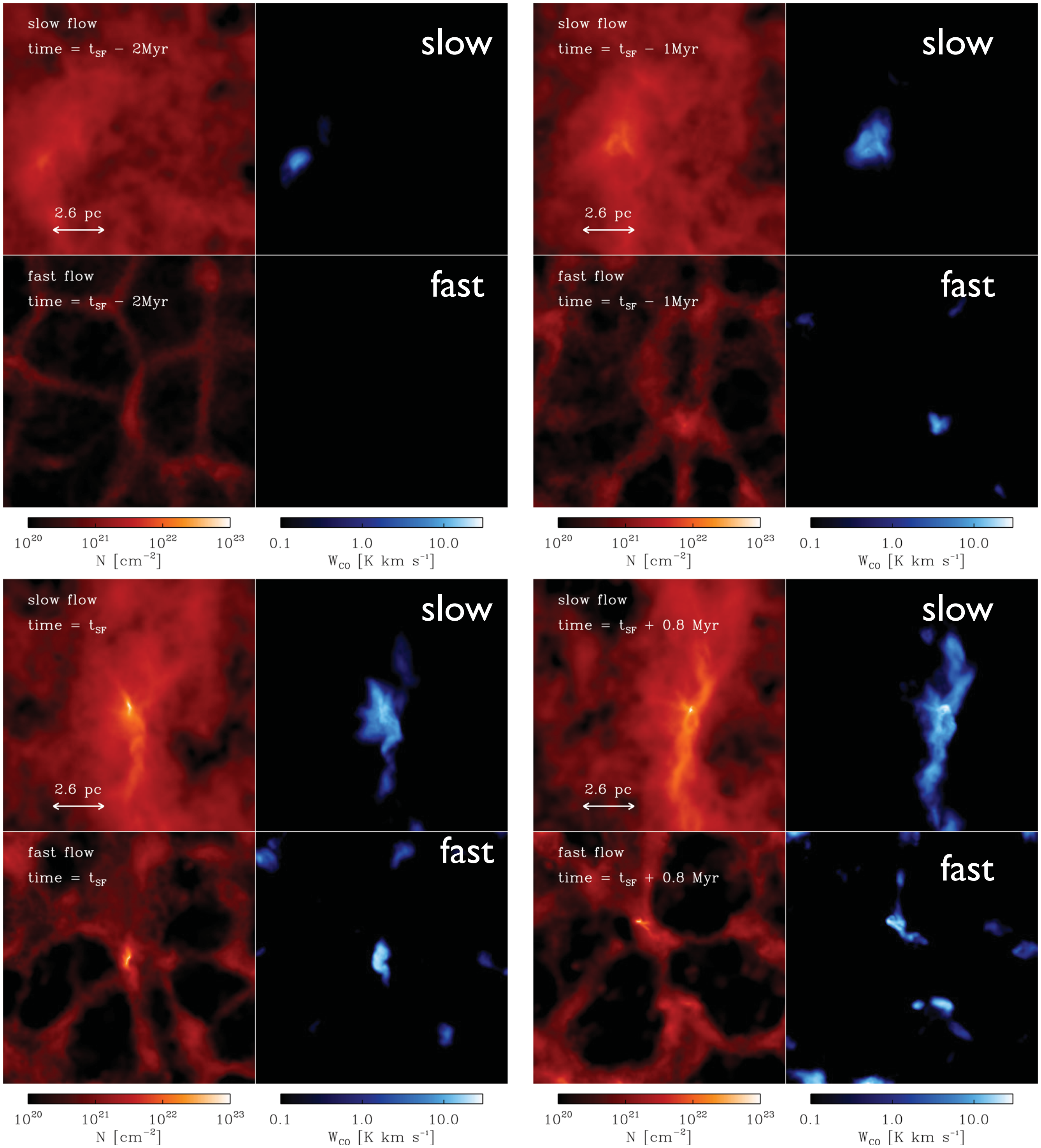

H_2 column

CO emission

fraction of CO dark gas will also change with metallicity and with ambient radiation field

Clark et al. (2012,MNRAS, 424, 2599)

Summary

summary

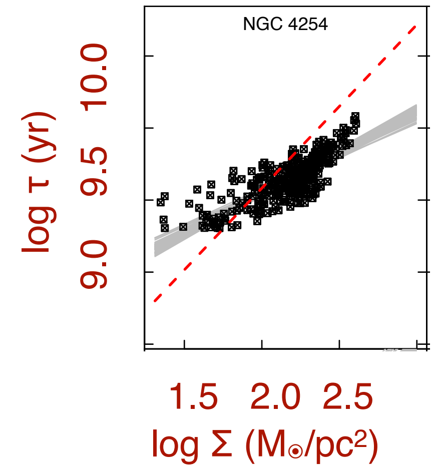

- hierarchical Bayesian statistics indicated galaxy to galaxy variations in the KS relation with typically sublinear slope
  → *is there lots of diffuse CO gas in galaxies?*

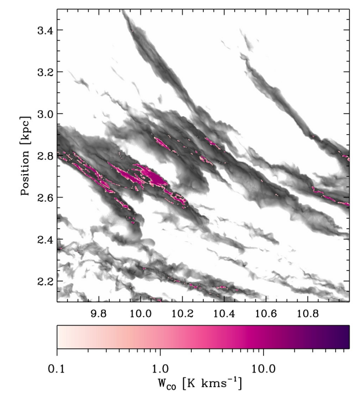

- detailed (M)HD calculations with time-dependent chemistry allow us to study the properties of CO-dark H_2 gas
  → *implications for interpreting observational data?*

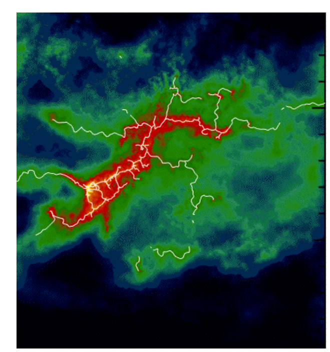

- molecular clouds are filamentary, but the filament parameters (width, slope, central density) may vary significantly
  → *what does it mean for star cluster formation?*

- next steps: *improved multi-scale and multi-physics simulations with Arepo and FLASH* thanks